University of Alberta

Mixing Effects on Chemical Demulsifier Performance in Diluted Bitumen and Froth

by

Jeng Yi Chong

A thesis submitted to the Faculty of Graduate Studies and Research
in partial fulfillment of the requirements for the degree of

Master of Science in Chemical Engineering

Chemical and Material Engineering

© Jeng Yi Chong
Fall 2013
Edmonton, Alberta

Abstract

The impact of mixing on water removal from diluted bitumen and bitumen froth is studied, with the goal of maximizing demulsifier performance. The relative effects of bulk concentration, mixing intensity, mixing time and injection concentration on the demulsifier performance are evaluated. A Confined Impeller Stirred Tank (CIST) with a more uniform turbulence distribution and mixing field than a conventional stirred tank is used in the experiments. Mixing is as important as the bulk concentration at a bulk concentration close to the minimal requirement, and can avoid the "overdosing" problem at a very high bulk concentration. The total mixing energy, J, which combines mixing intensity and mixing time, is the first mixing variable and the injection concentration is the second key mixing variable. Mixing strategies developed from the diluted bitumen system were equally applicable to bitumen froth. Addition order affected the demulsifier performance.

Table of Contents

List of Tables

List of Figures

List of Symbols

B_d	agglomerate birth rate (class size d)
C	off-bottom clearance (m)
d_{32}	sauter mean diameter (m)
d_i	class size (m)
d_p	mass-mean particle diameter (m)
D	impeller Diameter (m)
D_d	agglomerate death rate (class size d)
D_t	local turbulent diffusivity (m^2/s)
g	gravitational constant, (m/s^2)
H	tank height, (m)
k	turbulent kinetic energy (m^2/s^2)
M	mass (kg)
N	shaft rotational speed, (s^{-1})
N_P	power number
N_Q	flow number
P	energy dissipation (W)
Q	volumetric flow rate (m^3/s)
Q_I	injection volumetric flow rate (m^3/s)

Re	Reynolds number
S	impeller submergence (m)
t	settling time (s)
t_m	mixing time (s)
t_{meso}	mesomixing time (s)
t_{micro}	micromixing time (s)
T	tank width, (m)
$\vec{U}$	average fluid velocity (m/s)
V_{IMP}	impeller volume (m)
V_{TANK}	tank volume (m)
V_s	settling velocity (m/s)
We	Weber number
X_{BC}	bulk concentration
X_{IC}	injection concentration
X_J	mixing energy
X_t	mixing time
X_ε	mixing intensity
β	regression coefficient

ε	local energy dissipation rate per mass (W/kg)
ε_{avg}	average local maximum energy dissipation rate per mass (W/kg)
ε_{max}	local maximum energy dissipation rate (W/kg)
η	Kolmogorov length scale (m)
θ_{95}	dimensionless mixing time to 95% homogeneity
μ	viscosity, (Pa*s)
ν	kinematic viscosity (m^2/s)
ρ	density, (kg/m^3)
σ	interfacial tension (kJ/m^2)
v'	local fluctuating velocity (m/s)

Chapter 1: Mixing and Oil Sands Processing

Canada has the third largest oil reserves in the world (OCJ 2012) and 97% of these reserves are in the oil sands, with remaining reserves of 167.9 billion barrels (ERCB 2013). Alberta produced 1.9 million barrels of oil sands crude per day in 2013 and is projected to reach 3.8 million barrels per day by 2022. Alberta oil sands will continue to play an important role in the world economy, with the continual dependency on oil around the world.

Oil sands are a natural mixture of bitumen, sand, clay and water. Oil is extracted from these black ores to yield bitumen. Bitumen is hydrocarbon which is too heavy or thick to flow or be pumped without being diluted or heated. Oil sands bitumen has to be treated to reduce viscosity and increase the quality (e.g. minimal water and solids contents) before it can be fed to upgraders and refineries to produce fuel products such as gasoline, jet fuel and diesel oil.

Mixing is commonly defined as the reduction of inhomogeneity in order to achieve a desired process result. However, a more comprehensive mixing definition requires three specifications: uniformity of concentration, a specified scale of segregation, and a required rate of mixing, or mixing time (Kukukova et al. 2009). Mixing is commonly involved in agitating fluid-like systems. There are many types of mixing such as blending of miscible liquids, immiscible liquid-liquid mixing, solid-liquid mixing and gas-liquid mixing. Mixing is involved in reactions, precipitations, crystallizations, extractions, emulsion productions and many other processes. It plays an important role in a wide range of industries: petrochemical, pharmaceuticals, polymer processing, cosmetic products, food, wastewater treatment, pulp and paper, and mineral processing (Paul et al. 2004).

In oil sands processing, mixing is involved from the very beginning of the process, when bitumen ores are mixed with water and caustic in water-based extraction to yield bitumen froth. Bitumen froth is mixed with organic diluent and chemical

additive in the next stage of the process. Mixing is important throughout the process and will affect the efficiency of separation and processing, especially in multiphase viscous systems like bitumen, with water droplets and fine solids.

1.1   Oil Sands Extraction

Oil sands are mined from the surface for shallow oil sands, with overburden depth up to 75 meters. They are also extracted in situ with steam injected to the well for deep deposits. Surface mined oil sands are transported to the nearest extraction plant as a thick water and oil sands slurry by hydrotransport pipeline. Extraction starts with the water-based Clark extraction process (Masliyah et al. 2004).

Oil Sands
(from surface mining)
6-15% Bitumen

Water Based Extraction

- Hot Water
- Caustic and polymer
- Air bubbles

Bitumen Froth
∼ 60% Bitumen
∼ 30% Water
∼ 10% Solids

Froth Treatment

Naphthenic or Paraffinic

Diluted Bitumen

Solvent Recovery & Upgrader
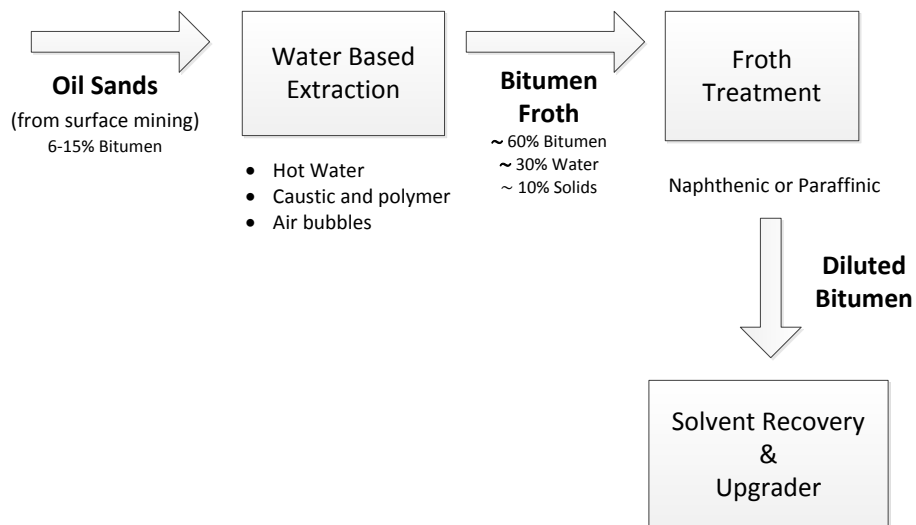
Figure 1-1: Overview of Oil Sands Extraction

1.1.1 Water-Based Extraction

The Karl Clark Water-Based Extraction is the primary extraction step to separate bitumen from mineable oil sands, with the use of hot water, surfactants and pH

modifiers. The fact that water-based technology can be successfully applied to Athabasca oils sands is due to the hydrophilic sand grains in the oil sands (Masliyah et al. 2004). The oil is not in direct contact with the grain as the grain is surrounded by a thin water layer. Air bubbles are used to entrain bitumen to the top of the slurry, forming aerated froth. The froth is deaerated before being fed to the froth treatment unit. The dearated froth typically contains 60% bitumen, 30% water and 10% solids. The bitumen recovery rate is largely affected by the ore grade (bitumen content), fines content, ionic composition, weathering and ageing (Liu et al. 2005).

1.1.2 Froth Treatment

Bitumen froth cannot be fed directly to upgrading or refining as the viscosity, water and solids contents are too high. The water usually contains dissolved salts and will cause corrosion in downstream equipment. Coarse solids can cause wear in pipelines and fine solids may plug reactors and stabilize water emulsions (Angle 2001). The main objective of froth treatment is to reduce water and solids content and this is normally done by adding hydrocarbon diluent. The addition of diluent will reduce the viscosity of bitumen and increase the density difference between the bitumen and water droplets which eases the separation of water. The diluted bitumen is fed to inclined plate settlers (IPS) or scroll and disk centrifuges to separate water and solids.

There are two types of commercial froth treatment operations: naphtha-based and paraffin-based. In naphtha-based froth treatment, naphtha is added at a naphtha-bitumen (N/B) ratio of 0.65–0.7. This is below critical dilution and there is no precipitation of asphaltenes at this dilution ratio. The overall oil losses to tailings are much lower in the naphtha-based froth treatment than in paraffinic froth treatment (Masliyah et al. 2011). Water content is reduced to 2–4 % and solids to 1–2 %. The remaining water and solids are kinetically stable. Diluted

bitumen clarification can be used to further reduce the water and solids content. This is done by attacking the stability of the emulsion chemically using a demulsifier.

In paraffinic froth treatment, the solvent added can be natural gas condensate, or a cut from the bitumen upgrading product containing mostly straight paraffinic hydrocarbon. The solvent-bitumen (S/B) ratio is about 2 or higher. Paraffinic solvent addition exceeds the onset of asphaltene precipitation and the precipitating asphaltenes act both as flocculants for emulsified water droplets and fine solids (Long et al. 2007) and as stabilizers at the drop interface. The diluted bitumen product from this process is very clean with a very low water content and is virtually solids free. However, the paraffinic solvent is usually more expensive and oil losses to tailing are greater (Masliyah et al. 2011).

There are pros and cons to both of these froth treatment processes. The decision on selecting the technology is always site-specific and depends on the downstream upgrading plant. There is more information on the selection of froth treatment processes in a review by Shelfantook (2004). Current processes are predominantly naphtha based.

1.1.2.1   W/O Emulsion Stability

The presence of water-in-oil emulsions creates problems throughout the petroleum industry, and stabilized water droplets with diameters ranging from 1 to 10 µm are also formed in bitumen froth. These small water droplets are very stable and difficult to remove. The stability of this emulsion has been studied extensively. In earlier works, Menon and Wasan (1988) observed a sludge layer at the water/oil interface which prevented the coalescence of droplets. Bhardwaj and Hartland (1994) later confirmed that stabilizing agents in the bitumen slowly migrated to the surface of the water droplets. An emulsifying

agent is present to form stable water-in-crude oil emulsions (Sjöblom et al. 2001). Asphaltenes and resins are acknowledged as the most important components in stabilizing the emulsified water droplets. Fine solids and the presence of naphthenic acids also contribute to the stabilization (Sullivan and Kilpatrick 2002; Ese and Kilpatrick 2004). The stability of water-in-oil emulsions is complex due to the combined effects of different components.

Asphaltenes are a fraction of crude oil that is insoluble in paraffinic solvent, like pentane and heptane, but soluble in toluene. Emulsions are stabilized by asphaltenes through the formation of a viscoelastic, physically cross-linked network of asphaltenic aggregates at the W/O interface (McLean and Kilpatrick 1997). The ability of asphaltenes and resins to form elastic crude oil-water interfaces is also an important factor contributing to emulsion stability. Emulsions are to a small extent stabilized by individual asphaltene molecules as compared to emulsions stabilized by colloidal asphaltene aggregates (Mullins et al. 2007).

Fine solids have a strong stabilizing effect on the W/O emulsion. The stability of the emulsion is affected by the wettability of solids, which depends on the surface properties and structure (Yan et al. 2001). Clay solids have much larger radii compared to surfactants, thus the energy to remove a solid particle from the W/O interface is much larger (Masliyah et al. 2011), so fine solids stay at the interface to make the film more rigid, acting as a barrier to coalescence.

1.1.2.2 Demulsifier Use in Froth Treatment

Stabilized water droplets in a water-in-oil emulsion are difficult to remove; and external mechanical, electrical or chemical interactions are required for effective demulsification. Chemical demulsifier is widely used in the oil and gas industry. Demulsifier is a surface active substance, or surfactant, which can destabilize

emulsions by changing the interfacial film properties and promote coalescence. Coalescence is a process where two or more drops combine to form one or more bigger drops. It is a complicated process involves multiple steps, such as demulsifier partitioning and film rupture between droplets (Kim and Wasan 1996). Demulsifier also causes flocculation by bridging the water droplets. In flocculation, water droplets and fine solids cluster together to form flocs. Flocculation occurs due to adhesive forces and depends on the relative magnitude of the attractive and repulsive forces among the droplets. Demulsification in industry normally involves both coalescence and flocculation and better results were shown when coalescing and flocculating additives were used together (Peña et al. 2005). Since contact of water droplets is required for coalescence to occur, flocculation is shown to be an important step for coalescence (Feng et al. 2010).

Commercial demulsifiers contain mixtures of surfactants and the most common active ingredients are the copolymers ethylene oxide (EO) and propylene oxide (PO) of various molecular masses and EO-PO ratio. Polymer molecular masses affect the demulsification rate and EO-PO ratio determines the hydrophobicity of the polymer (Masliyah et al. 2011). Branched demulsifiers are also found to be more effective in demulsification (Zhang et al. 2005).

Agglomerates, flocs and big water droplets formed during demulsification are separated through settling, based on Stokes Law,

$$V_s = \frac{1}{18} \frac{(\rho_p - \rho_f)}{\mu} g D^2 \qquad \textbf{1-1}$$

where V_s is the terminal settling velocity of a spherical particle, ρ_p and ρ_f are the densities of the settling particle and the continuous fluid, μ is the continuous fluid viscosity, g is the gravity acceleration, and D is the particle diameter (Shelfantook 2004).

1.2   Mixing and Multiphase Systems

When a small amount of demulsifier is added in the naphtha-based froth treatment to remove stabilized water droplets and solids, it is first dispersed and dissolved into the bulk liquid phase of diluted bitumen. Dissolved demulsifier then attaches to the water droplet surfaces and flocculation and coalescence begin to occur. Mixing of demulsifier is a multiphase mixing problem. Mixing enhances the dispersion of demulsifier in the viscous diluted bitumen and will also promote collisions among water droplets. An increase of collision frequency will increase the flocculation and coalescence rates, and improve the separation of water and solids.

1.2.1   Characterization of Mixing

The objectives of mixing can be different in varied fields. Mixing can be described with three parameters: the intensity of segregation, the scale of segregation, and the exposure of the dispersed phase (Kukukova et al. 2009). These parameters are illustrated in Figure 1-1.

1. Intensity of segregation drops

most visible in turbulent blending

2. Scale of segregation drops

most visible in laminar blending

3. Exposure increases

most visible in mass transfer
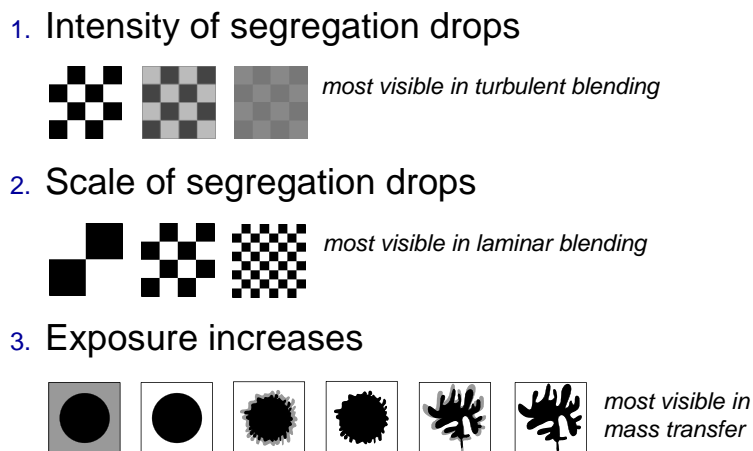
Figure 1-2: The dimensions of segregation, reproduced from (Kresta 2013) with permission

The intensity of segregation is the variance in concentration. In the case of demulsifier dispersion, it is the uniformity of concentration. The scale of segregation is used to define the length scale of mixing and to capture the distribution of phases. It is a measure of droplet size during flocculation and coalescence. Exposure is to measure the driving force of change indicating the rate of mixing, and is the mixing time required for the demulsifier dispersion.

The mixing regime can be estimated using a common dimensionless number, the Reynolds number, which is the ratio of inertial to viscous forces. In a stirred tank, the Reynolds number is defined as

$$Re = \frac{\rho N D^2}{\mu} \qquad \text{1-2}$$

where ρ is the fluid density (kg/m^3), N is the rotational speed (s^{-1}), D is the impeller diameter (m) and μ is the fluid viscosity (Pa.s). Laminar mixing takes place at low Reynolds number below 10 while fully turbulent mixing takes place at Reynolds numbers greater than 20,000. The flow is dominated by viscous forces in laminar flow and becomes dependent on inertial forces in the turbulent regime. Between the two mixing regimes is the transitional region, where local turbulence is experienced near the impeller (Paul et al. 2004). The energy consumption in an impeller stirred tank is characterised by the power number (Rushton et al. 1950), which is defined as

$$N_P = \frac{P}{\rho N^3 D^5} \qquad \text{1-3}$$

where P is the shaft power consumed by the impeller (W). The pumping power of an impeller stirred tank is characterised by the flow number (Rushton et al. 1950), which is defined as

$$N_Q = \frac{Q}{N D^3} \qquad \text{1-4}$$

where Q is the average volumetric flow rate through the impeller (m^3/s). In the fully turbulent regime, the flow number and power number converge to a constant value reflecting their full proportionality to inertial forces. Table 1-1 shows the power numbers of several commonly used impellers.

Table 1-1: Power numbers of various impellers under turbulent conditions (Paul et al. 2004)

Impeller Type	N_P
Lightnin A310	0.3
Chemineer HE3	0.3
45° PBT; 4 blades	1.3
Rushton; 6 blades	5

Blend time in a stirred tank (H=T) is defined as the mixing time required to reach 95% homogeneity. For miscible fluids, blend time is correlated for all impeller types as (Grenville 1992):

$$N\theta_{95} = \frac{5.20}{N_P^{1/3}} \left(\frac{T^2}{D^2} \right) \qquad\qquad \text{Re} > 10,000 \qquad\qquad \textbf{1-5}$$

However, the blend time is not applicable if there is a dissolution limit between two liquids. The time required for blending of naphtha and froth, and for demulsifier dispersion in diluted bitumen, is longer than the miscible fluid blend time.

1.2.2 Liquid-Liquid Dissolution

Diluted bitumen is highly viscous and there is a dissolution barrier between the demulsifier and diluted bitumen. There is a solubility limit in partially miscible

liquid and liquid dissolution can be a mesomixing problem as formation of striations at the addition point is possible. The time required for dissolution is much longer than for blending. The miscibility gap between two fluids depends on the solubility limit of the dispersed liquid and the concentration difference between two phases (Ibemere and Kresta 2007). Mass transfer between two phases is important to increase the dissolution rate. At a high mixing energy dissipation, demulsifier will break into tiny droplets and have a larger interfacial area. Therefore, mass transfer and dissolution rate can be improved by higher mixing energy. The injection concentration of the dispersed phase will also affect the dissolution rate. Prediluted demulsifier will dissolve to the diluted bitumen phase more easily and attain a homogeneous bulk concentration in a shorter time.

1.2.3 Liquid Dispersion and Drop Breakup

In immiscible liquids, a dispersed phase and a continuous phase exist during mixing. Dispersed drop breakage occurs when the external forces exceed the surface and internal viscous forces. The breakup of a dispersed phase in turbulent mixing is largely dependent on the energy dissipation in the system. The turbulent eddies will break the drop if the energy dissipated by the eddy overcomes the resistance forces of the drop (Hinze 1955). The length scale of the smallest eddies is characterized by the Kolmogorov length scale:

$$\eta = \left(\frac{v^3}{\varepsilon}\right)^{1/4} \qquad \text{1-6}$$

where v is the kinematic viscosity (m^2/s) and ε is the local dissipation rate of turbulent kinetic energy per unit mass. At this length scale, the viscous forces in the eddy are approximately equal to the inertial forces due to turbulent velocity fluctuations (Paul et al. 2004). The smallest drop sizes will be limited to the Kolmogorov scale and other fragments produced during breakup (Zhou and

10

Kresta 1998). The maximum stable drop size in a breakup-dominated system will be some multiple of the Kolmogorov length scale.

The energy dissipation in a stirred tank has been found to vary by up to a factor of 100 (Zhou and Kresta 1996). The maximum and minimum energy dissipations of some commonly used impeller geometries have also been quantified by Zhou and Kresta (1996). In cases where no correlations exist, a reasonable estimate of the relative maximum energy dissipation is made by assuming all energy is dissipated in the impeller volume:

$$\varepsilon_{IMP} \sim \frac{P}{\rho V_{Impeller}} \qquad \text{1-7}$$

Energy dissipation affects the dispersion of immiscible liquid and Kolmogorov length scale, and is therefore a suitable variable for the study of mixing effects. The local maximum energy dissipation rate is defined as mixing intensity (ε) in our study. A Confined Impeller Stirred Tank (CIST) with multiple impellers is used in the experiments. The ratio of $\varepsilon_{IMP}/\varepsilon_{avg}$ in the CIST is lower compared to a conventional stirred tank, indicating a more uniformly distributed energy dissipation (Machado and Kresta 2013), where $\varepsilon_{avg} = P/\rho V_{TANK}$.

Drops are found in a distribution of sizes as the energy dissipations are varied in a stirred tank. The Sauter mean diameter, d_{32}, is commonly used to represent these distributions. The diameter of drops has been correlated with Weber number, $We = \rho_C N^2 D^3/\sigma$ in non-coalescing systems (Chen and Middleman 1967),

$$\frac{d_{32}}{D} \propto We^{-3/5} \qquad \text{1-8}$$

The Weber number is the ratio of inertial (disruptive) to surface (cohesive) forces and σ is the interfacial tension between the two dispersed liquids. This relation assumes a proportional relationship between d_{32} and d_{max}, an assumption that

holds true if geometric similarity is maintained. Davies (1987) correlated a rough estimate of ε_{avg} with the maximum stable drop size, and illustrated that

$$d_{max} \propto \varepsilon_{avg}^{-2/5} \qquad \textbf{1-9}$$

The rate of breakage increases as the circulation time decreases. The rate also increases as the distance from the equilibrium drop size distribution goes up. Accordingly, the kinetics of droplet breakage has been approached in a way similar to reaction kinetics:

$$\frac{d\Omega}{d\theta} \propto -C_1 \Omega^{C_2} \; where \; \Omega = \frac{d_{32}(t) - d_{32}^{\infty}}{d_{32}^{\infty}} \; and \; \theta = Nt \qquad \textbf{1-10}$$

where N is the impeller speed, $d_{32}(t)$ the Sauter mean diameter of the dispersed phase at time t and d_{32}^{∞} is the value at equilibrium. Exponential decay functions with a value of C_2 equal to 1 and 2 have been reported (Paul et al. 2004). These correlations will be useful in understanding the water droplets breakup and size distribution in diluted bitumen during mixing.

1.2.4 Flocculation and Coalescence

Water droplet breakage, flocculation and coalescence occur simultaneously when the demulsifier is mixed with the diluted bitumen. When the impellers are stopped, settling begins while flocculation and coalescence continue. All these processes happen at different rates and a population balance model is a practical approach to determine the size distribution in a system. The population balance equation is essentially a mathematical mass balance over a discrete volume and drop size. The most general population balance equation can be written as:

$$\frac{\partial n_d}{\partial t} + \nabla \cdot \left(\vec{U} n_d \right) - B_d + D_d = 0 \qquad \textbf{1-11}$$

For a given agglomerate size, n_d is the number of drops, $\vec{U}$ is the velocity vector, B_d is the birth rate and D_d is the death rate of the agglomerates. The equation

can be solved using numerical methods but the solution is difficult due to the numerical complexities and model uncertainties. Various approaches applying population balances in CFD simulations are outlined by Ramakrishna (2001). Population balances are not used in this study but it is a useful approach for future work.

1.3   Mixing Studies in Froth Treatment

There are limited studies of mixing in froth treatment. In an early work, Bhardwaj and Hartland (1994) showed that most of the coalescence of water in diluted bitumen systems occurs in the first few minutes, and a very long mixing time may not be necessary. Effects of mixing time and demulsifier dosage on the drop size distribution of water in diluted bitumen were also studied by Mason et al. (1995). An increase of demulsifier bulk concentration and longer mixing time both lead to a larger final water drop size and a faster separation. Therefore, demulsifier bulk concentration and mixing time are two variables that can be further explored in this study.

For paraffinic based froth treatment, the floc size distribution of asphaltenes has been shown to vary with shear rate in laminar flow regimes (Rahmani et al. 2004). The kinetics of asphaltene flocculation by varying ratios of toluene and heptane as solvents at different levels of shear were also studied. (Rastegari et al 2004). We can infer from these studies that the shear effect is an important variable in flocculation. Diluted bitumen is mixed in a turbulent regime in our study and the energy dissipation during mixing can be an important variable for demulsification.

1.4   Objectives for This Work

There is a knowledge gap between the field of mixing and oil sands froth treatment studies. Mixing parameters in oil sands research are rarely defined well and are not easily transferred to industrial conditions. Shaker tables, magnetic stirrers and jar tests with low energy dissipation are still commonly used in testing the performance of chemical additives. In Laplante's (2011) study, results obtained from the shaker table did not compare well with the results from the stirred tank. Since not all studies are conducted under the same mixing conditions, comparison and prediction of demulsifier performance at the large scale is currently difficult.

Only the bulk concentration of demulsifier is reported in many demulsifier studies and demulsifiers are possibly injected with varied injection concentration (Xu et al 2005; Peña 2005). Injection concentrations below 5 % of active ingredient are also reported (Feng et al. 2009), and the low injection concentration may not be feasible in industrial applications due to the large injection volume required. Injection method and location are other limitations in many studies. As dispersion at the beginning of the demulsification process is important, varying injection method and location will affect the outcome of the test.

In this study, a Confined Impeller Stirred Tank (CIST) is used to standardize the mixing protocols in demulsifier testing. The CIST with confined multiple impellers is able match mixing conditions in the plant and has defined mixing parameters. The dispersion of demulsifier in diluted bitumen is affected by the energy dissipation. Flocculation and coalescence may be improved by mixing due to a higher collision frequency. Therefore the effect of mixing on the demulsifier performance is an interesting question to answer. Mixing is tested with two different variables, mixing intensity and mixing time. Injection concentration is also an important variable to study as it affects the dissolution of demulsifier in a

highly viscous multiphase fluid system, and potentially affects the performance of the demulsifier. The injection of demulsifier in this study is carried out in a more systematic way and at a fixed location to maximize the initial dispersion. Finally, the effect of bulk concentration is studied as its significance may be different under varied mixing conditions.

Chapter 2: Evaluation of Mixing Effects on Demulsifier Performance in Dilute Bitumen Clarification

The performance of chemical additives is commonly evaluated based on the chemical dosage (Xu et al. 2005, Deng et al. 2005). However, there can be a dispersion problem with the addition of a small amount of additive, especially in a complex multi-phase fluid system such as diluted bitumen, which will affect the performance of the chemical additive. In this project, the effect of mixing on chemical additive performance is studied in a novel Confined Impeller Stirred Tank (CIST) with different chemical dosage and mixing variables. The experimental protocol is similar to the studies conducted by Laplante (2011) but a different type of demulsifier is tested to observe the effects of mixing when different demulsifier is applied. As mixing is an interactive variable and has a non-linear effect on the demulsifier performance, two experimental designs were carried out to identify the significance of mixing on diluted bitumen clarification at different ranges of chemical dosage.

2.1 Experimental Setup

A Confined Impeller Stirred Tank (CIST) designed previously was used throughout the experiments to have a standard mixing/settling apparatus and protocol (Laplante 2011). The experimental procedure can be divided into three stages: sample preparation, demulsifier dispersion and batch settling. A schematic of the experimental setup and procedure is shown in Figure 2-1. In the sample preparation step, diluted bitumen was heated and premixed in the sample can before being transferred to the CIST. Both demulsifier dispersion and batch settling were carried out in the CIST.

Step 1: Pre-Mixing
- Heating for 30 minutes to 60 °C
- Agitation at 1000 rpm for 15 minute while heating to 76.5 °C

Step 2: Mixing
- Add diluted demulsifier into CIST 1 and 2.
- Mix for time t and specified agitation level.

Step 3: Settling
- Batch gravity settling for 60 minutes
- Sample water content at 1, 3, 5, 7, 10, 30, 60 minutes settling
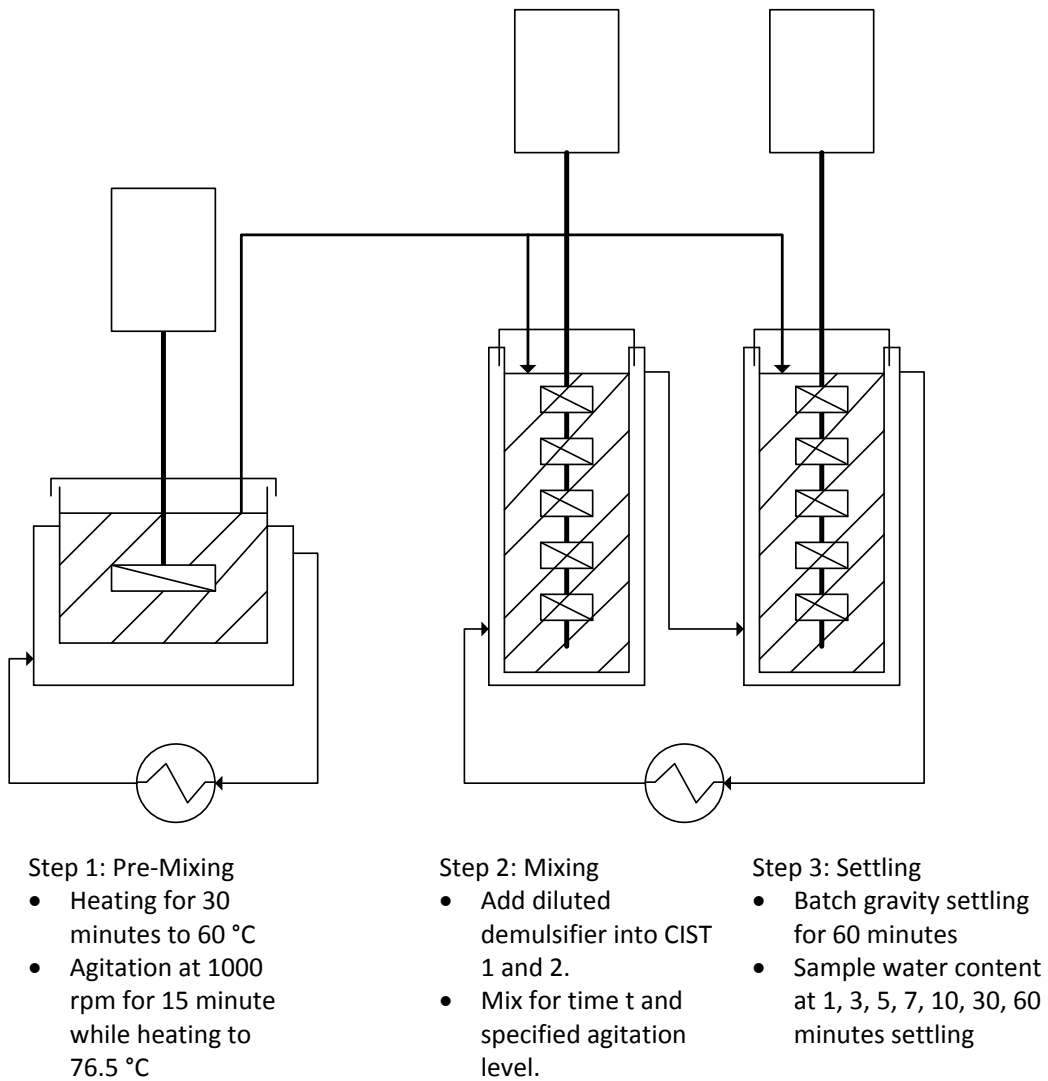
Figure 2-1: Schematic of experimental setup and procedure. Reproduced with permission (Laplante 2011).

Diluted bitumen from froth treatment as provided by Syncrude Research was used as the feed sample in the experiments. The properties and composition of diluted bitumen after pre-mixing are shown in Table 2-1. The composition was obtained using Karl Fischer titration and Dean Stark oil, water and solids (O/W/S) analysis. The diluted bitumen as supplied had a naphtha-to-bitumen ratio (N/B) of 0.7 by weight. The viscosity of diluted bitumen was measured using a Fenske viscometer at 80 °C and the density was measured using a pycnometer at 80 °C. Demulsifier from Champion Technologies was also provided by Syncrude Research with a concentration of 39 wt%.

Table 2-1: Properties and composition of diluted bitumen

Average Water Content (wt%)	2.3 - 2.7
Average Solids (wt%)	0.3 - 0.6
Average Hydrocarbons Content (wt%)	96.7 - 97.4
N/B	0.7
Density, 80 °C (kg/m^3)	860
Viscosity, 80 °C (m^2/s)	6.1×10^{-6}

2.1.1 Premixing

All diluted bitumen samples in 4 L paint cans were stored upside down at 5 °C in a refrigerator. Before demulsifier dispersion, the diluted bitumen was re-suspended at a high energy dissipation level in order to ensure the feed sample was homogeneous and to provide a "worst case" emulsification scenario. The sample was first re-agitated by shaking by hand before heating. Then, the diluted bitumen was heated for 30 minutes to 60 °C without mixing and then for another 15 minutes with mixing at speed 1000 rpm to 76.5 °C. A 45° pitched

blade turbine (PBTD) impeller was used and standard T/10 baffles were attached to the can to promote turbulence. The premixing tank dimensions and mixing parameters are shown in Table 2-2. At the end of premixing, a sample of 100 ml was withdrawn for O/W/S analysis and Karl Fischer titration to determine the composition of the sample. A small sample was retained for microscopic observation. The premixed diluted bitumen was then transferred to two CISTs using a Masterflex Pump and disposable tubing for demulsifier dispersion.

Table 2-2: Premixing tank dimensions and mixing parameters

Impeller Type	PBTD (45)
Tank diameter, T (m)	0.16
Impeller diameter, D (m)	0.08
Liquid height, H (m)	0.11
Off-bottom clearance, C (m)	0.04
Total Impeller Volume, V_{IMP} (m^3)	8.04×10^{-5}
Power Number, N_P	1.30
Impeller speed, N (rpm)	1000
P/ρ V_{TANK} (W/kg)	9.20
P/ρ V_{IMP} (W/kg)	245
Reynolds Number, Re	17558
Mixing time (min)	15

2.1.2 Mixing and Settling

The CIST with 1 L volume has an H/T ratio of 3. The high H/T ratio enables demulsifier dispersion and settling to be conducted in the same tank without transferring to a settling cell. The CIST with T/12 baffles was agitated with either 6 Intermig impellers, 5 A310 impellers or 5 Rushton impellers to achieve different mixing intensities while maintaining the circulation velocities and Reynolds numbers. In a standard stirred tank, one impeller is used for every H=T (Paul et al. 2004). The number of impellers used in the CIST was larger in order to have more turbulence per unit volume. The relatively high viscosity of diluted bitumen leads to lower Reynolds numbers than in a conventional mixing experiment. The CIST is able to keep the flow turbulent at small Re, 2000 for Rushton turbines and 3200 for Intermigs (Machado and Kresta 2013). Multiple impellers provide a large amount of turbulence per volume.

The impellers were installed on a 0.25" shaft with an off-bottom clearance of the bottom impeller of 1/3*D and a submergence of 1*D for the top impeller, where D is the diameter of the impeller. Successive impellers were staggered at 60°, 30° and 90° to each other for the A310s, Rushtons, and Intermigs, respectively. The shaft was supported by a steady bearing at the CIST bottom. The stainless steel Intermigs were supplied by Ekato, while the Nickel plated resin A310 and Rushtons were supplied by Lightnin. The impellers were plated with Nickel to minimize chemical attack and provide thermal stability. The total power number of the impellers as a function of Reynolds number was measured by Machado and Kresta (2013) as shown in Figure 2-2. Triethylene glycol at 25 °C, with kinematic viscosity (6×10^{-6} m^2/s), similar to diluted bitumen at 80 °C, was used to determine the power number of impellers in this experimental set-up.
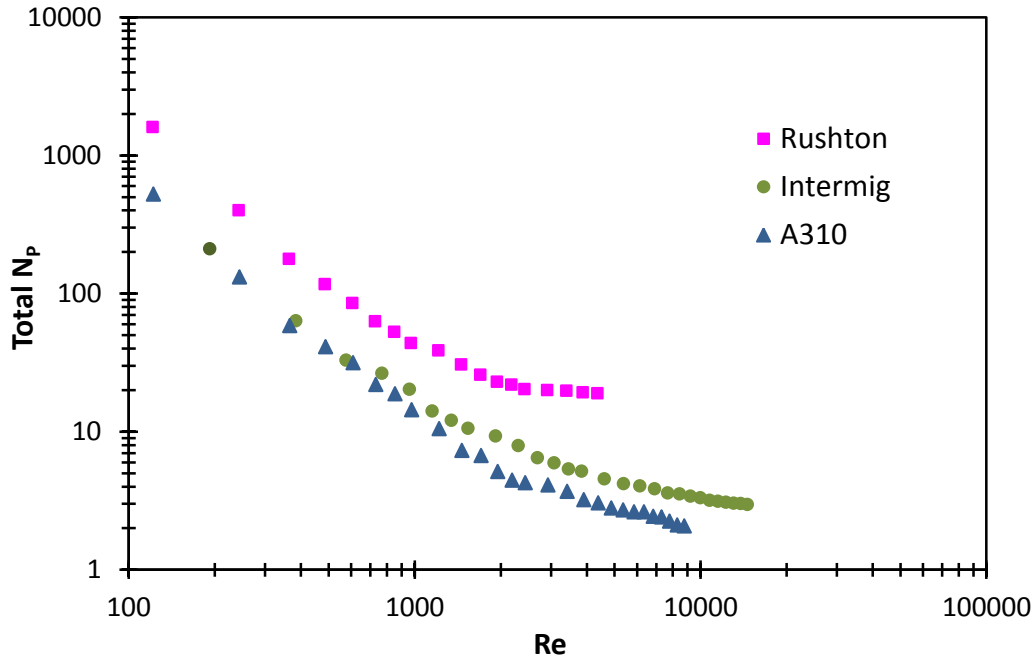
Figure 2-2: Total power number as a function of Reynolds number for different impellers in the CIST. Data reproduced with permission (Machado and Kresta 2013).

The tank was jacketed to allow circulation of heating fluid and to maintain the temperature of diluted bitumen at 76.5 °C. Stainless steel 3/8" sampling and injection ports protruded from the tank lid. Figure 2-3 shows the schematic of the CIST design and Table 2-3 gives the geometry of CIST and mixing specifications.

Demulsifier was diluted using xylene to the desired injection concentration. The demulsifier was injected 1 minute after the impellers were turned on using an appropriately sized syringe or 1/8" tubing connected to a syringe pump. The syringe and tubing were inserted to the CIST through the injection port. The injection took place directly above the upper impeller blade tip to promote high initial dispersion of demulsifier. Demulsifier was mixed with the diluted bitumen for a specific mixing time and the sample was allowed to settle for 60 minutes after mixing.
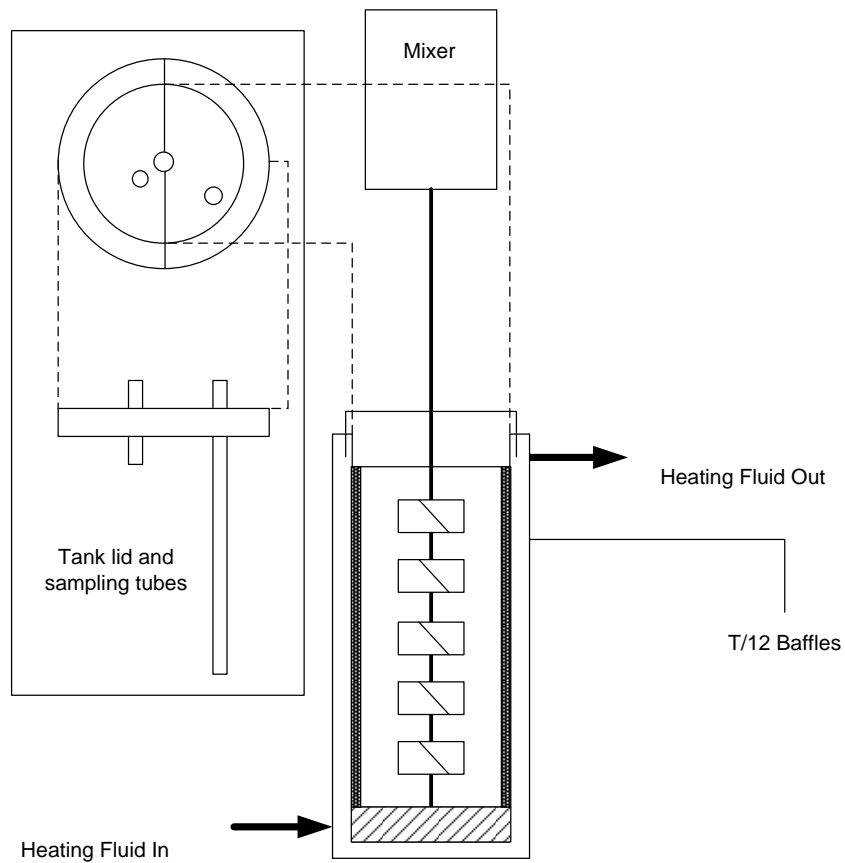
Figure 2-3: CIST design schematic: the glass stirred tank has a volume of 1 L, a tank diameter T of 7.5 cm, and T/12 baffles. A ¼ in shaft is supported at the tank bottom using a steady bearing. Stainless steel 3/8" sampling and injection ports protrude from the tank lid. Impellers are equally spaced between distance D/3 from tank bottom and D below fluid surface. Reproduced with permission from (Laplante 2011).

Table 2-3: CIST geometry and mixing specifications

Impeller Type	Intermig	A310	Rushton
Tank diameter, T (m)	0.075	0.075	0.075
Number of impellers	6	5	5
Impeller diameter, D (m)	0.050	0.038	0.038
Impeller speed, N (rpm)	250	1000	600
Liquid height, H (m)	0.225	0.225	0.225
Off-bottom clear, C (m)	0.017	0.013	0.013
Submergence, S (m)	0.050	0.038	0.038
Tank volume, V_{TANK} (m^3)	9.94×10^{-4}	9.94×10^{-4}	9.94×10^{-4}
Total impeller vol, V_{IMP} (m^3)	1.68×10^{-4}	5.23×10^{-5}	4.31×10^{-5}
Transitional N_p per impeller	1.3	0.65	4.6
$P/\rho\ V_{TANK}$ (W/kg)	0.18	1.13	1.71
$\varepsilon \sim P/\rho\ V_{IMP}$ (W/kg)	1.08	21.45	39.48
Reynolds number, Re	1715	3858	2315
Mixing time (min)	2, 6 and 10 min		

2.1.2.1 Mesomixing

Mesomixing can occur during injection of demulsifier if the injection volume and the injection flow rate are too high. The formation of a plume will possibly increase the local concentration of demulsifier and affect the performance of the demulsifier. In these experiments, mesomixing was avoided by following a more systematic injection procedure. For cases with large volumes of diluted demulsifier, larger than 1 ml, injections were carried out using a syringe pump with a controlled flowrate. The mesomixing time constant indicates the rate-limiting mesomixing step. A plume may form if it is greater than 20% of the characteristic micromixing time constant (Anthieren 2003). Therefore, the injection flowrate is calculated based on the mesomixing time scale, $t_{meso} <$ $0.2\ t_{micro}$. The injection flowrate, Q_I can be expressed as below with the derivation given in Appendix A:

$$Q_I = 0.54 \frac{v^{0.5} \cdot U_z \cdot d_p^{\ 1.5}}{v_z'^{\ 0.5}} \qquad \textbf{2-1}$$

In this equation, v is the kinematic viscosity, U_z is the mean velocity of surrounding fluid at the feed, d_p is the feed pipe diameter and v_z' is the local fluctuating velocity. The U_z and v_z' values in CIST were obtained from measurement by Machado and Kresta (2013).

Table 2-4: Summary of injection flowrate and injection time

Impeller	Flowrate Calculated (ml/hr)	Flowrate Used (ml/hr)	Injection time* (s)
Intermig	122.0	120	49
A310	207.7	200	56
Rushton	634.7	630	9.3

*Based on the largest volume injected when the respective impeller is used

2.1.3 Experimental Design

Four variables were studied in the experiments, bulk demulsifier concentration (BC), mixing intensity (ε), mixing time (t_m) and injection concentration of demulsifier (IC). Both bulk concentration and injection concentration are calculated on a mass basis. An estimate of local maximum energy dissipation rate, $\bar{\varepsilon}$ is obtained from:

$$\bar{\varepsilon} \propto \frac{P}{\rho V_{Impeller}}$$

2-2

where P is the energy dissipation (W), ρ is the density of the sample (kg/m^3) and $V_{Impeller}$ is the impeller swept volume (m^3).

2.1.3.1 Campaign 1: 4-Variable Box-Behnken Design

The effects of the variables were studied using the Box-Behnken fractional factorial design in the first experimental campaign (Box and Behnken 1960). The variables are coded according to equally spaced intervals using the relationship:

$$X_A = 2\frac{(A - A_{MIN})}{A_{MAX} - A_{MIN}} - 1$$

2-3

Each variable was varied at three levels to observe the quadratic effects. The variables X_{BC}, X_{ε}, X_{tm} and X_{IC} were coded as -1, 0 and +1. 30 experiments were carried out to complete a 3 level Box-Behnken fractional factorial. Table 2-5 summarizes the experimental conditions for the variables at three levels with the full Box-Behnken factorial design is shown in Table 2-6.

Demulsifier was added to the diluted bitumen at a bulk concentration, BC, of 5, 50 and 95 ppm. These BC values were set based on a few preliminary tests and were within the commercial application range. The injection concentration was varied from 3 wt% to the stock solution concentration of 39 wt%. The mixing intensity from 1 to 40 W/kg was selected to include energy dissipation levels ranging from agitation in an empty pipe to agitation with a static mixer.

Table 2-5: Variable coding for Box-Behnken fractional factorial design

Variable	-1	0	1
Bulk Demulsifier Concentration, BC (ppm)	5	50	95
Mixing Intensity, ε (W/kg)	1	21	40
Mixing Time, t_m (min)	2	6	10
Injection Concentration, IC (wt. %)	3	21	39

Table 2-6: Box-Behnken factorial design

Block/ Variable	Bulk Concentration X_{BC}	Mixing Intensity X_ε	Mixing Time X_{tm}	Injection Concentration X_{IC}
X_{BC}, X_ε	-	-	0	0
	-	+	0	0
	+	-	0	0
	+	+	0	0
X_{BC}, X_{tm}	-	0	-	0
	-	0	+	0
	+	0	-	0
	+	0	+	0
X_{BC}, X_{IC}	-	0	0	-
	-	0	0	+
	+	0	0	-
	+	0	0	+
X_ε, X_{tm}	0	-	-	0
	0	-	+	0
	0	+	-	0
	0	+	+	0
X_ε, X_{IC}	0	-	0	-
	0	-	0	+
	0	+	0	-
	0	+	0	+
X_{tm}, X_{IC}	0	0	-	-
	0	0	-	+
	0	0	+	-
	0	0	+	+
Central Design Point	0	0	0	0
	0	0	0	0
	0	0	0	0
	0	0	0	0
	0	0	0	0
	0	0	0	0

2.1.3.2 Campaign 2: Effect of Dropping Maximum Demulsifier Concentration

Mixing intensity and mixing time did not show a significant effect in the first experimental campaign. This could be due to the high demulsifier bulk concentration and the injection concentration range tested. A bulk concentration of 95 ppm may be too high to observe the effect of mixing and a new high range (+) of BC was set to 50 ppm in the second experimental campaign. It was also noted that the demulsifier tends to work best at a lower injection concentration, between 3 to 21 wt%. To test if further improvement is possible inside this range, a mean value of 12 wt% was set as the high IC (+) in the second experimental design.

Instead of repeating the complete Box-Behnken factorial design, which involves a minimum of 27 runs for 4 variables, a 2-level factorial design was carried out for a smaller group of experiments. With this, quadratic effects of the variables would not be observed. A lumped variable of the mixing intensity and mixing time, J, was used to further reduce the number of experiments. $J = \bar{\varepsilon} \times t_m$ is the mixing energy and is a representative mixing variable. The new set of experiments was used to test the effect of lowering concentrations, IC to 12 wt% and BC to 27 ppm, but also to identify mixing effects at different bulk concentrations.

Table 2-7: Variables of 2-level factorial design

Variable	-1	1
Bulk Demulsifier Concentration, BC (ppm)	27	50
Mixing Energy, J	Low*	High**
Injection Concentration, IC (wt. %)	3	12

* Low   : $\varepsilon = 1$ W/kg, $t_m = 2$ min
** High : $\varepsilon = 40$ W/kg, $t_m = 10$ min

Table 2-8: 2-level factorial design

Run	BC	J	IC
1	–	–	–
2	–	–	+
3	–	+	–
4	–	+	+
5	+	–	+
6	+	+	–
7	+	–	+
8	+	–	–

2.1.4 Sampling and Test

During the dispersion of demulsifier, samples were obtained 60 seconds after demulsifier injection and 30 seconds before the end of mixing. These samples were obtained for water content determination and microscope analysis, by sampling the bulk mixtures 3.2 cm below the liquid surface using 0.25" ID polyethylene tubing attached to an auto-pipette. After the mixing time was reached, the impellers were stopped and the sample in the CIST was allowed to settle by gravity for 60 minutes. Samples were taken at 3.2 cm below the liquid surface at 1, 3, 5, 7, 10, 30 and 60 minutes. Microscope images of samples were obtained after 1, 3, 5, 7, 10 and 30 minutes of settling. To observe the vertical profile of water content during the settling, samples were also taken at height $z/H = 0.45$ and 0.8, at 10 and 30 minutes, in a few selected runs. The z/H ratio is measured from the surface of the liquid, $z/H = 0$. At the end of the 60 minute settling, 100 mL samples were obtained for O/W/S analysis at height $z/H = 0.1$, 0.5 and 0.9. Table 2-9 summarizes the sampling time, location and methods in the experiments.

Table 2-9: Summary of sampling during the experiment

Label	Time	Location	Method	Volume (ml)
A	End of premixing		Tubing attached to an auto-pipette	1
DS_A	End of premixing		Tubing connected to a 100 ml syringe	100
B,C	During Mixing (60 s after demulsifier added and 30 s before mixing ends)	3.2 cm below the liquid surface	Tubing attached to an auto-pipette	1
1, 3, 5, 7, 10, 30, 60	During settling	3.2 cm below the liquid surface	Tubing attached to an auto-pipette	1
10b, 10c, 30b, 30c	During settling (10 and 30 min)	At z/H = 0.4, 0.8	Tubing attached to an auto-pipette	1
DS_0.1, DS_0.5, DS_0.9	End of settling	At z/H = 0.1, 0.5, 0.9	Tubing connected to a 100 ml syringe	100

2.1.4.1 Karl Fischer Titration

Karl-Fischer titration was used to measure the water content in the samples. This method is more accurate and consistent compared to Dean Stark extraction at low water content (Laplante 2011). Samples containing approximately 1 mL diluted bitumen were obtained once after pre-mixing, 2 times during mixing and 7 times during the settling. These samples were pre-dissolved before the analysis using Unisol, a 1:3 isopropyl alcohol and toluene mixture, which was dried using silica gel and sampled for water content prior to dilution. The samples were analyzed using a Kam Controls Karl Fischer titration apparatus and standard reagents. The titration apparatus was calibrated using 1 wt% water standard and the calibration curve is shown in Figure 2-4. During the titration, samples were agitated using a vortex mixer for 6 seconds and a 50 µL spring loaded Hamilton syringe was used to inject the sample. Samples were weighed before and after dilution to determine the dilution factor, and syringes were weighed before and after injection to measure the amount of sample injected. Three repetitions were made from each sample to ensure the precision of the results.
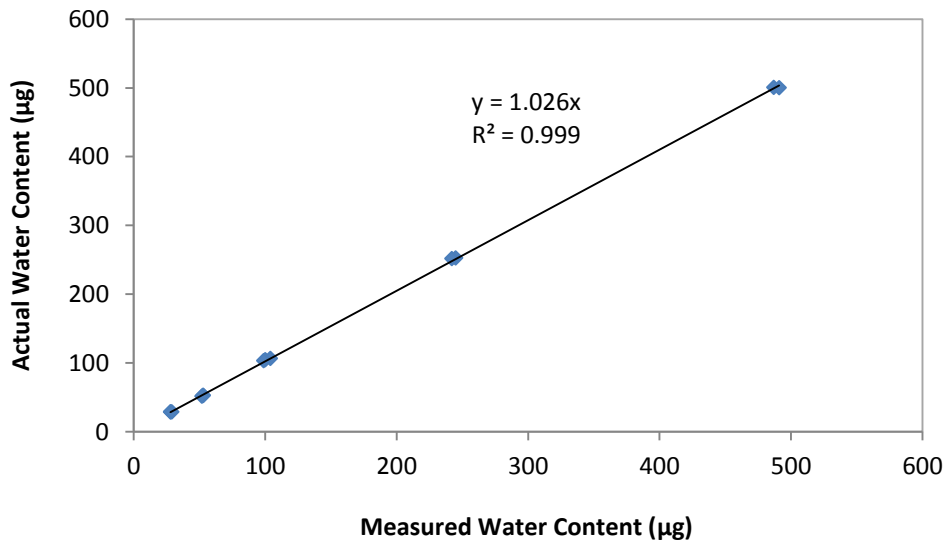
Figure 2-4: Kam Controls Karl Fischer calibration

2.2 Results and Discussion

Demulsifier is added to the diluted bitumen to remove water droplets and fine solids. Demulsifier causes flocculation and coalescence of water droplets. Flocs together with solid particles settle to the tank bottom after mixing. Therefore, the performance of the demulsifier is evaluated by the water and solids content in diluted bitumen during settling. The complete set of experimental data is given in Appendix B.

2.2.1 Campaign 1

The six centre point repeats are shown in Figure 2-5. All six runs show a similar trend of reduction of water content over time and the final water content reaches about 1.4 wt% at the end of the settling. These runs show the repeatability of the experiments and provide an estimate of variability from run to run.
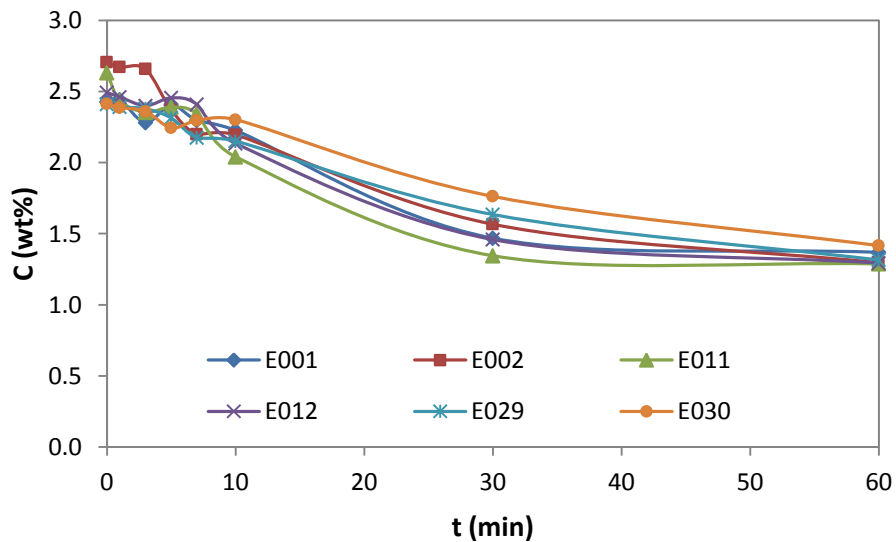
Figure 2-5: Diluted bitumen water content during batch gravity settling, centre point repeats (0,0,0,0)

Figure 2-6 shows all 30 experimental runs as a function of settling time. The initial water content varies from 2.3 to 2.7 wt% while the final water content varies from 0.13 to 1.76 wt%. However, for most of the cases, the final water content is higher than 1 wt% and there is a continuous progression from 1 to 1.8 wt%.
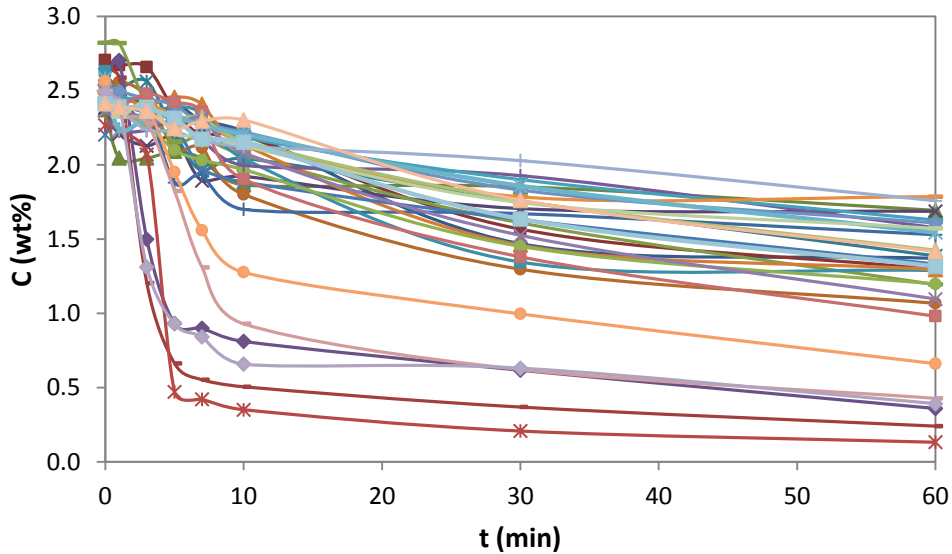
Figure 2-6: Diluted bitumen water content during batch gravity settling for all 30 runs

Figure 2-7 shows all runs with final water content higher than 1.5 wt%, cases where demulsifier does not perform well. The majority of these cases are either with low bulk concentration, 5 ppm, or high injection concentration, 39 wt%. Bulk concentration 5 ppm is too low to meet the product quality, whereas if the injection concentration is too high, the demulsifier is not well dispersed and does not work effectively. If these two unfavourable conditions do not happen, then at least one of the mixing conditions (mixing intensity or mixing time) is unfavorable. This suggests that increasing the demulsifier bulk concentration has a low impact on product quality if the mixing conditions are not properly selected.
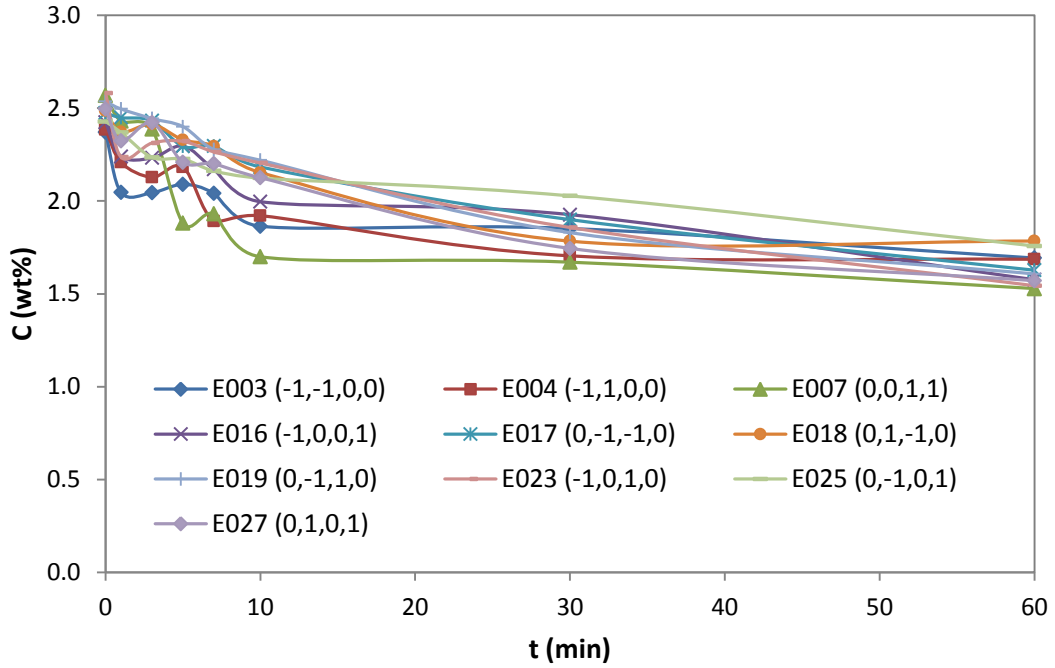
Figure 2-7: Diluted bitumen water content during batch gravity settling, with final water content exceeding 1.5 wt%. Variable order: (X_{BC}, X_ε, X_{tm} and X_{IC})
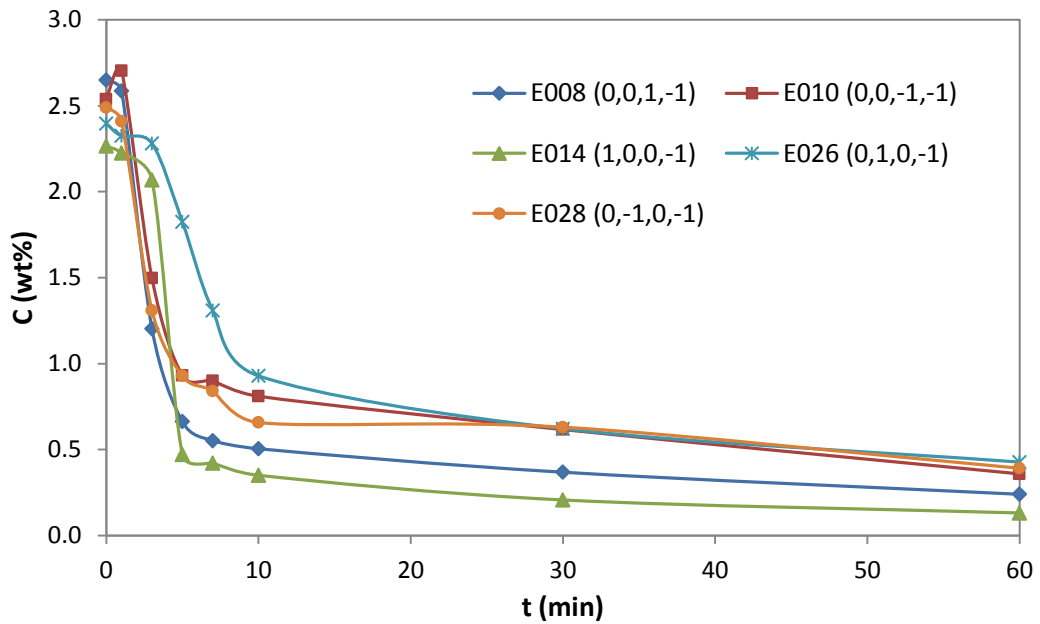
Figure 2-8: Diluted bitumen water content during batch gravity settling with final water content less than 0.5 wt%. Variable order: (X_{BC}, X_ε, X_{tm} and X_{IC})

Figure 2-8 shows the cases where the demulsifier works the best and the final water content falls below 0.5 wt%. The initial settling is fast for all of these cases and water content drops below 1 wt% before 10 minutes of settling. The rapid action of demulsifier to remove water in the first 10 minutes is critical for successful demulsifier application. The short settling duration is also important in real plant operation.

All 5 of these runs are with low injection concentration and a bulk concentration 50 ppm or 95 ppm. Dilution of injection concentration appears to be the key factor in obtaining a low final water content in this experimental design. It can also be observed that a bulk concentration of 50 ppm is high enough to obtain a final water content below 0.5 wt% if the injection concentration is low (3 wt%). Though good performance happens even at low mixing intensity and short mixing time, experiment E010 and E028, this could be due to the high BC used, which outweighs the mixing effect.

Dilution of demulsifier before injection reduces the mixing requirement in CIST and eases the dispersion of demulsifier. Good dispersion enables the demulsifier to reach water droplets faster and improves the performance by promoting more coalescence and flocculation, while poor dispersion creates high local concentration and limits the performance of the demulsifier. The effect of dilution is similar to premixing the chemical additive at the injection point and is therefore considered as a mixing variable.

2.2.1.1 Mixing and Demulsifier Effects on Settling

The density of the data acquired and the multiple factors involved make it difficult to proceed with a visual analysis of the results. The batch gravity settling data was subjected to a 4-factor multiple linear regression analysis at each instant in time using the regression equation:

$$C(t) = \beta_0 + \beta_{BC}x_{BC} + \beta_{\varepsilon}x_{\varepsilon} + \beta_{t_m}x_{t_m} + \beta_{IC}x_{IC} + \beta_{BC*BC}x_{BC}{}^2 + \beta_{\varepsilon\varepsilon}x_{\varepsilon}{}^2$$
$$+ \beta_{t_m t_m}x_{t_m}{}^2 + \beta_{IC*IC}x_{IC}{}^2 + \beta_{BC*\varepsilon}x_{BC}x_{\varepsilon} + \beta_{BC*t_m}x_{BC}x_{t_m}$$
$$+ \beta_{BC*IC}x_{BC}x_{IC} + \beta_{\varepsilon*t_m}x_{\varepsilon}x_{t_m} + \beta_{\varepsilon*IC}x_{\varepsilon}x_{IC} + \beta_{t_m*IC}x_{t_m}x_{IC} \qquad \textbf{2-4}$$

where C(t) is the water content in mass percentage as a function of time. The regression coefficients were calculated using the Data Analysis tool in Microsoft Excel. The effects of the variables from 3 minutes settling onwards are shown in Figures 2-9, 2-10 and 2-11, with confidence intervals of 95 %.
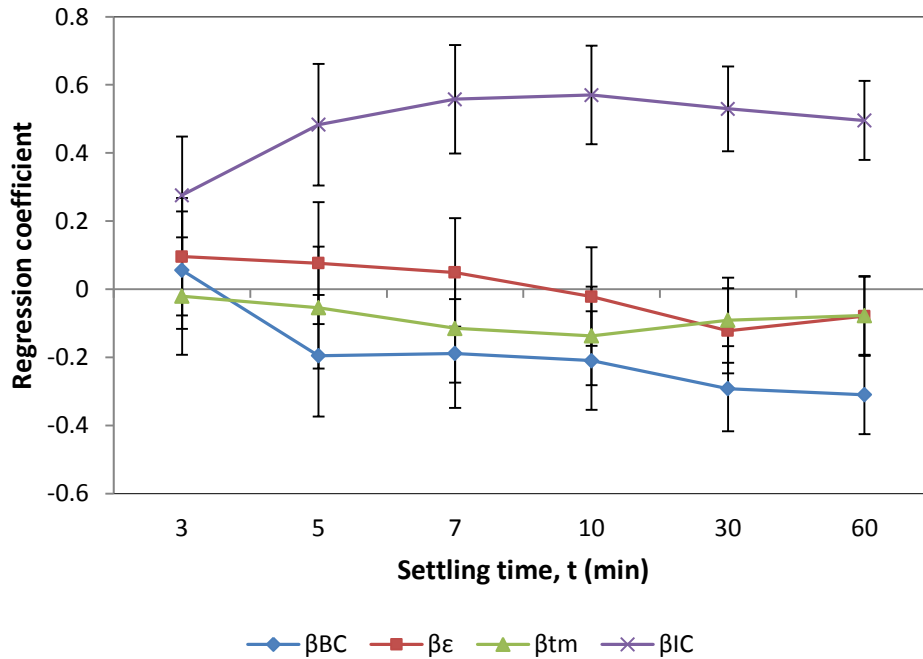
Figure 2-9: Regression coefficients and their confidence intervals for four variable multiple linear regression

As shown in Figure 2-9, injection concentration has the most significant impact on the water reduction throughout the entire settling and the impact is about twice that of the other variables. The bulk concentration does not have a significant effect on the water content at the beginning of settling but the effect gets larger from 5 minutes onwards. However, the significance of bulk concentration is not as high as the injection concentration. For both mixing intensity and mixing time, the effects on water content are relatively small throughout the whole settling process. This may be due to high bulk concentration over-shadowing the mixing effects.

The quadratic effect of all variables is small except for injection concentration, as shown in Figure 2-10. The large negative value of the quadratic effect could indicate that the effect of dilution of injection concentration from 21 to 3 wt% ($x_{IC} = -1$) is much higher than the effect from 39 to 21 wt%. ($x_{IC} = +1$). This provides the range of injection concentration where the demulsifier will perform effectively. As for the interaction effect, interaction between bulk concentration and injection concentration suddenly appears at 5 minutes and continues to be significant until the end of the settling. Interactions between other variables are not significant throughout the whole settling period.

Two different demulsifiers were tested in these experiments and the experiments conducted by Laplante (2011). Both studies have the same experimental set-up and protocol. The only major difference is the bulk concentration used; 5, 50, 95 ppm in this campaign while 2, 26, 50 ppm in Laplante's experiments. Both of the demulsifiers work best with low injection concentration, mid- or high bulk concentration and adequate mixing.
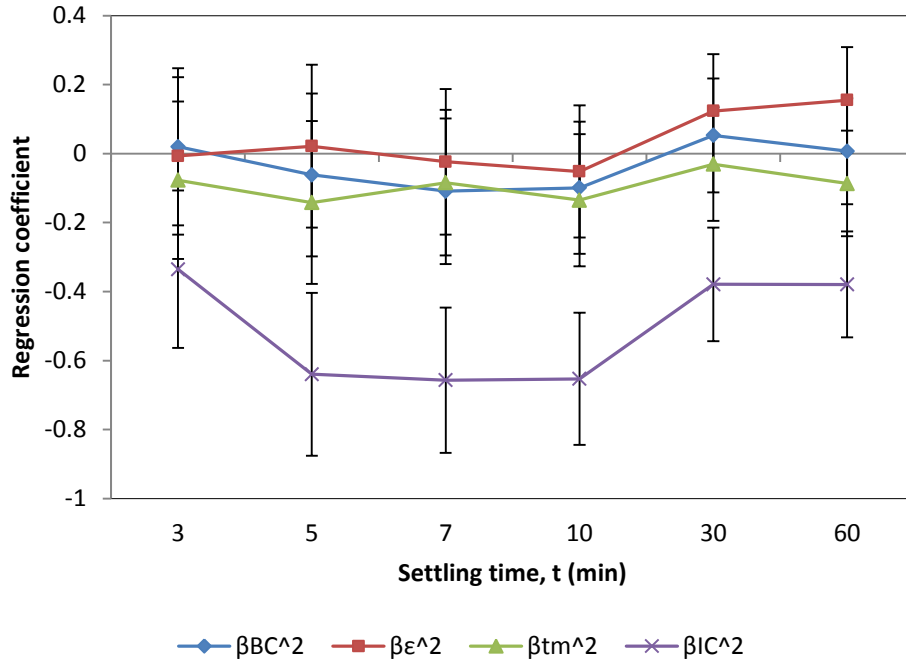
Figure 2-10: Regression coefficients and their confidence intervals for four variable multiple linear regression (quadratic effect)
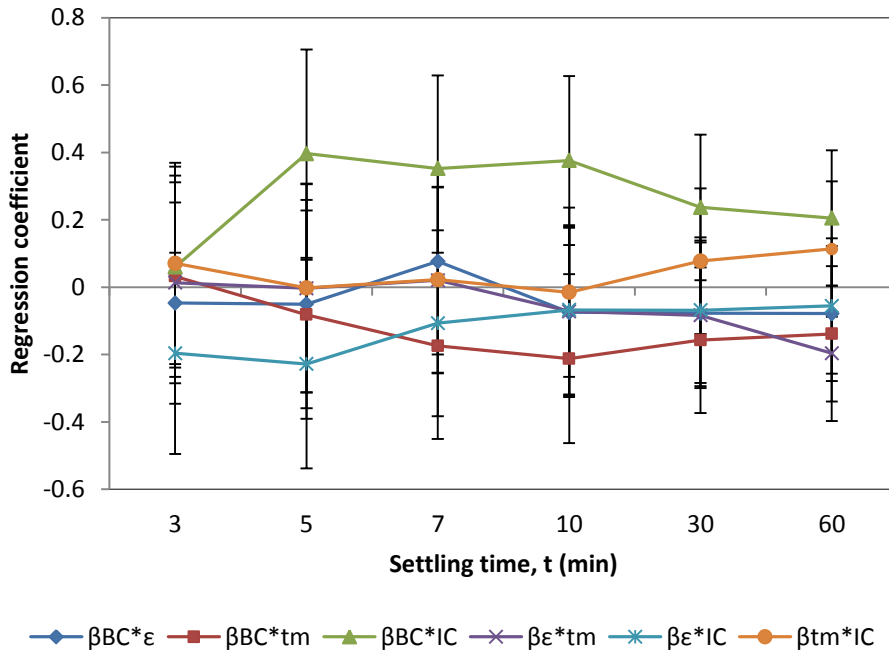
Figure 2-11: Regression coefficients and their confidence intervals for four variable multiple linear regression (interaction effect)

2.2.1.2 Lumped parameter

To see the effect of mixing as a total energy, mixing intensity and mixing time are lumped as a single variable:

$$J = \bar{\varepsilon} * t_m \qquad\qquad \textbf{2-5}$$

where J is proportional to the total energy injected at the impeller volume. The regression equation can then be expressed as:

$$C(t) = \beta_0 + \beta_{BC}x_{BC} + \beta_J x_J + \beta_{IC}x_{IC} + \beta_{BC*BC}x_{BC}{}^2 + \beta_{JJ}x_J{}^2$$

$$+ \beta_{IC*IC}x_{IC}{}^2 + \beta_{BC*J}x_{BC}x_J + \beta_{BC*IC}x_{BC}x_{IC} + \beta_{J*IC}x_J x_{IC} \qquad \textbf{2-6}$$

Similar to the four-variable multiple linear regression, the effect of injection concentration is dominant throughout the whole settling process, as shown in Figure 2-12. The lumped mixing effect is still not significant though it is getting larger from 10 minutes onwards and the combined variable effect, β_J is larger than the individual variable.
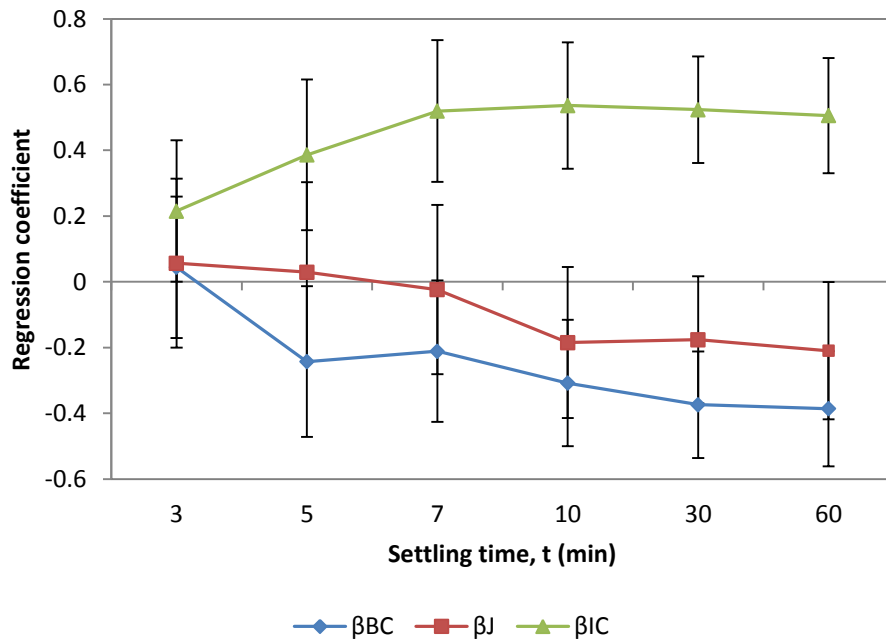
Figure 2-12: Regression coefficients for three variable multiple linear regression
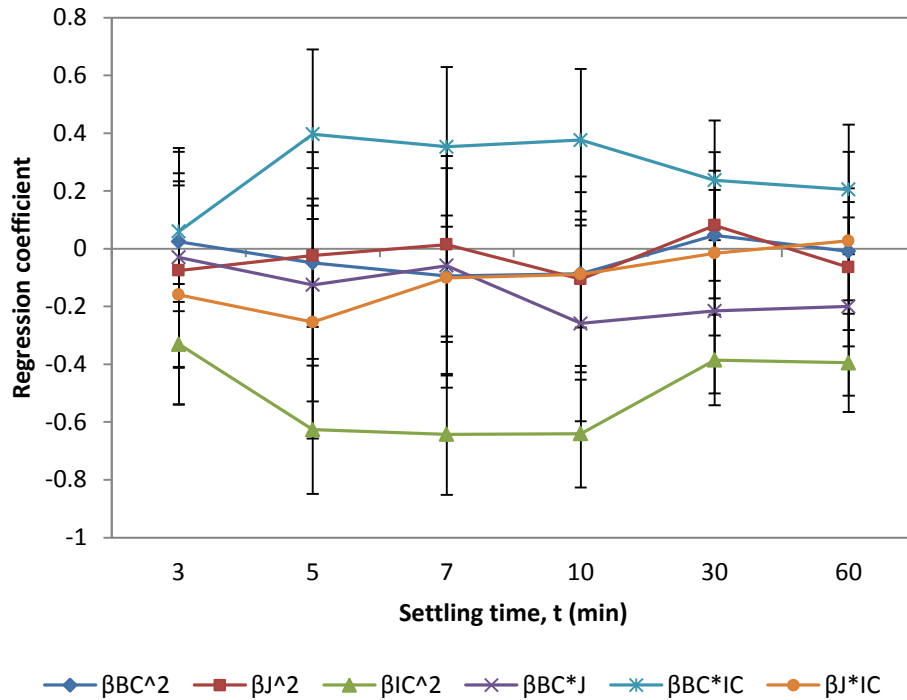
Figure 2-13: Regression coefficients for three variable multiple linear regression

The effects of the variables are still similar after combining mixing time and mixing intensity. Injection concentration has a large quadratic effect on the demulsifier performance. Therefore, mixing energy can be a representative mixing variable used to simplify both mixing tests and scale-up.

2.2.1.3 Vertical Water Profile

As the samples are only taken at the top layer of the CIST, 3.2 cm below the diluted bitumen surface, during the settling, it is important to ensure that the settling along the whole CIST is uniform so that the samples taken are representative. Several sets of experiments were chosen to have a full-profile sampling where an additional 2 samples were taken at $z/H = 0.4$ and 0.8, at 7 and 30 minutes of settling to test the water content in different sections of the CIST.

Table 2-10: Water content of diluted bitumen at different sections of CIST

Time (min)	Height (z/H)	C (wt%)					
		E004 (-1,1,0,0)	E006 (1,1,0,0)	E014 (1,0,0,-1)	E016 (-1,0,0,1)	E022 (1,0,-1,0)	E030 (0,0,0,0)
7	0.15	1.89	2.07	0.42	2.17	2.31	2.30
	0.4	2.04	2.09	0.38	2.47	2.27	2.25
	0.8	1.97	2.13	1.80	2.36	2.23	2.24
30	0.15	1.70	1.30	0.21	1.93	1.52	1.76
	0.4	1.63	1.41	0.24	1.85	1.54	-
	0.8	1.66	1.30	1.26	1.98	1.44	1.70
60	0.15	1.69	1.08	0.13	1.58	1.10	1.42

For almost all of the cases, the water content at the three different sections was similar, which indicates uniform settling. For E014, case where the demulsifier works effectively, the water content at z/H = 0.8 was higher than the other two sections at both 7 and 30 minutes. This is due to good water reduction and settling in the experiment where the water layer started to build up at the bottom of the CIST.

2.2.1.4 Solids Reduction in Clarification Step

The main objective of diluted bitumen clarification is to remove water droplets as well as fine solid particles. Good performance of demulsifier will also lead to effective solids removal. Initial and final solids contents of each experiment were measured through Dean Stark extraction. As shown in Figure 2-14, there is no correlation between water and solids contents in the feed samples used in the

experiments, as they are dependent on the upstream process and the quality of oil sands. The solids content at the top and middle sections of the CIST show a linear relationship with the final water content after 60 minutes of settling, as shown in Figure 2-15 and 2-16. The solids content in these two sections is also directly proportional to each other (Figure 2-17) which confirms the uniformity of settling of solids along the CIST.

Both solids and water settled to the bottom of the CIST but there is no clear correlation between solids at the bottom and the final water content which was measured at the top part of the CIST. However, when the final water content is very low, more solids were found at the bottom of CIST (Figure 2-18). To satisfy the mass balance, the increase of solids content at the bottom will be same as the reduction of solid at the top section of the CIST. Therefore, high solids content at the bottom indicates good settling of solids if the demulsifier works well in the system, when the final water content is low at the top of the CIST.
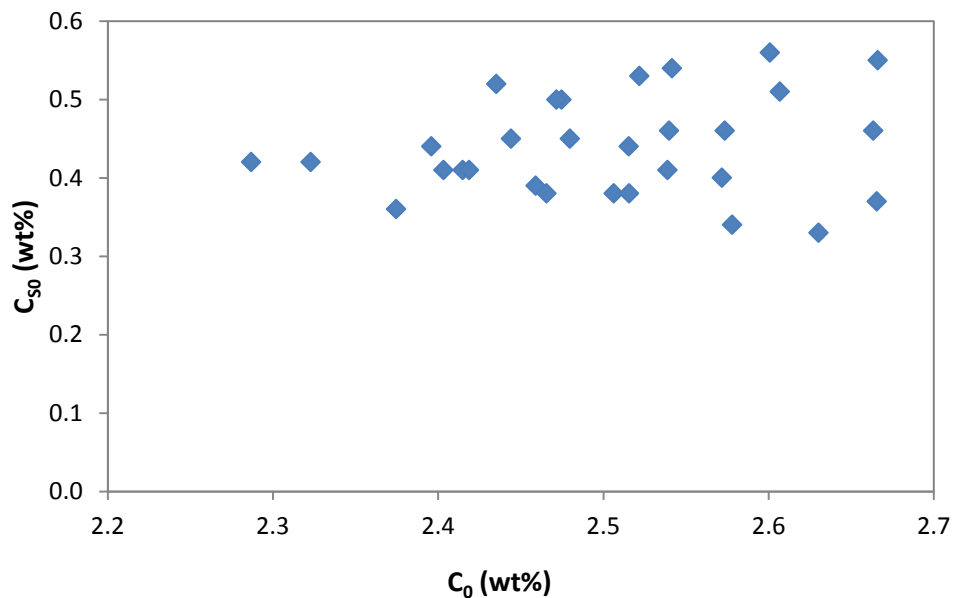
Figure 2-14: Initial solids content, C_{S0} vary from 0.3 - 0.6 wt% while initial water content, C_0 varies from 2.3 - 2.7 wt%
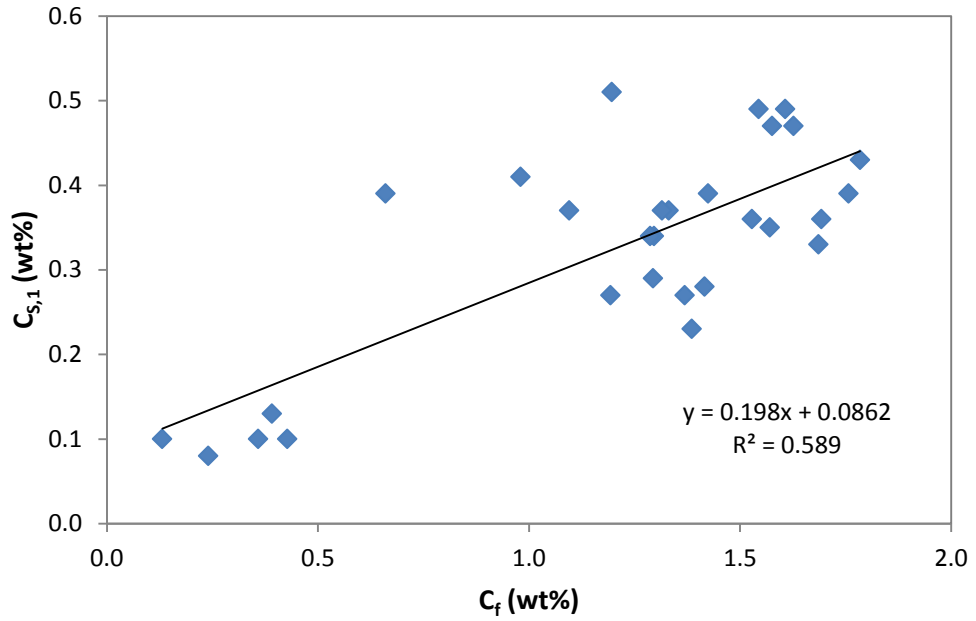
Figure 2-15: Product solids content at the top section of CIST, $C_{S,1}$ as a function of final water content, C_f
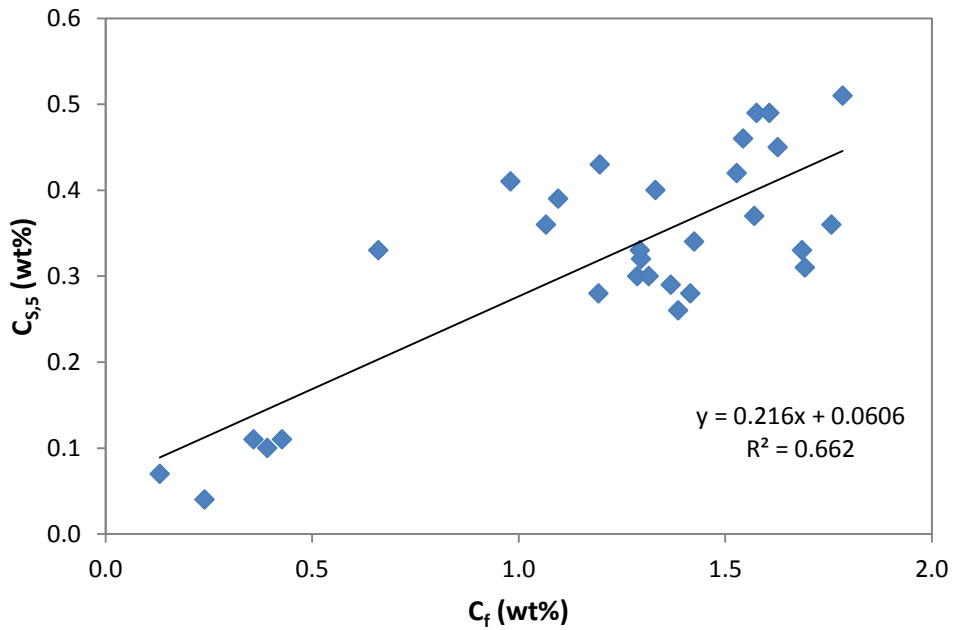
Figure 2-16: Solids content at the middle section of CIST, $C_{S,5}$ as a function of final water content, C_f
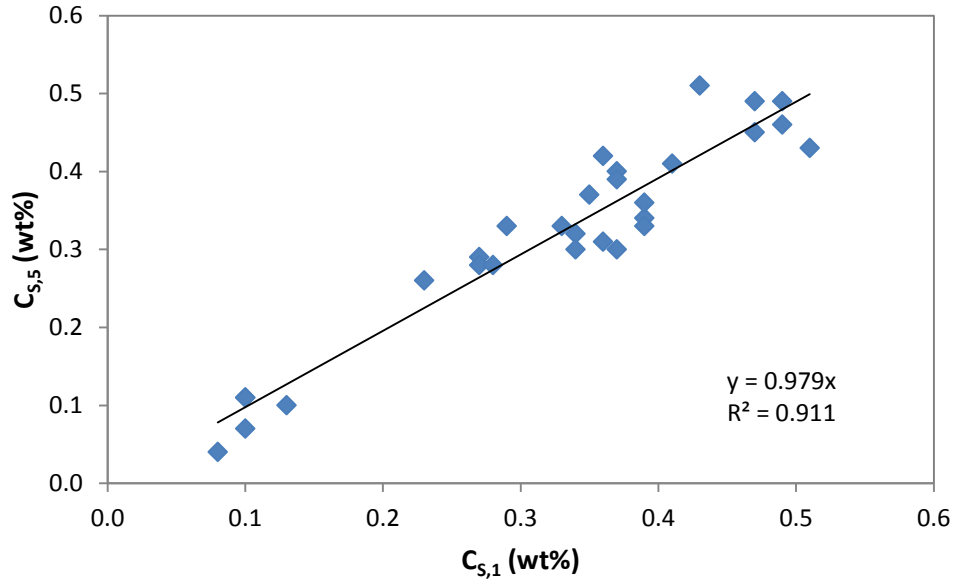
Figure 2-17: Solids content at the top, $C_{S,1}$ and middle, $C_{S,5}$ section of CIST after 60 minutes settling
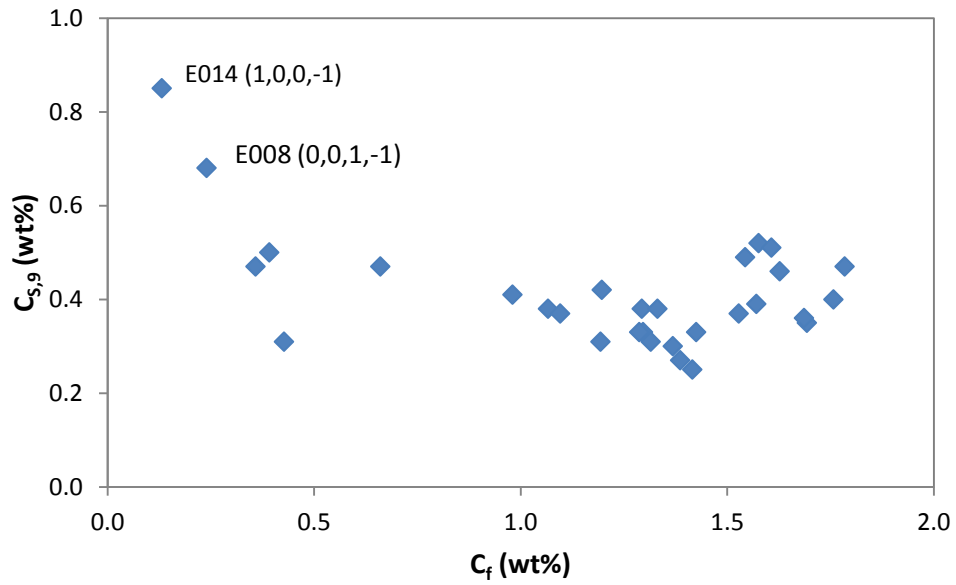
Figure 2-18: Solids content at the bottom section of CIST, $C_{S,9}$ as a function of final water content, C_f

The dewatering of diluted bitumen is normally used as a useful approach to predict the reduction of suspended solids in the diluted bitumen product. However, the reduction of solids content at the top part of the CIST does not show any correlation with the reduction of water content when the reduction of water content is below 1.5 wt%, as shown in Figure 2-19. However, when the reduction of water content is higher than 1.5 wt%, reduction of solids will have the same trend with the reduction of water.
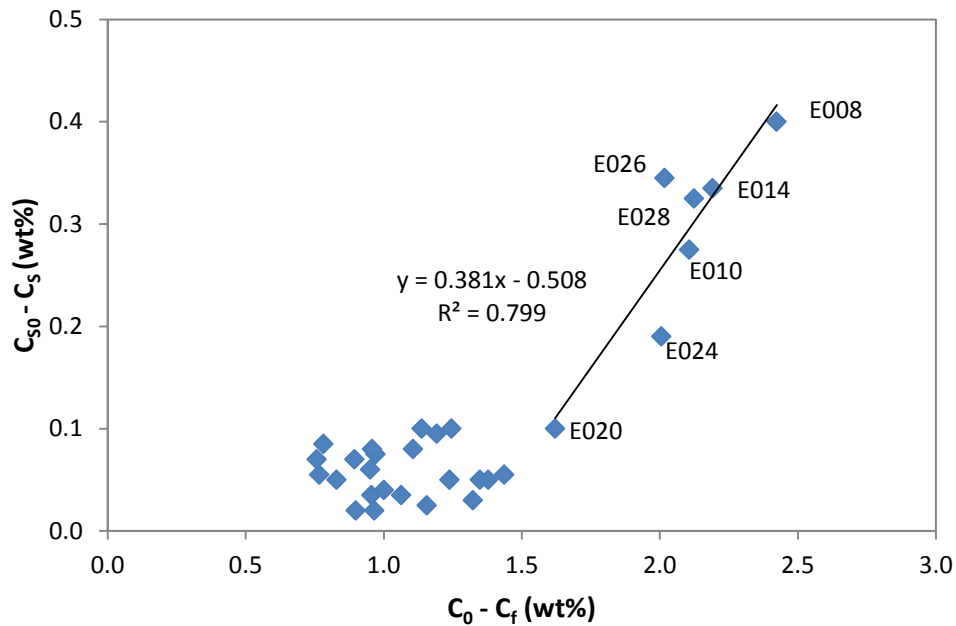
Figure 2-19: Reduction of solids as the function of reduction of water content

The seven points with water reduction, C_0-C_f larger than 1.5% in Figure 2-19, are from experiment E020 (0,1,1,0), E024 (1,0,1,0), E010 (0,0,-1,-1), E026 (0,1,0,-1), E028 (0,-1,0,-1), E014 (1,0,0,-1) and E008 (0,0,1,-1). Dilution of injection concentration, which has the largest effect on the water reduction, also results in high reduction of solids, C_{S0}-C_S. It can be deduced from the two separate groups of data that the reduction of solids requires better performance of demulsifier. This also indicates that the majority of solids are removed with the water.

46

The reduction of solids at the top and middle part of the CIST can be due to the nature of settling. To study the effect of demulsifier on solids reduction, the average solids content at the top and middle part of the CIST after settling are plotted as the function of the initial solids content. For most of the cases, the final solids content shows a linear relationship with the initial solids content. For cases where the final solids content deviates from the linear relationship, the final water contents are much lower as well, generally below 0.5 wt% (E010, E014, E028, E026, E008 and E024). Therefore, demulsifier will only work well on solids in the conditions where it works exceptionally on water; otherwise, the settling of solids will be strongly affected by the initial solids content. Even when the demulsifier works effectively, the solids content can only be reduced to about 0.1 wt%. The remaining solids may be oil wet solids which are difficult to remove using the demulsifier.
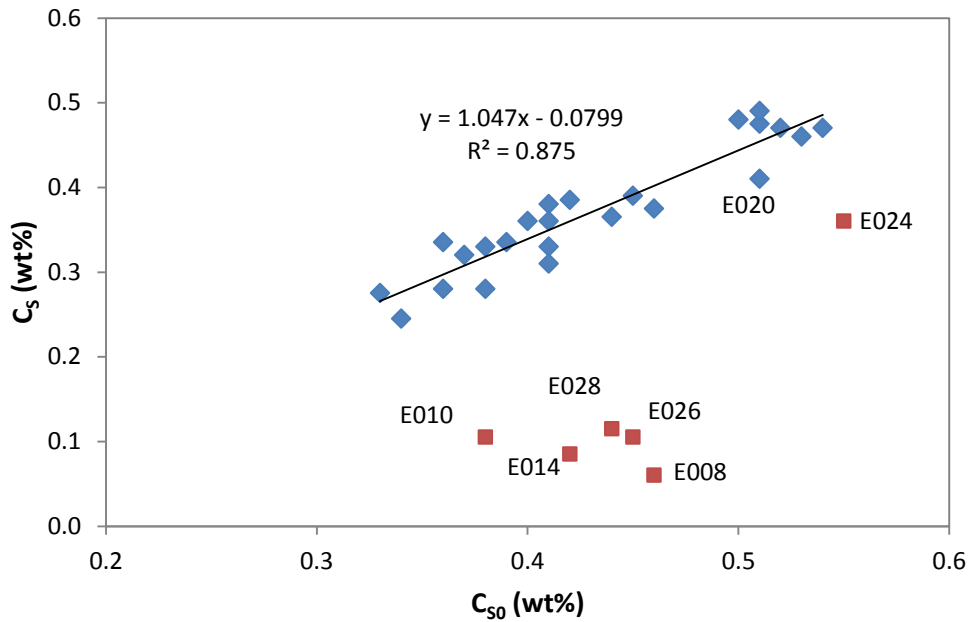
Figure 2-20: Average final solids content as the function of initial solids content (top and middle part of the CIST)

The relationship between the final water content and the initial solids content is also investigated. The final water content has a weak linear relationship with the initial solids content if the demulsifier does not perform well. This might suggest that solids in the sample will hinder the settling of water if the demulsifier does not work well.
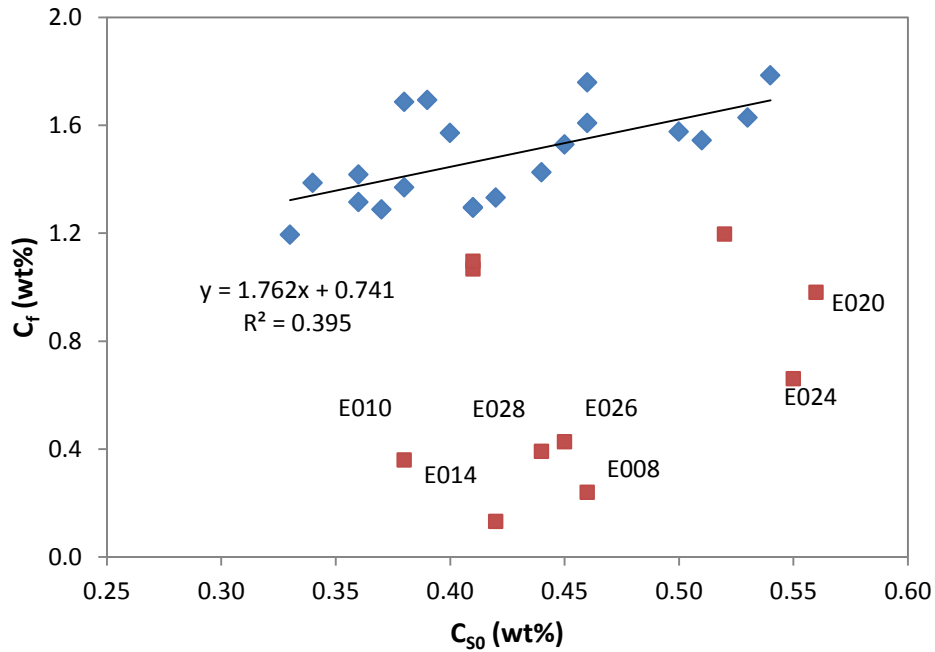
Figure 2-21: Final water content as the function of initial solids content

A 4-factor multiple linear regression analysis is used to observe the effects of each variable on solids removal.

$$C_s = \beta_0 + \beta_{BC}x_{BC} + \beta_\varepsilon x_\varepsilon + \beta_t x_t + \beta_{IC}x_{IC} + \beta_{BC*BC}x_{BC}{}^2 + \beta_{\varepsilon\varepsilon}x_\varepsilon{}^2$$
$$+ \beta_{tt}x_t{}^2 + \beta_{IC*IC}x_{IC}{}^2 + \beta_{BC*\varepsilon}x_{BC}x_\varepsilon + \beta_{BC*t}x_{BC}x_t + \beta_{BC*IC}x_{BC}x_{IC}$$
$$+ \beta_{\varepsilon*t}x_\varepsilon x_t + \beta_{\varepsilon*IC}x_\varepsilon x_{IC} + \beta_{t*IC}x_t x_{IC} \qquad \textbf{2-7}$$

where C_s is the solids content in mass percentage at the top section of CIST at the end of the settling.

From the multiple linear regression (Figure 2-22), it is shown that injection concentration is the dominant factor affecting the demulsifier performance in reducing the solids content. The large quadratic effect of injection concentration is also observed for solids reduction. Dilution of injection concentration improves the reduction of both water and solids content, and the approach of predicting the reduction of solids with the reduction of water content is practically reasonable.
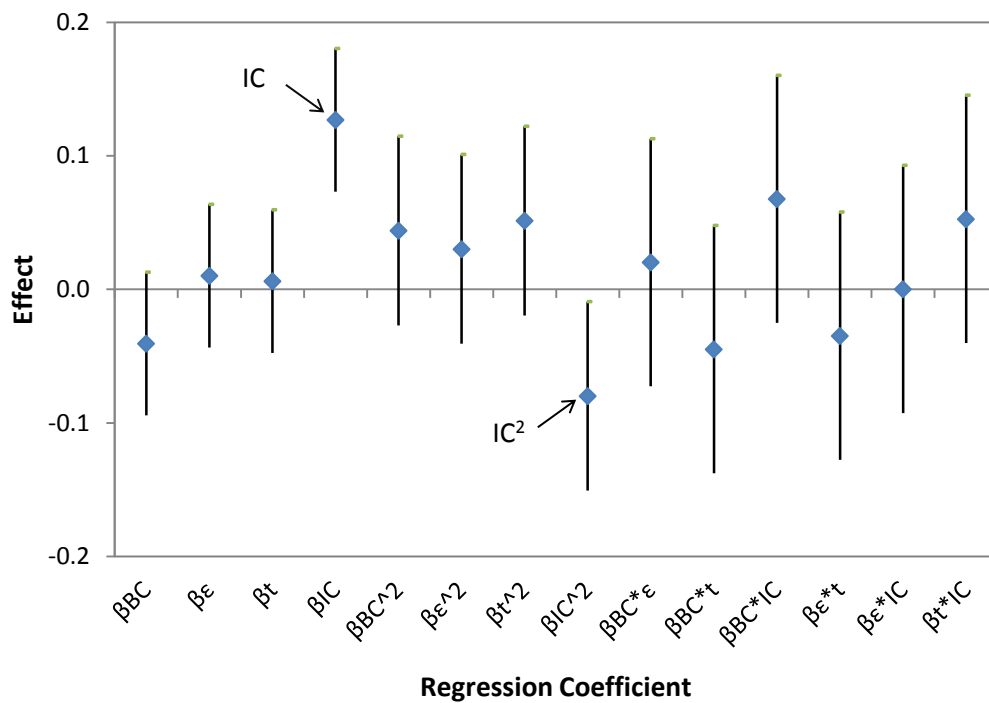
Figure 2-22: Regression coefficients and their confidence intervals for four-variable multiple regression on solids content at the top section of CIST

2.2.2 Campaign 2

In Campaign 1, injection concentration had the greatest impact on the performance of demulsifier. Mixing intensity and mixing time did not appear to have significant effects and this could be due to the high bulk concentration used and the injection concentration range tested. As mixing has strong interactions with other variables, a good experimental design is required to study the mixing effect.

In the first campaign, the final water content dropped below 0.5 wt% even at BC 50 ppm (experiment E008, E010, E026 and E028) if the injection concentration was sufficiently low. A decrease of injection concentration from 39 to 21 wt% only slightly improved the demulsifier performance compared to dilution from 21 to 3 wt%. Therefore, in campaign 2, the high range of BC (+) was set at 50 ppm and IC below 21 wt% was used to study the significance of mixing.

2.2.2.1 Mixing and Demulsifier Effects on Settling

A different set of diluted bitumen samples was used in the second campaign and the initial water content of the feed diluted bitumen was lower, varying from 1.0 to 1.4 wt% compared to 2.4 to 2.7 wt% in the previous campaign. The final water content still dropped below 0.5 wt% although the bulk concentration used was only 50 ppm. Due to the large difference in initial water content among samples, normalized water content was plotted against settling time in Figure 2-24 in order to have a more representative analysis.
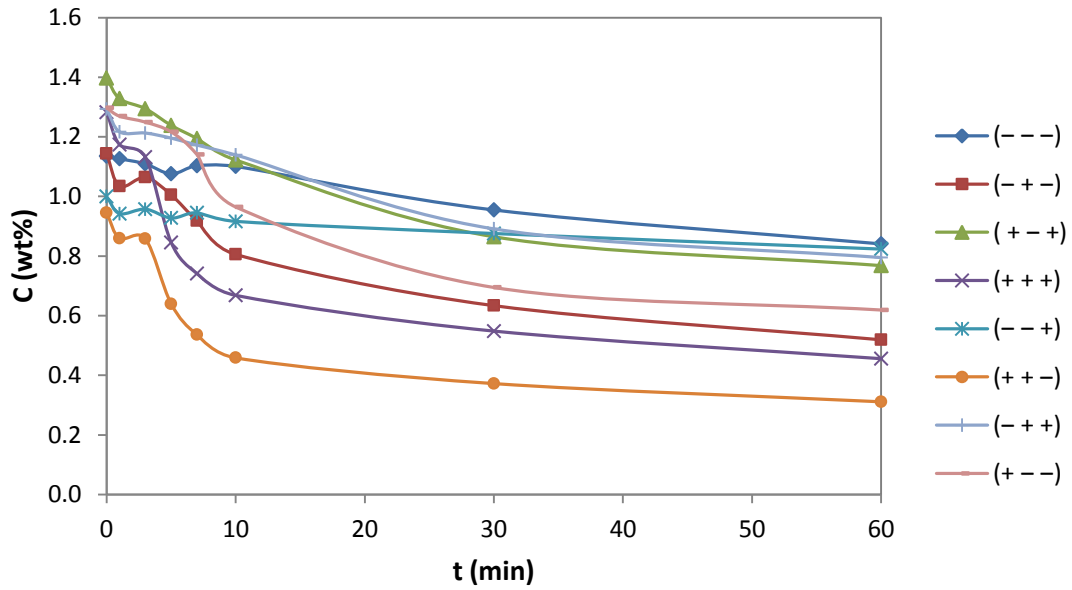
Figure 2-23: Diluted bitumen water content during batch gravity settling.
Variable order: (X_{BC}, X_J, and X_{IC})
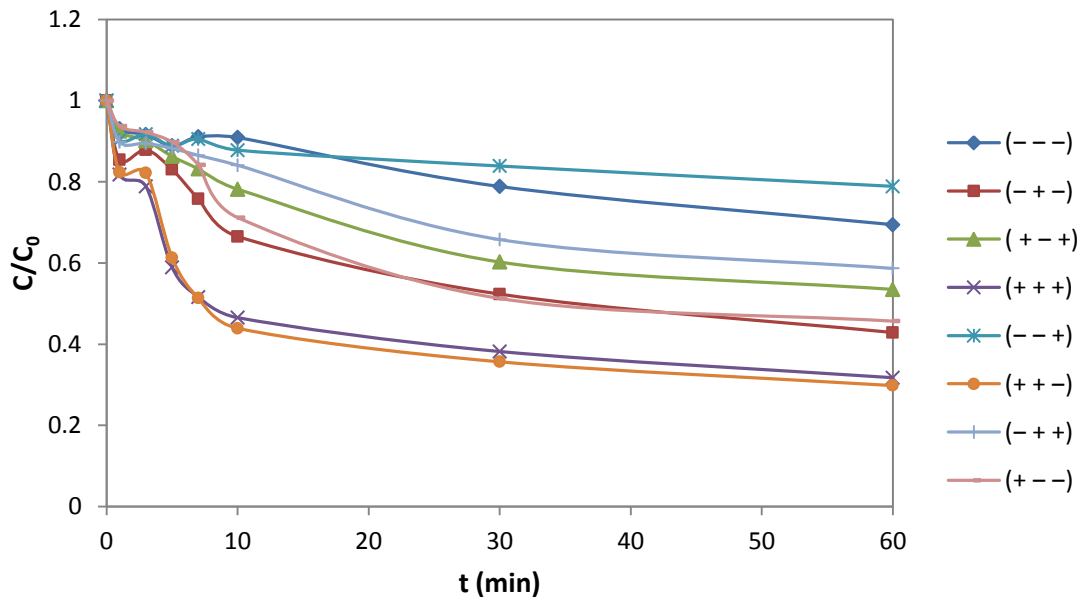
Figure 2-24: Normalized diluted bitumen water content during batch gravity settling. Variable order: (X_{BC}, X_J, and X_{IC})

From both absolute and normalized plots, the ideal conditions to determine low final water content are high bulk concentration, high mixing energy and low injection concentration. However, the normalized water content in experiment (+ + +) was almost as low as the water content in experiment (+ + −), although a slightly higher injection concentration of 12 wt% was used. This in fact shows that dilution of the injection concentration does not have a strong effect on the demulsifier performance if the injection concentration is 12 wt% or lower. The higher workable injection concentration is particularly important to injection volume, injection time, and the control of mesomixing at the injection point. It potentially eases the injection in real operation with a lower injection volume required.

When mixing is insufficient or when bulk concentration is low, but the other conditions are favorable, experiment (+ − −) and (− + −), the final water contents were higher than the ideal case (+ + −). This shows the importance of bulk concentration and mixing in this experimental range. Besides, these two cases had similar water contents at the end of settling. Therefore, low bulk concentration can be compensated by high mixing energy and a lower bulk concentration can be used if mixing conditions are favorable.

From the results in Campaign 1, experiments with low bulk concentration, low mixing energy and high injection concentration will have poor demulsifier performance. The results obtained in the second campaign are consistent with that conclusion as experiment (− − +) has the highest water content at the end of settling. Changing one of these 3 variables to a favorable condition improves the demulsifier performance.
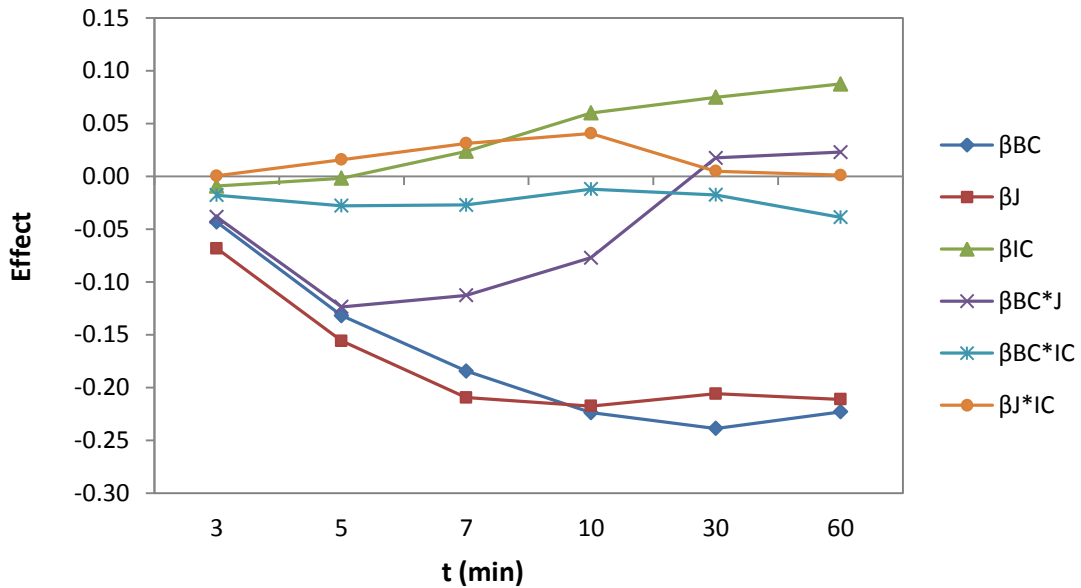
Figure 2-25: Effects of the variables at different time of settling

From the effect analysis of the factorial design, the same observation is seen; injection concentration does not a have large effect in the testing range from 3-12 wt%. This does not mean the injection concentration is unimportant but indicates both 3 wt% and 12 wt% are sufficiently low for good demulsifier performance. Mixing energy and bulk concentration have more significant effects on the performance of demulsifier throughout the whole settling process especially from 5 minutes onwards.

By combining this result with the previous campaign, dilution of injection concentration has a significant effect on the demulsifier performance and the demulsifier works better when injection concentration is below 21 wt% and performs excellently when it is 12 wt% or lower. Mixing effects become more significant when the demulsifier bulk concentration is reduced and can be an important variable to manipulate in reducing demulsifier use.

2.2.2.2 Mixing Effects on Solids Settling

The initial solid contents of the samples used in this experimental campaign are lower, ranging from 0.34 to 0.44 wt%. At the end of the settling, solids contents at the top and middle section of the CIST show a linear relationship with the final water content, as shown in Figure 2-26 and 2-27. The same trend in these two sections confirms the uniformity of the solids settling along the CIST. Solids are reduced to below 0.2 wt% when the demulsifier performs effectively. In experiment D06 (+ + −) and D04 (+ + +), the performance of demulsifier is good with high mixing energy, high bulk concentration and sufficiently low injection concentration. The effectiveness of demulsifier is also reflected from the solids content.
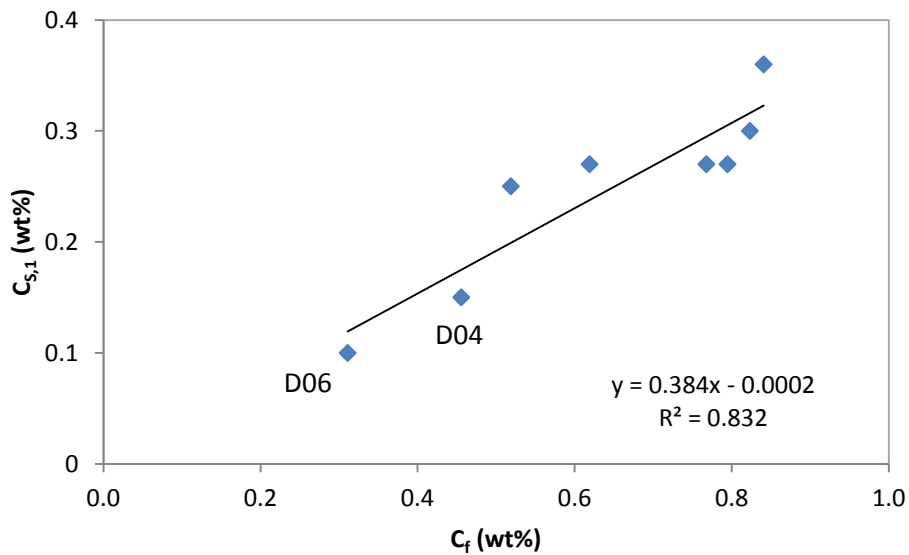
Figure 2-26: Product solids content at the top section of CIST, $C_{S,1}$ as a function of final water content, C_f
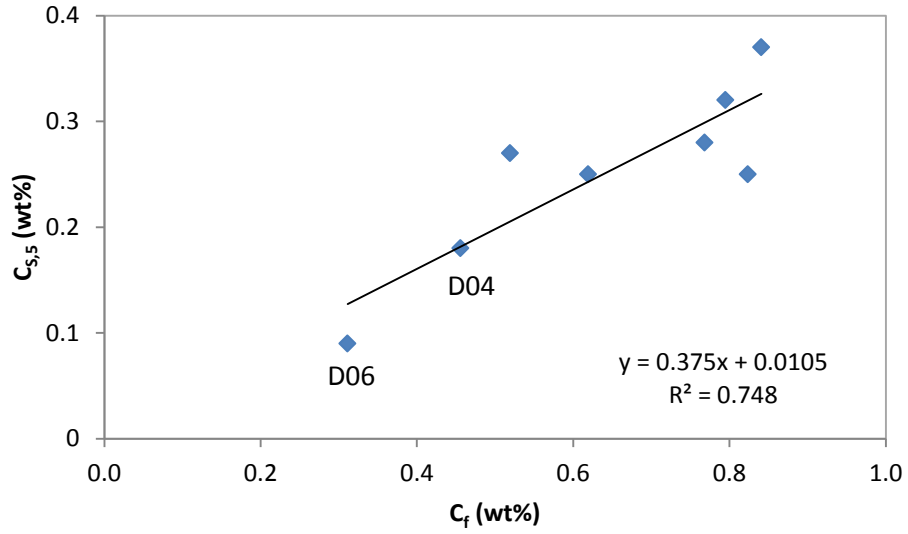
Figure 2-27: Solids content at the middle section of CIST, $C_{S,5}$ as a function of final water content, C_f
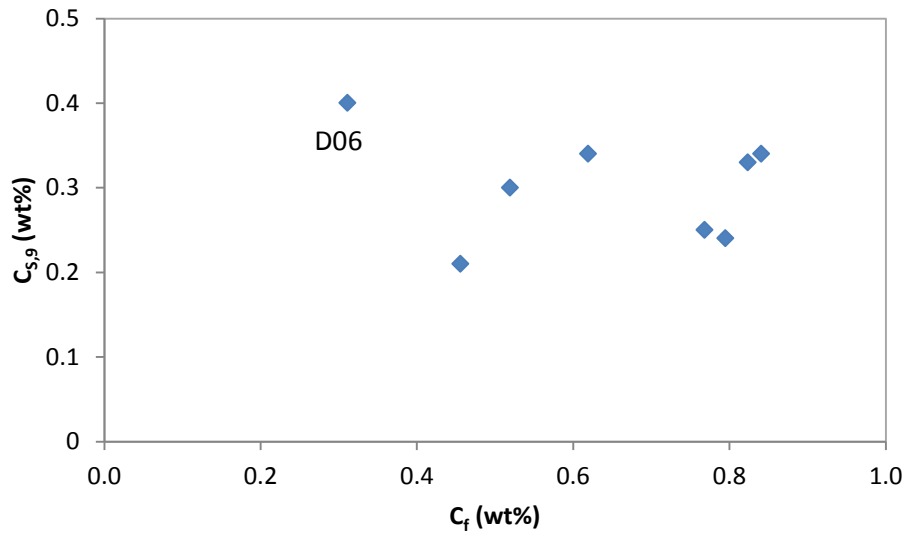
Figure 2-28: Solids content at the bottom section of CIST, $C_{S,9}$ as a function of final water content, C_f

At the end of settling, solids accumulate at the bottom of the CIST. The solids content at the bottom of the CIST does not show a clear relationship with the final water content which is measured at the top section, Figure 2-28. However, D06 has the highest solids content at the bottom section compared to other runs due to good settling resulted from good demulsifier performance.
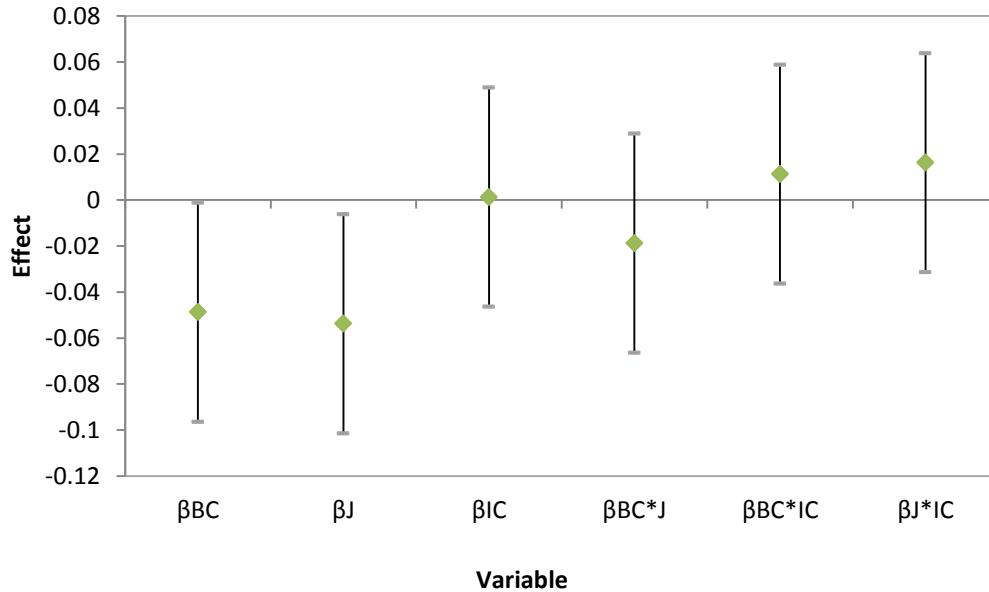
Figure 2-29: Effect of variables on solids content at the top section of CIST

Both bulk concentration and mixing energy have significant effects on the solids reduction. The effects are similar to the results obtained in water removal. Good performance of demulsifier which yields low water content will also improve solids removal. Water wetted solid particles form flocs with water droplets when demulsifier is added. Big flocs formed will then settle to the bottom of CIST and may sweep other solid particles during the settling. Therefore, the mixing strategies which improve the dewatering process can also be applied in solids removal.

2.2.3 Initial Settling and Demulsifier Performance

The initial settling of water droplets is critical to have an effective water removal. Figure 2-30 shows two typical cases of good and bad settling of water droplets. In almost all cases, the initial settling rate is constant in the first 10 minutes. However, in cases where demulsifier has a very good performance, the initial settling rate is faster, and lasts for 5 to 7 minutes. The initial settling rate, Ri of each of the experiments was calculated by linear regression at the first 10 minutes, or from 0 to 5 or 7 minutes if the initial settling rate changes before 10 minutes. The initial settling rate is compared with the final water content and the results are shown in Figure 2-31 and 2-32 for Campaign 1 and 2, respectively.
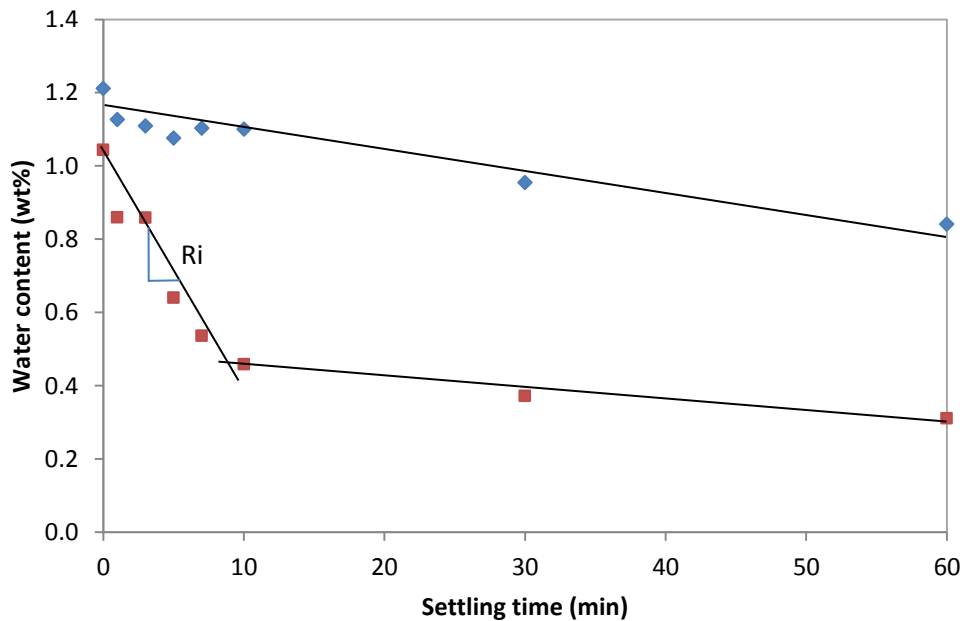
Figure 2-30: Typical settling curves of experiment with good (red) and poor (blue) water removal. Ri is the initial settling rate calculated from linear regression
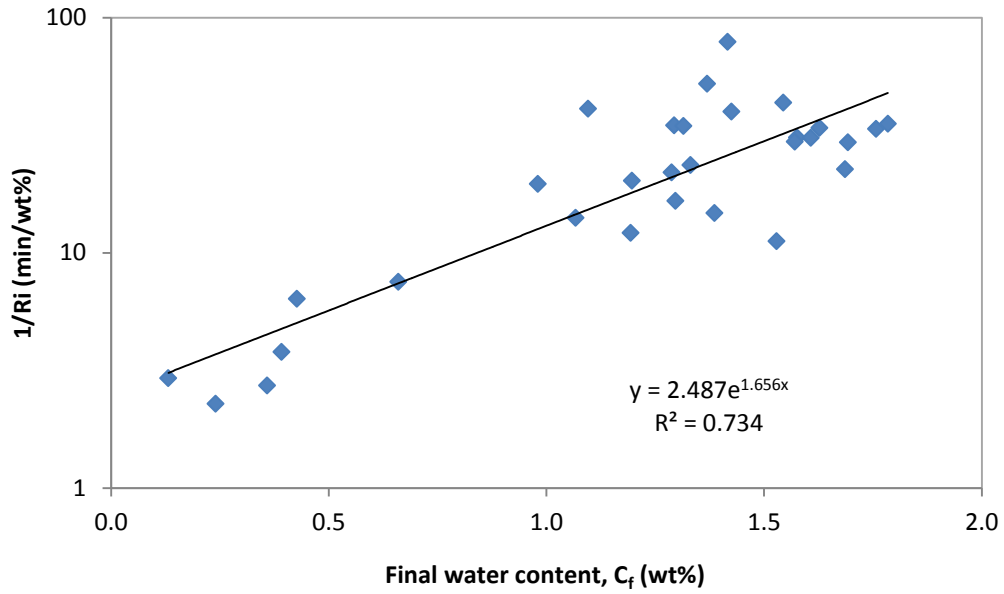
Figure 2-31: Initial settling rate as a function of final water content (Campaign 1)
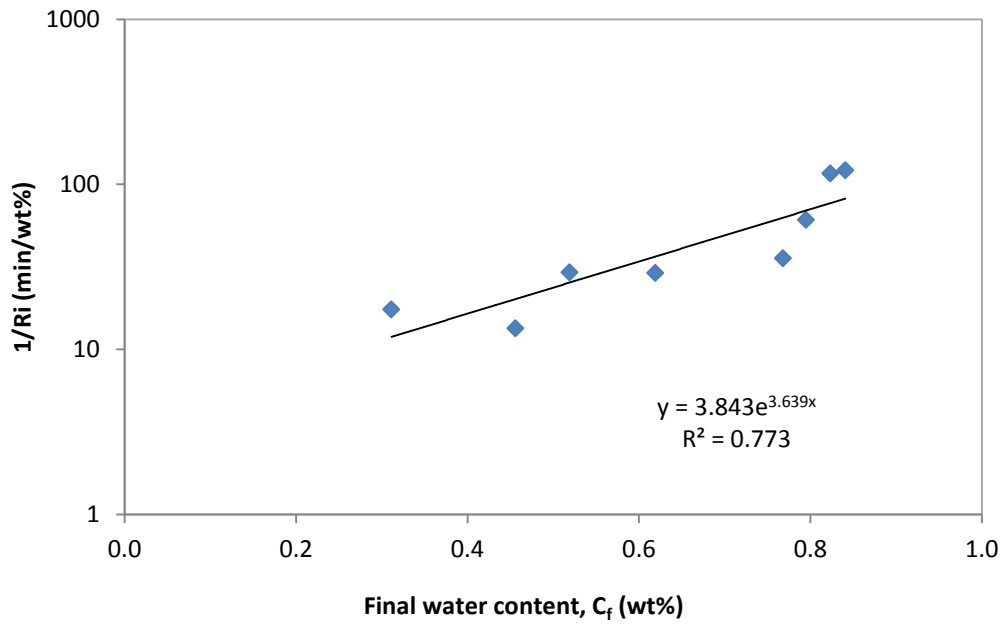
Figure 2-32: Initial settling rate as a function of final water content (Campaign 2)

Final water content has an exponential relationship with the initial settling rate. The initial settling is fast for a good water removal. Fast settling can only be achieved if the water droplets are bigger or if big flocs are formed. Therefore, the final water content will be lower only when the demulsifier works effectively to enhance the coalescence and flocculation of water droplets.

In a study conducted by Czarnecki et al., it was observed that low density fluffy flocs formed at high flocculant concentration due to rapid flocculation (2007). At lower concentration, the droplets and particles will move within the forming structure, and form denser flocs with neighbouring droplets and particles. Therefore, a high injection concentration which can cause high local concentration may promote less dense flocs and results in low initial settling rate. By having low injection concentration and better mixing, water droplets will form denser flocs. Mixing also promotes movement of water droplets and increases the collision frequency among water droplets, which is expected to result in the formation of denser flocs.

2.3 Conclusions

In the first campaign, the dilution of injection concentration overwhelmed all other variables. This result reinforces the importance of dilution of demulsifier at the injection point. Injection concentration is also considered to be an important mixing variable as the demulsifier is premixed before injection. Bulk concentration has a significant effect on demulsifier performance but does not dominate the performance. The results also illustrate the range of workable injection concentrations for the tested demulsifier which allowed a more focused experimental design in the second campaign to observe the effects of mixing.

The second campaign was reduced to a smaller set of experiments to test the performance of demulsifier at a lower bulk concentration and to further study mixing effects. Mixing appears to be important in conditions where injection concentration is low and bulk concentration is near the minimum requirement. The demulsifier works well for both injection concentrations 3 wt% and 12 wt%, which gives more flexibility in the real operation. It was also found that mixing energy and bulk concentration are equally important and the decrease of bulk concentration can be overcome by having better mixing.

In conclusion, low injection concentration, sufficient chemical dosage and adequate mixing are the three key strategies to have good chemical additive performance in a complex fluid system.

Chapter 3: Evaluation of Mixing Effects at a Very High Demulsifier Bulk Concentration

Demulsifier bulk concentration and mixing conditions are equally important especially at the minimum demulsifier dosage as shown in Chapter 2. Bulk concentration is often used to control the performance of demulsifier in situation where mixing is not fully understood. In general, the performance of demulsifier improves with an increase in demulsifier bulk concentration up to a certain limit. Demulsifier can reach surface saturation and past this point, further addition of demulsifier does not improve performance. A drop in demulsifier performance at a very high bulk concentration is observed in many demulsifier tests (Xu et al. 2005; Dimitrov 2012) and is commonly described as an overdosing effect. However, there is a limited understanding of the overdosing phenomenon.

As demulsifiers are a type of surfactant, the characteristics and performance of the demulsifier may be adverse when the concentration is too high. In Gao's (2010) study, the crumpling ratio of a water droplet becomes large at a very high demulsifier concentration. The high ratio indicates a more rigid water droplet surface which results in low coalescence probability. Re-emulsification is also possible due to excess demulsifier adsorption when the concentration is too high. In a plant operation, the overdosing of demulsifier can cause upset of a process and problems in downstream. Poor treatment of product, dirty water and interface pad build-up are all symptoms of overdosing of demulsifier (Stewart et al. 2009).

Overdosing of chemical additive is not only observed in processes involving water-in-oil emulsion. It has also been reported in water treatment where flocculent is added. Overdosing of flocculent reduces the aggregation of colloidal solids and affects the separation process (Christensen et al. 1993). The question is whether overdosing is solely a chemistry interfacial problem, or whether it can

be due to the dispersion mixing and high local concentrations, especially when chemical additive is added to a complex multiphase system.

The flocculation mechanisms in water-in-oil emulsions and water treatment can be different but it is also possible that the adverse results are due to high local concentration during the addition of chemical additives. The injection volume becomes larger at high chemical dosage, which will subsequently make the dispersion of chemical additive difficult and may lead to meso-mixing limitation and plume formation. In this part of the study, the objective is to determine if overdosing is still observed with sufficient mixing, and with predilution of demulsifier.

3.1 Experimental Setup

The experimental setup to study the overdosing effect is same as the setup in the previous campaigns in Chapter 2. Diluted bitumen from froth treatment as provided by Syncrude Research was used as the feed. At the beginning of the experiment, diluted bitumen was heated and premixed at a high energy dissipation level to ensure the feed sample was homogeneous. Diluted bitumen was then transferred to the CISTs for demulsifier dispersion. The specified amount of demulsifier was injected using an appropriately sized syringe or a 1/8" tubing connected to a syringe pump. After mixing, the diluted bitumen was allowed to settle for 60 minutes in the CIST.

During the dispersion of demulsifier, samples were obtained 60 seconds after demulsifier injection and 30 seconds before the end of mixing by sampling the bulk mixtures 3.2 cm below the liquid surface using 0.25" ID polyethylene tubing attached to an auto-pipette. These samples were used for water content determination and microscope analysis. During settling, samples were taken at the same position below liquid surface at 1, 3, 5, 7, 10, 30 and 60 minutes. Microscope images of samples were obtained after 1, 3, 5, 7, 10 and 30 minutes of settling. At the end of the 60 minutes of settling, 100 mL samples were obtained for O/W/S analysis at heights $z/H = 0.1$, 0.5 and 0.9.

The performance of the demulsifier was evaluated by water and solids content during the batch settling. The water content was measured by Karl Fischer titration and the solids content was obtained from the O/W/S analysis. Microscope images were also taken to observe the behavior of water droplets at a very high demulsifier dosage.

3.1.1 Experimental Design

In previous experiments, it was shown that a demulsifier bulk concentration (BC) of 50 ppm is sufficiently high for good separation of water droplets. In this overdosing study (Campaign 3), a BC of 300 ppm was used in the experiments. This value is 6 times the concentration used in Campaign 2, and is much higher than the normal operating concentration. As shown in Chapter 2, total mixing energy can be used to test the effect of mixing. Only two variables, mixing energy and injection concentration were varied in this study.

Table 3-1: Variables of 2-level factorial design

Variable	−	+
Mixing Energy, J (W)	Low*	High**
Injection Concentration, IC (wt%)	12	39

* Low   : $\varepsilon = 1$ W/kg, $t_m = 2$ min

** High   : $\varepsilon = 40$ W/kg, $t_m = 10$ min

Bulk concentration = 300 ppm

Table 3-2: 2-level factorial design

Run	J	IC
1	−	−
2	−	+
3	+	−
4	+	+

3.2   Results and Discussion

The water contents of diluted bitumen during settling are shown in Figure 3-1. As the initial water contents of the samples were very different, ranging from 1.21 to 1.45 wt%, the normalized water contents were plotted in Figure 3-2 to prove a more representative analysis.

When the mixing conditions are unfavorable, low mixing energy and high injection concentration, (− +), the water content is still high after 60 minutes of settling. Less than 20 % of the initial water content was reduced by the end of settling. The final water content was also higher than all the experiments conducted in the first and second campaign, based on the normalized value. This phenomenon can be caused by bad mixing, high injection concentration or overdosing problems.

By changing one of the mixing variables to a favorable condition, for case (− −) and (+ +), the performance of the demulsifier was considerably improved. It can also be observed that the effect of mixing was greater compared to the dilution of injection concentration at a BC = 300 ppm. The final water content in experiment (+ +), 0.52 wt%, was lower than in experiment (− −), 0.77 wt%.

The final water content dropped to 0.21 wt% at high mixing energy and low injection concentration. This again demonstrates the importance of both mixing energy and injection concentration in demulsifier dispersion. The results are compared with experiments from the previous campaign in Figure 3-3. For the same mixing energy and injection concentration, the final water content continues to drop when the bulk concentration is increased to 300 ppm. This suggests that demulsifier is still functioning well even at a very high bulk concentration, with no appearance of overdosing phenomenon, if the mixing and injection concentration are favorable.
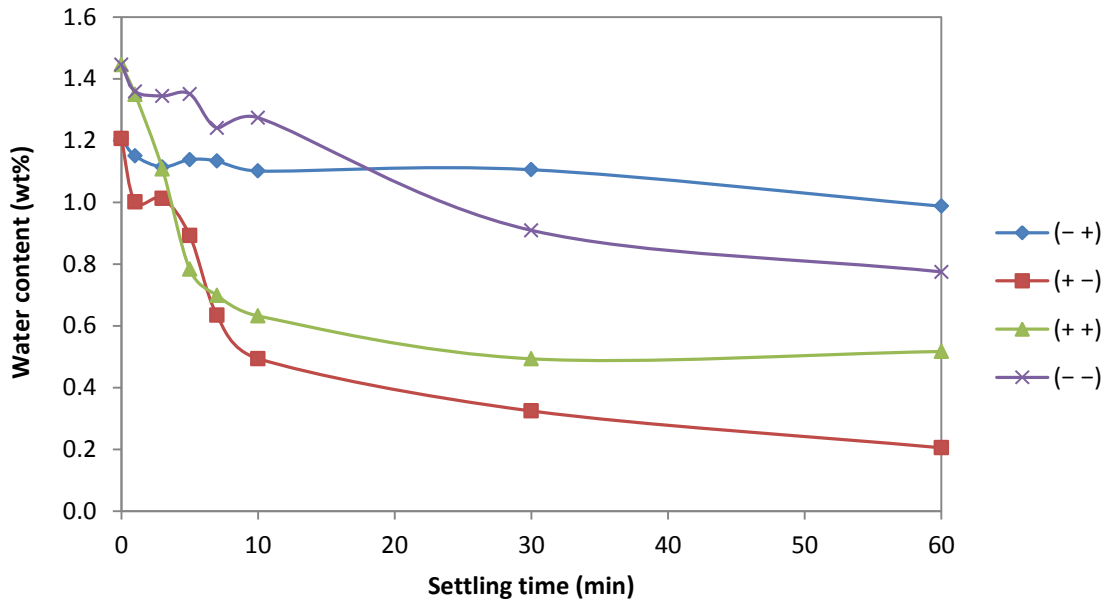
Figure 3-1: Diluted bitumen water content during batch gravity settling at BC = 300 ppm. Variable order: (X_J, X_{IC})
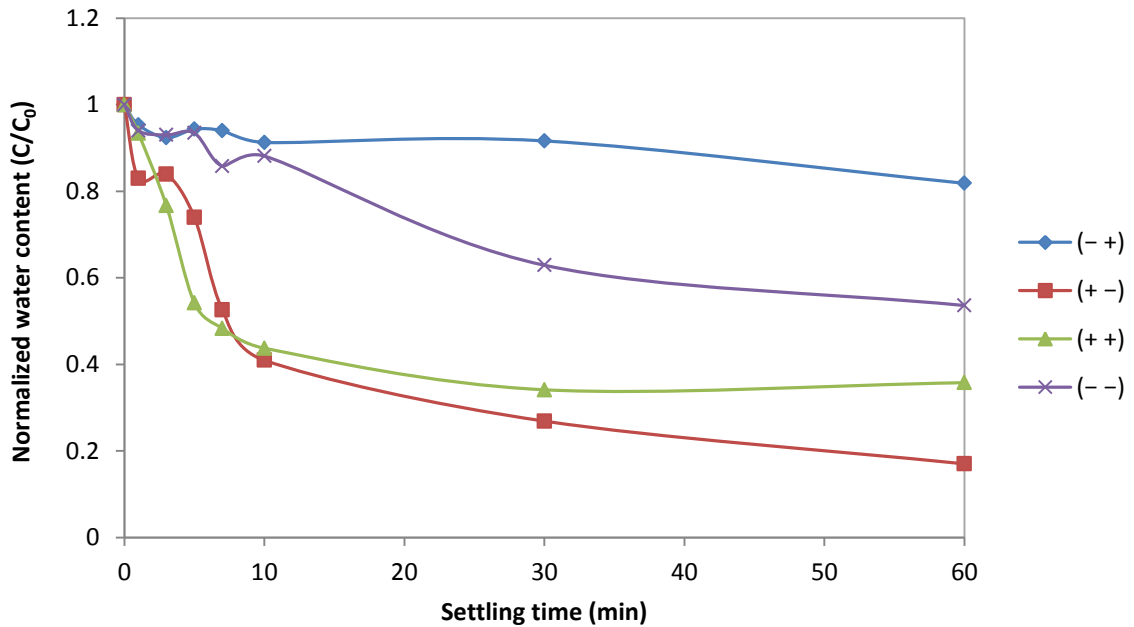
Figure 3-2: Normalized diluted bitumen water content during batch gravity settling at BC = 300 ppm. Variable order: (X_J, X_{IC})
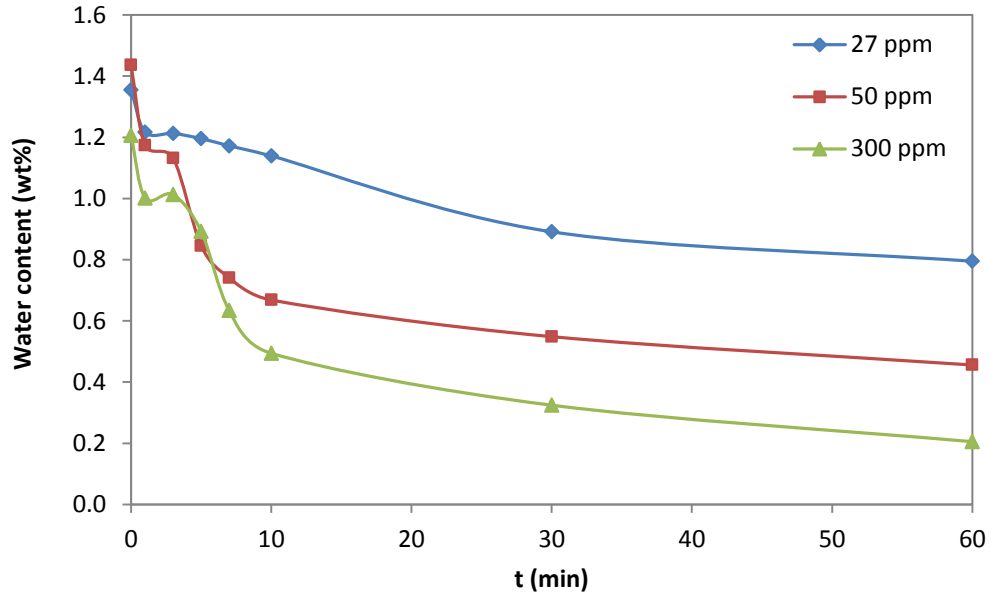
Figure 3-3: Diluted bitumen water content during batch gravity settling for different bulk concentration at high mixing energy. X_J = High (ε = 40 W/kg, t_m = 10 min), X_{IC} = 12 wt%
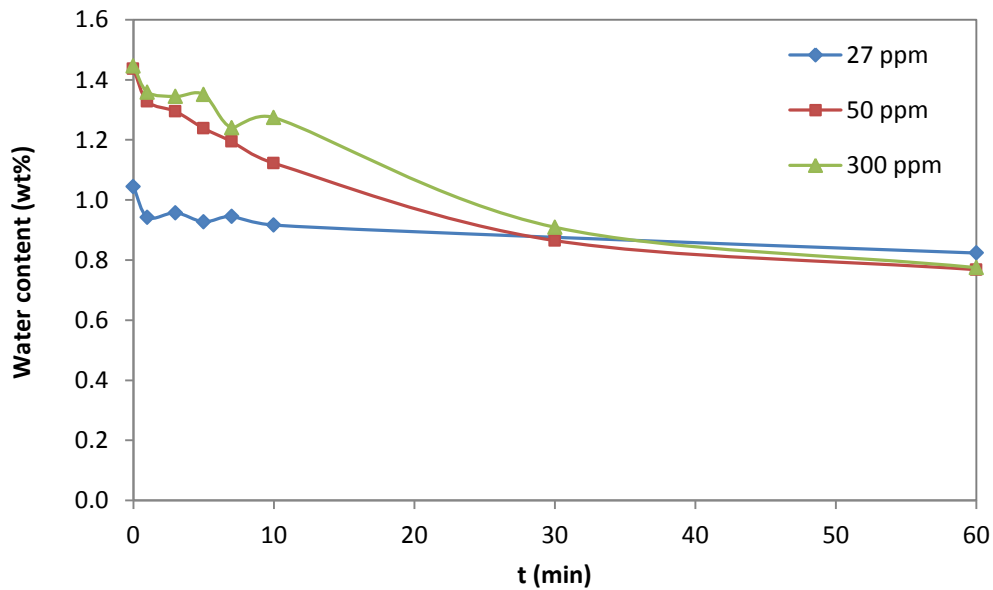
Figure 3-4: Diluted bitumen water content during batch gravity settling for different bulk concentration at low mixing condition. X_J = Low (ε = 1 W/kg, t_m = 2 min), X_{IC} = 12 wt%

However, an increase in bulk concentration does not improve the performance of the demulsifier if the mixing energy is not favorable even if the injection concentration was low, as shown in Figure 3-4. Low injection concentration alone is not sufficient to ensure good demulsifier dispersion at a very high bulk concentration of 300 ppm.

Diluted bitumen samples were also observed using a microscope to study the behavior of water droplets when the demulsifier dosage was very high. Figure 3-5 top is the micrograph from experiment (+ −) and bottom is from experiment (− −) after 30 minutes of settling. For (− −), abundant tiny water droplets are formed and spread evenly when mixing is insufficient at a very high bulk concentration. These stabilized discrete water droplets are not observed when mixing is sufficient at high concentration (300 ppm), or in all of the experiments involving lower bulk concentration in the previous campaigns. The high final water content in experiment (− +) at bulk concentration 300 ppm is due to the formation of these water droplets that are difficult to settle and separate. The formation of tiny water droplets at high dosage which do not separate is commonly described as overdosing effect.

This phenomenon occurs in experiment (− +), (− −) and (+ +) where either one or both of the mixing conditions are unfavorable. The tiny water droplets were not observed in experiment (+ −) and the final water content was also the lowest among all the runs. Therefore, the overdosing problem can be overcome with good mixing and good demulsifier dispersion. The overdosing problem might be more accurately described as undermixing.
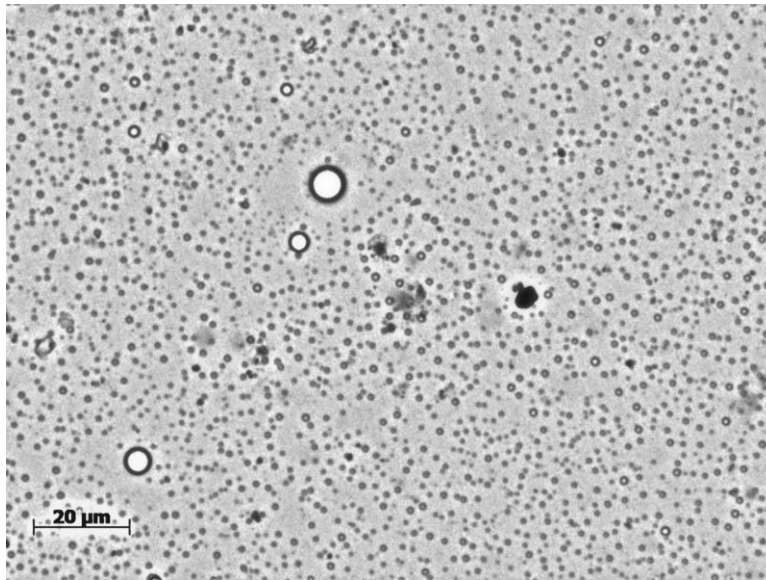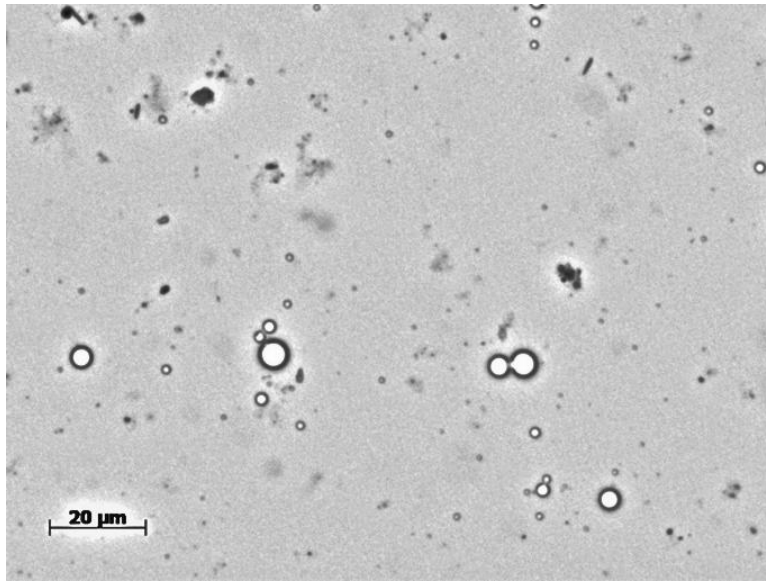
Figure 3-5: Micrographs after 30 minutes of settling for BC = 300 ppm. Top: (+ −); Bottom: (− −). Variable order: (X_J, X_{IC}). Pictures taken by Shaun Leo with a Zeiss Axio Scope A1 Light Transmission Microscope and a Zeiss Axio Cam ICc 1 (1.4-megapixel CCD camera)
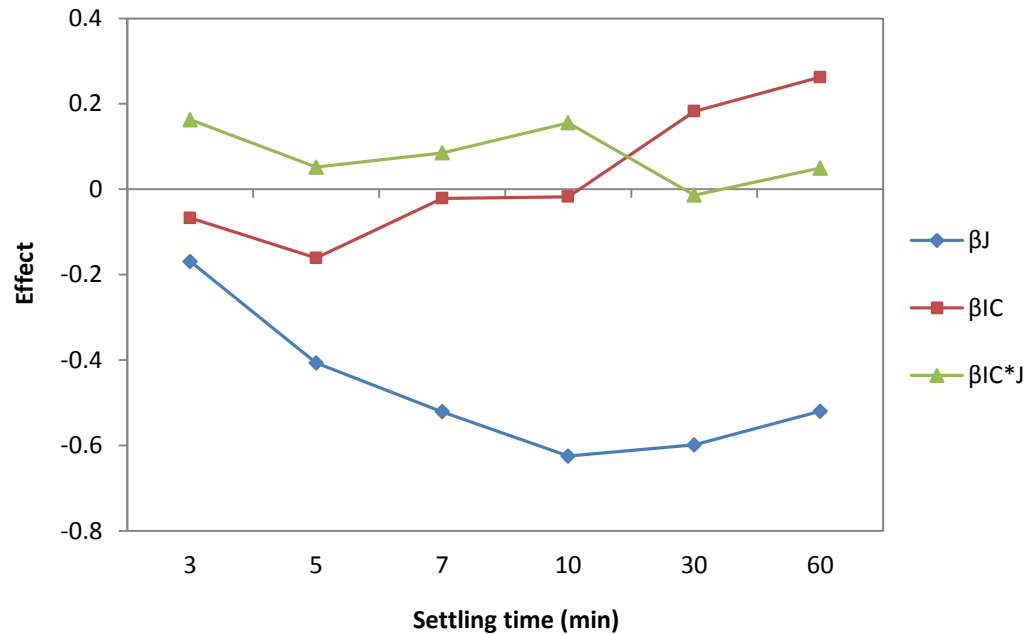
Figure 3-6: Effects of the variables at different time of settling for BC = 300 ppm

The effect analysis of the factorial design in Figure 3-6 shows that mixing is the key variable affecting the performance of demulsifier when the bulk concentration is very high (300 ppm). The effect of mixing is large throughout the settling. Injection concentration does not show a significant impact on the water content at this bulk concentration, although the effect is slightly higher at the end of the settling.

The best result in the overdosing condition is when mixing is good and injection concentration is dilute. When one of the mixing variables is unfavorable, the final water content is higher and stabilized tiny water droplets are observed. At extremely high chemical dosage, all mixing variables need to be optimum in order to avoid a highly stabilized condition.

3.2.1 Undermixing and emulsification

Overdosing phenomena does not occur at a bulk concentration of 300 ppm if the mixing of demulsifier is sufficient. However, undesired emulsification happens when the system is under-mixed. The formation of stable fine water droplets may not be due to high average bulk concentration but could be caused by high local concentration resulting from bad mixing.

Overdosing is potentially harmful to a process as demulsifier will self-associate and form micelles if the concentration is higher than the critical micelle concentration (CMC). However, there is no evidence of micelle formation in this work and the CMC of the demulsifier used is unknown. 300 ppm may not be considered overdosing in average but it may cause micelle problem if the concentration is too high locally.

High local concentration will also the change surface properties of water droplets which causes coalescence problem. In Gao's (2010) study, it is found that there is an optimum demulsifier concentration for water droplets to coalesce. The probability of water coalescence is almost zero if the concentration is too high due to the change of surface properties. The presence of high local concentrations is the most probable reason for low coalescence and poor separation of water droplets.

During demulsification, demulsifier is first adsorbed on water droplets surface before forming flocs. When the local concentration is too high, excessive adsorption will occur and the surface of water droplets will be saturated with demulsifier. Steric repulsion among water droplets will cause coalescence and flocculation difficult to occur. Therefore, water droplets are observed to form distinct water droplets and difficult to settle. Besides, the adsorption step is relatively irreversible (Gregory and Barany 2011). High concentration at the beginning of dispersion cannot be improved at a later stage of the process.

3.2.2 Solids Settling at High Demulsifier Bulk Concentration

The initial solids contents in the samples in this experimental campaign ranged from 0.39 to 0.44 wt%. At the end of settling, solids contents at the top and middle section of CIST show a linear relationship with the final water content, as shown in Figure 3-7. The trends in these two sections are similar which confirm the uniformity of solids settling along the CIST.
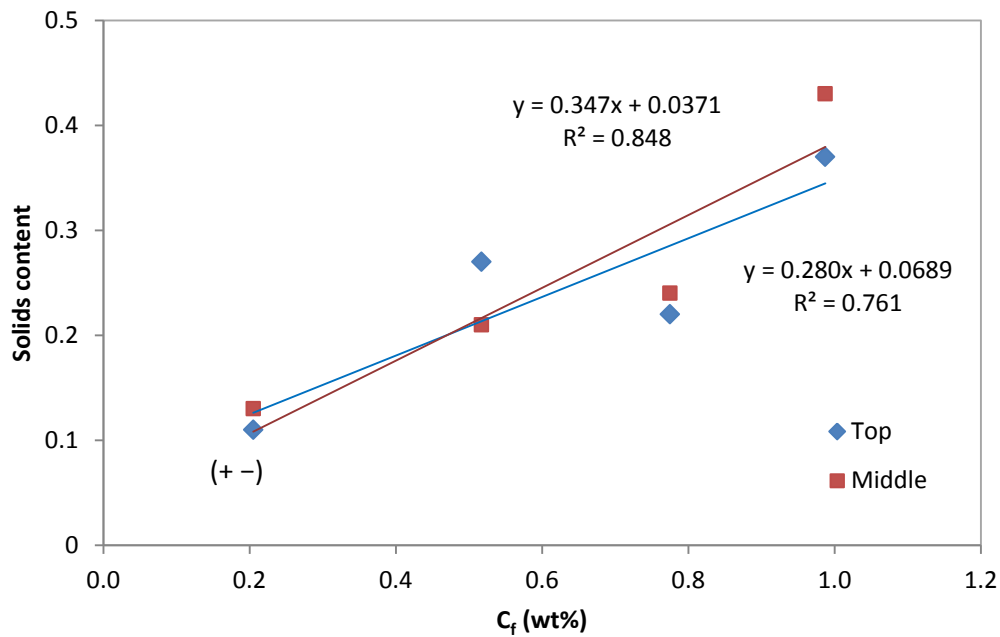
Figure 3-7: Solids content at the top and middle section of CIST as a function of final water content, C_f

Solids removal was effective when the mixing energy was high and the injection concentration was low, (+ −). Solids product dropped to 0.11 wt% from an initial concentration of 0.39 wt% at the end of settling. Solids removal is effective under conditions where the demulsifier has good performance and the result is similar to observations in the previous campaigns in Chapter 2.

However, the product solids content when BC = 300 ppm is similar to the experiment when BC = 50 ppm was used, approximately 0.1 wt% at the end of

settling. The large increase in bulk concentration does not further remove the fine solids. The remaining solids may be oil wetted and cannot be removed together with water droplets easily. This also indicates that another solids removal method is necessary if a lower solids content is desired.

When the mixing condition was the worst case, low mixing energy and high injection concentration, the solids removal was minimal. In experiment (− +), the final solids contents at the top and middle of CIST were 0.37 and 0.43 wt% respectively, where the initial solids content was 0.37 wt%. The high demulsifier bulk concentration may also stabilize the fine solids and minimize the formation of flocs when mixing is insufficient. The lack of big floc formation has also reduced the sweeping of fines to remove solids during settling.

Solids contents at the bottom of CIST do not have a linear relationship with the final water content which is measured at the top section of CIST, Figure 3-8. Since solids accumulate at the bottom of CIST during settling, a good solid removal will cause high solids content at the bottom. In experiment (+ −), solids contents at the top and middle section of CIST were low and therefore solids content at the bottom was high 1.34 wt%.

The linear relationships between solids and water contents at the top and middle section of CIST show that most of the solids are removed together with water droplets. The water content at the bottom of CIST was also measured and the relationship between water and solids contents at the bottom of the CIST is shown in Figure 3-9. Solids content has a linear relationship with water contents which supports the hypothesis that most solids are removed together with water droplets. Therefore, strategies to improve removal of water droplets will work reasonably well for reducing solids content as well.
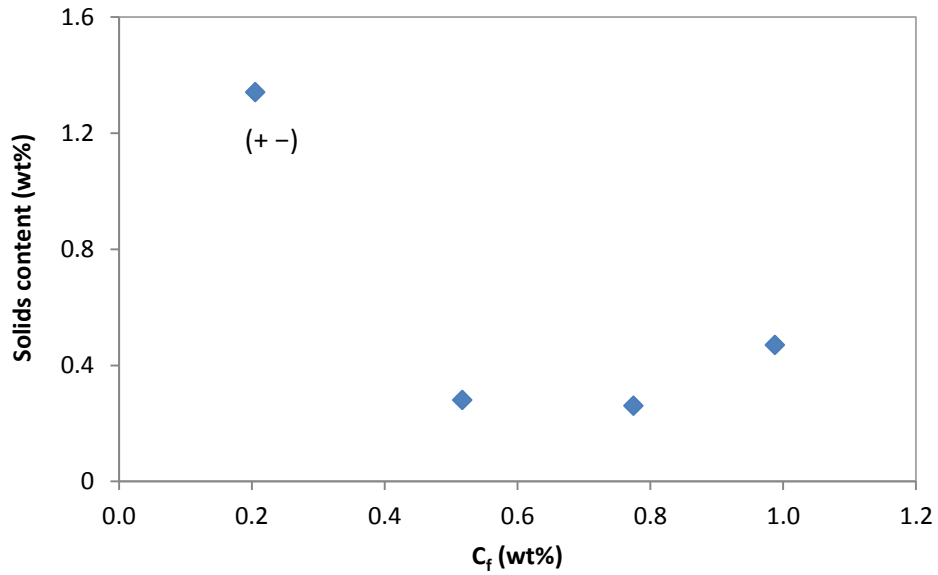
Figure 3-8: Solids content at the bottom section of CIST as a function of final water content, C_f
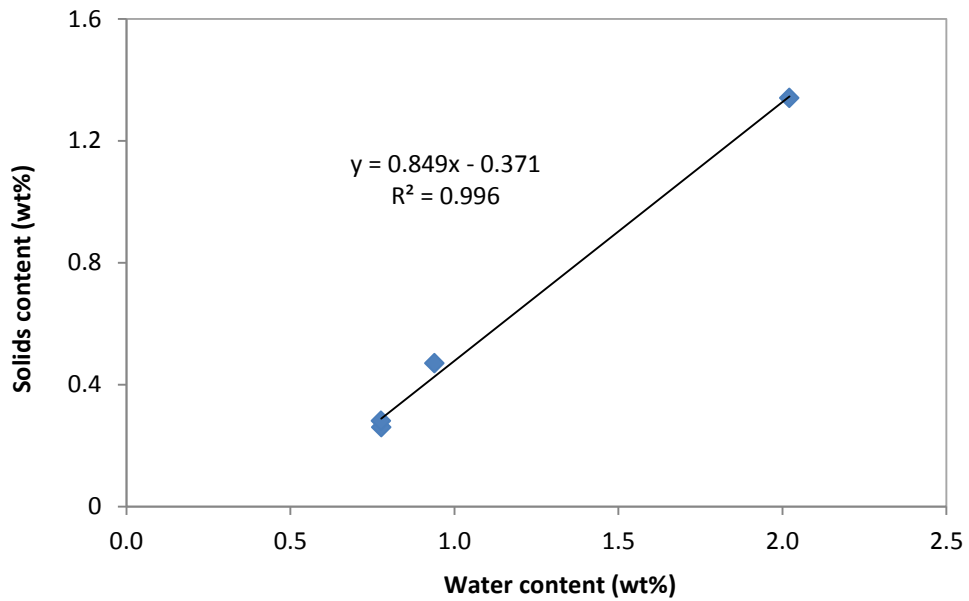
Figure 3-9: Solids content as a function of water content at the bottom section of CIST

3.2.3 Conclusions:

Mixing becomes more important at an extremely high bulk concentration as high local concentration will occur more easily due to the large amount of demulsifier injected. Insufficient mixing leads to high local concentration and affect the performance of the demulsifier.

At a very high bulk concentration (300 ppm), all mixing variables need to be favorable in order to avoid the overdosing problem. Although the final water content can still reach below 1 wt% when only one mixing variable is favorable, the formation of tiny water droplets was consistently observed. These stabilized water droplets cause further water reduction to become more difficult.

A bulk concentration of 300 ppm is very much higher than the normal operating dosage but the demulsifier can still work effectively when mixing is sufficient. The overdosing problem is more aptly described as undermixing.

Chapter 4:   Evaluation of Mixing Effects on Demulsifier Performance in Froth Treatment

The performance of the demulsifier in diluted bitumen clarification can be improved by adequate mixing and low injection concentration at sufficient bulk concentration. The effect of mixing is significant particularly at both bulk concentration near the minimum requirement and at very high bulk concentration. In this chapter, the effect of mixing is studied using a different material, bitumen froth before naphtha is added. Froth with its higher viscosity, water, and solids content is a more complex multiphase fluid for demulsifier dispersion. This part of the study aims to test the mixing strategies developed based on diluted bitumen behaviour in a more complex system, and to evaluate the effects of mixing in froth treatment.

4.1   Experimental Setup

The Confined Impeller Stirred Tank (CIST) was used throughout the experiments to have a standard mixing/settling apparatus and protocol (Laplante 2011). The experimental procedures can be divided into four stages: sample preparation, naphtha blending, demulsifier dispersion and batch settling. Naphtha was added to bitumen froth at a naphtha-to-bitumen ratio (N/B) of 0.7. Demulsifier was added either to the froth or to the naphtha diluted froth. Two addition orders were performed in the experiments:

a) **(F+N)+D:** Demulsifier added to Naphtha Diluted Froth
b) **(F+D)+N:** Demulsifier added to Froth, Naphtha added to (F+D)

For case (F+N)+D, naphtha was blended with the froth before demulsifier was dispersed. For case (F+D)+N, demulsifier was dispersed in the froth before naphtha was blended. A schematic of the experimental setup and procedure are

shown in Figure 4-1. In the sample preparation step, bitumen froth and diluent naphtha were heated, and bitumen froth was premixed in the sample can. The sample preparation step was same in both addition orders. Naphtha and froth sample were then transferred to the CIST following the addition order. All naphtha blending, demulsifier dispersion and batch settling were carried out in the CIST.

Bitumen froth provided by Syncrude Research was used as the feed in the experiments. The properties and composition of the bitumen froth after pre-mixing are shown in Table 4-1. The composition was obtained using Karl Fischer titration and Dean Stark oil, water and solids (O/W/S) analysis. The density and viscosity of froth are based on data provided by Syncrude Research. Diluent naphtha and demulsifier with concentration 39 wt% from Champion Technologies were also provided by Syncrude Research.

Table 4-1: Properties and composition of bitumen froth

Average Water Content (wt%)	24.6 - 27.4
Average Solids (wt%)	24.1
Average Bitumen (wt%)	49.2
Density, 80 °C (kg/m^3)	1138.1
Viscosity, 80 °C (m^2/s)	7.03×10^{-4}
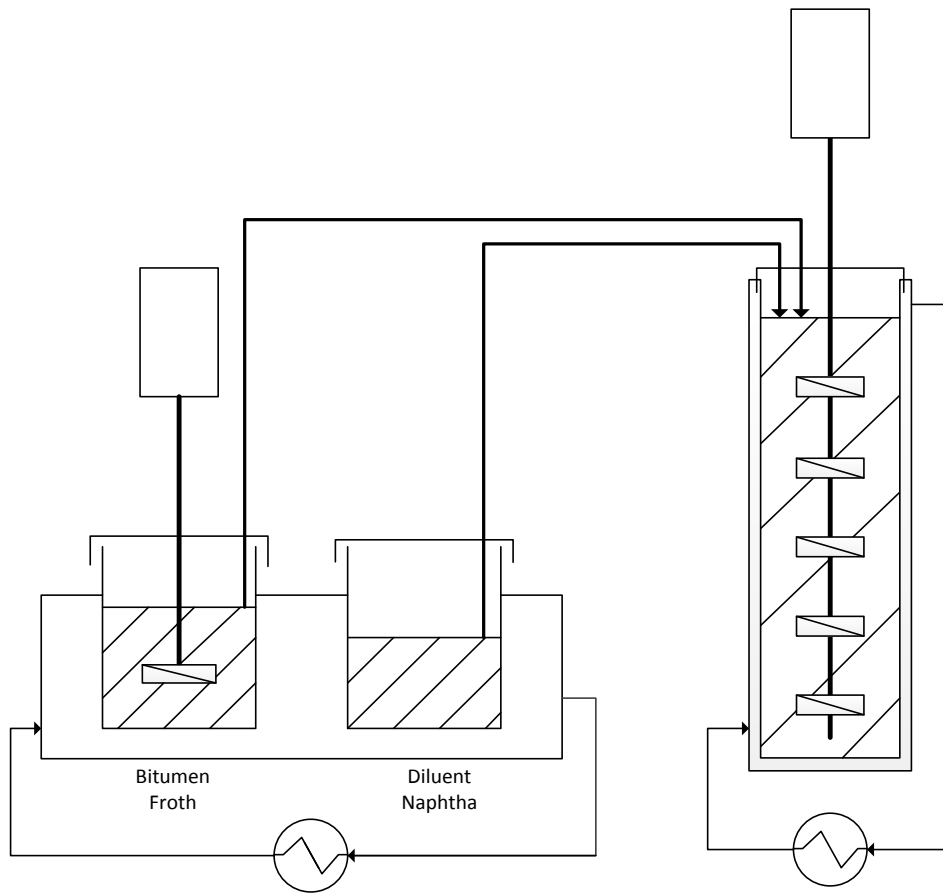
Step 1: Pre-Mixing and Heating

- Heat froth for 1.5 hours to 70 °C
- Agitation at 1000 rpm for 15 minutes
- Heat naphtha to 80 °C

Addition Order: (F+N)+D

Step 2: Naphtha Blending

- Transfer naphtha and froth to CIST
- Mix for 2 minutes at specified speed

Step 3: Demulsifier Dispersion

- Add demulsifier into CIST
- Mix for t_m at specified agitation level

Step 4: Batch Settling

- Batch gravity settling for 60 minutes
- Sample water content at 1, 3, 5, 7, 10, 30 and 60 minutes settling

Addition Order: (F+D)+N

Step 2: Demulsifier Dispersion

- Transfer froth to CIST
- Add demulsifier to CIST
- Mix for 3 minutes at specified speed

Step 3: Naphtha Blending

- Transfer naphtha to CIST
- Mix for 9 minutes at specified speed

Step 4: Batch Settling

- Batch gravity settling for 60 minutes
- Sample water content at 1, 3, 5, 7, 10, 30 and 60 minutes settling

Figure 4-1: Schematic of experimental setup and procedure

4.1.1 Premixing

As the viscosity of bitumen froth was higher and the premixing sample volume was smaller than the diluted bitumen sample in the previous experiments, a new premixing protocol was tested and developed. Figure 4-2 shows the water contents at the top and bottom of the can at different mixing times at a rotational speed of 1000 rpm. In the beginning of premixing, water was not fully suspended and the water contents were low at both top and bottom of the can. The sample was almost homogeneous after 5 minutes of mixing. The premixing was also tested with rotational speeds of 350, 500 and 750 rpm as shown in Figure 4-3, 4-4 and 4-5, respectively. The rotational speed of 350 rpm was too slow as water was still not well dispersed after 15 minutes of mixing. Water droplets were well suspended after 5 minutes when the rotational speed was 500 rpm or higher. To ensure the re-suspension of solid particles, a full 15 minutes of premixing at a rotational speed of 1000 rpm was used in the experiments.
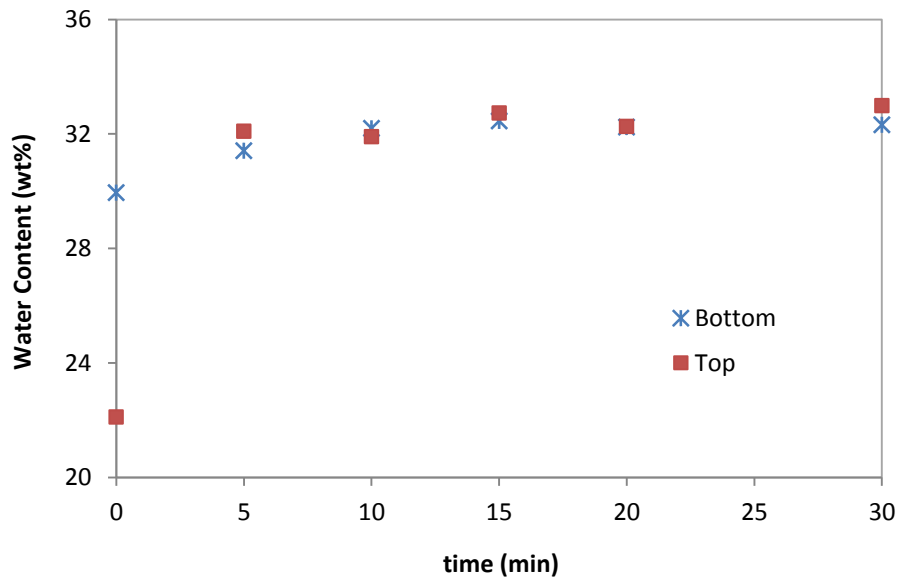
Figure 4-2: Bitumen froth water content at the top and bottom of the sample can at different mixing time at a rotational speed of 1000 rpm
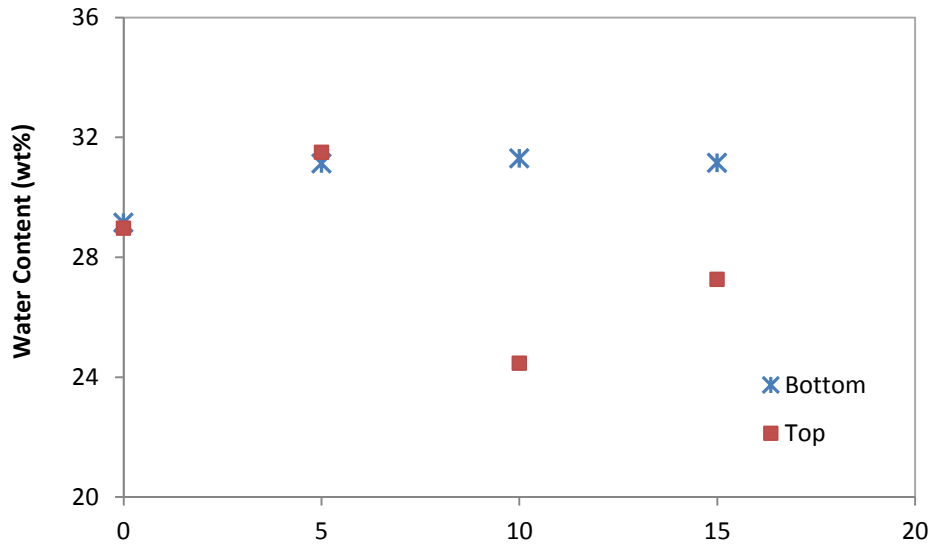
Figure 4-3: Bitumen froth water content at the top and bottom of the sample can at different mixing time at a rotational speed of 350 rpm
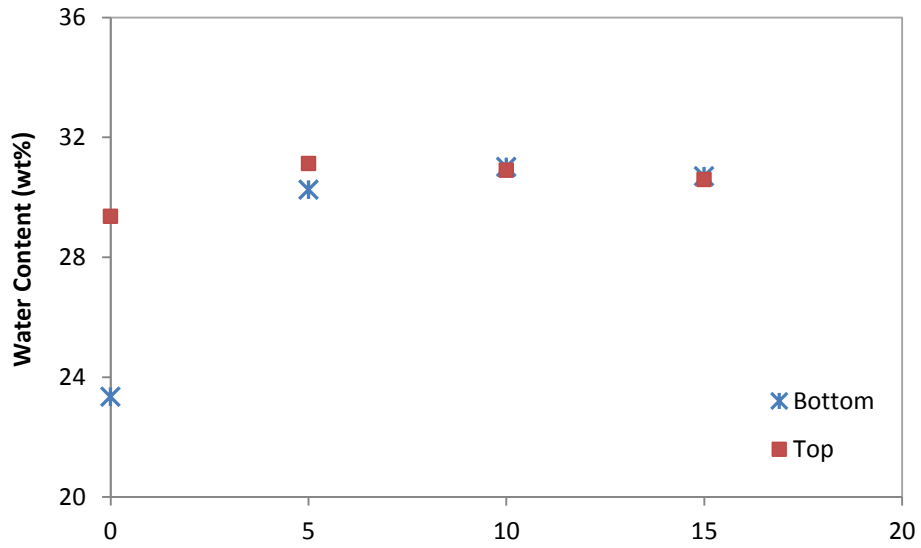
Figure 4-4: Bitumen froth water content at the top and bottom of the sample can at different mixing time at a rotational speed of 500 rpm
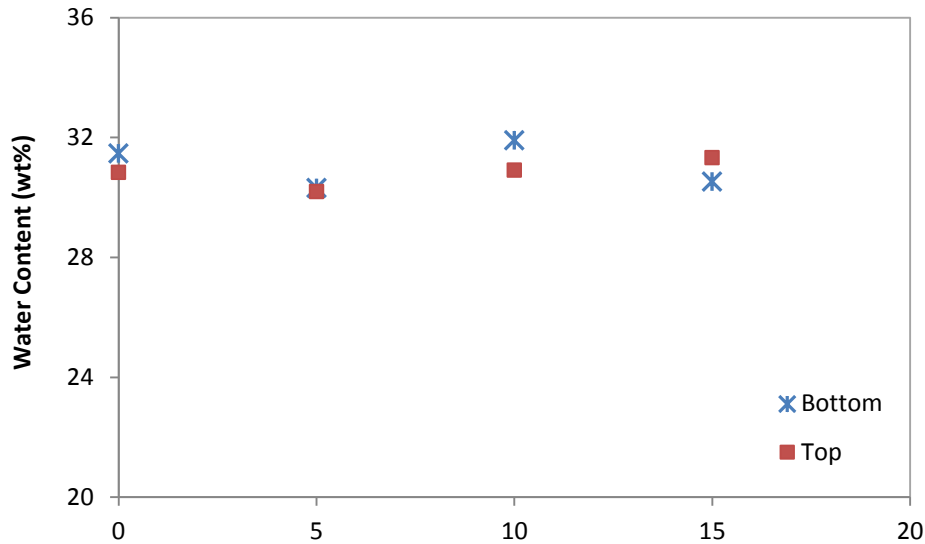
Figure 4-5: Bitumen froth water content at the top and bottom of the sample can at different mixing time at a rotational speed of 750 rpm

All samples in 1 L paint cans were stored at 5 °C in a refrigerator. The samples were left at room temperature overnight before the day of experiment to shorten the heating time. Froth was heated for 1.5 hour to 70 °C without mixing in a heating bath filled with ethylene glycol. The sample was then mixed at 1000 rpm for 15 minutes to 80 °C. A 45° pitched blade turbine (PBTD) impeller was used and a single T/10 baffle was attached to the can to improve solids re-suspension. The premixing tank dimensions and mixing parameters are shown in Table 4-2. At the end of premixing, a sample of 1 ml was taken for Karl Fischer titration to determine the water content of the sample. The froth sample was then transferred to the CIST using a temperature resistant glove.

Table 4-2: Premixing tank dimensions and mixing parameters

Impeller Type	PBTD (45)
Tank diameter, T (m)	0.10
Impeller diameter, D (m)	0.06
Liquid height, H (m)	0.08
Off-bottom clearance, C (m)	0.02
Impeller Volume, V_{IMP} (m^3)	2.54×10^{-5}
Power Number, N_P*	1.30
Impeller speed, N (rpm)	1000
$P/\rho \, V_{TANK}$ (W/kg)	7.28
$\varepsilon \sim P/\rho \, V_{IMP}$ (W/kg)	180
Reynolds Number, Re	78
Mixing time (min)	15

* Power Number in turbulent flow

4.1.2 Naphtha Blending and Demulsifier Dispersion

The blending and dispersion procedures were different for the two addition orders as demulsifier was dispersed into liquids with different viscosities.

4.1.2.1 (F+N)+D: Naphtha Blending

Naphtha was transferred to the CIST before bitumen froth. The impeller rotational speed was set to have a high energy intensity to ensure froth and naphtha were well blended and did not affect the study of mixing effects in demulsifier dispersion. The same impellers were used in blending and

demulsifier dispersion in every experiment. The impeller speeds were set so that the average energy dissipation in both impeller sets was the same for blending. Table 4-3 summarizes the mixing specifications the (F+N) blending step.

Table 4-3: Mixing specifications for naphtha blending at addition order (F+N)+D

Impeller Type	Intermig	Rushton
Tank Diameter, T (m)	0.075	0.075
Number of impellers	6	5
Impeller diameter, D (m)	0.050	0.038
Impeller speed, N (rpm)	1070	600
Liquid Height, H (m)	0.225	0.225
Off-bottom clearance, C (m)	0.017	0.013
Submergence, S (m)	0.050	0.038
Tank volume, V_{TANK} (m^3)	9.94E-04	9.94E-04
Total impeller vol, V_{IMP} (m^3)	1.68E-04	4.31E-05
N_p per impeller	0.63	4.6
P/ρ V_{TANK} (W/kg)	6.69	1.72
ε ~ P/ρ V_{IMP} (W/kg)	39.6	39.6
Reynolds number, Re	8365	2638
Mixing time (min)	2	

4.1.2.2 (F+N)+D: Demulsifier Dispersion

Demulsifier was diluted using xylene to the desired injection concentration. The specified amount of demulsifier was injected using an appropriately sized syringe or a 1/8" tubing connected to a syringe pump. The injection took place directly

above the upper impeller blade tip to promote high initial dispersion of demulsifier. Demulsifier was mixed with the naphtha diluted froth for the specified mixing intensity and mixing time. Table 4-4 summarizes the mixing specification for the demulsifier dispersion. Intermigs were used for low mixing energy while Rushtons were used for high mixing energy.

Table 4-4: Mixing specifications for demulsifier dispersion at addition order (F+N)+D

Impeller Type	Intermig	Rushton
Tank diameter, T (m)	0.075	0.075
Number of impellers	6	5
Impeller diameter, D (m)	0.050	0.038
Impeller speed, N (rpm)	250	600
Liquid height, H (m)	0.225	0.225
Off-bottom clearance, C (m)	0.017	0.013
Submergence, S (m)	0.050	0.038
Tank volume, V_{TANK} (m^3)	9.94E-04	9.94E-04
Total impeller vol, V_{IMP} (m^3)	1.68E-04	4.31E-05
N_p per impeller	1.3	4.6
P/ρ V_{TANK} (W/kg)	0.18	1.72
ε ~ P/ρ V_{IMP} (W/kg)	1.05	39.6
Reynolds number, Re	1954	2638
Mixing time (min)	2	10

4.1.2.3 (F+D)+N: Demulsifier Dispersion

The CIST was only partially filled with bitumen froth with 3 impellers below the liquid surface in the case where demulsifier was added to froth. The viscosity of bitumen forth was very high which resulted laminar mixing at the experimental scale. The power numbers of the impellers were estimated from an extrapolation from the power numbers measured by Machado and Kresta (2013). The impeller speeds were set so that the ratio between the low and high mixing energy in the demulsifier dispersion was same as the ratio in naphtha blending, which was 0.15:1. Table 4-5 summarizes the mixing specification for the demulsifier dispersion. A310s were used for low mixing energy while Rushtons were used for high mixing energy.

Demulsifier was diluted using xylene to the desired injection concentration. The specified amount of demulsifier was injected using an appropriately sized syringe or a 1/8" tubing connected to a syringe pump. The injection took place beside the first impeller below the liquid surface to promote high initial dispersion of demulsifier.

Table 4-5: Mixing specifications for demulsifier dispersion at addition order (F+D)+N

Impeller Type	A310	Rushton
Tank diameter, T (m)	0.075	0.075
Number of impellers	3	3
Impeller diameter, D (m)	0.038	0.038
Impeller speed, N (rpm)	760	1200
Liquid height, H (m)	0.145	0.145
Total impeller vol, V_{IMP} (m^3)	3.14E-05	2.59E-05
N_p per impeller	1600	2200
P/ρ V_{FROTH} (W/kg)	1128	6105
$\varepsilon \sim$ P/ρ V_{IMP} (W/kg)	2.31E+04	1.51E+05
Reynolds number, Re	25	40
Mixing time, t_m (min)	3	

4.1.2.4 (F+D)+N: Naphtha Blending

Naphtha was transferred to the CIST after the demulsifier dispersion. Two different mixing intensities were used in the experiments to study the effect of mixing on demulsifier performance. For high energy intensity, Rushton impellers were used and the rotational speed was set to match the high mixing intensity used in the previous experiments, 40 W/kg. For low mixing energy, the Intermig impellers used previously were not feasible in this experimental setup as blending of froth and naphtha required a higher mixing intensity and better fluid circulation. A310 impellers were used and the rotational speed was set so that the blending could be done in a reasonable period of time. The mixing energy

ratio between the high and low mixing intensity cases was set at 0.15:1. There was an additional 2 minutes blending time to blend froth and naphtha in the (F+N)+D experiments. Therefore, the total mixing time for (F+D)+N was set as 12 minutes, with 3 minutes demulsifier dispersion and 9 minutes naphtha blending. The longer blending time was to ensure naphtha and froth were well blended especially at low mixing intensity. Table 4-6 summarizes the mixing specifications for the naphtha blending step.

Table 4-6: Mixing specifications for naphtha blending at addition order (F+D)+N

Impeller Type	A310	Rushton
Tank diameter, T (m)	0.075	0.075
Number of impellers	5	5
Impeller diameter, D (m)	0.038	0.038
Impeller speed, N (rpm)	600	600
Liquid height, H (m)	0.225	0.225
Off-bottom clearance, C (m)	0.013	0.013
Submergence, S (m)	0.038	0.038
Tank volume, V_{TANK} (m^3)	9.94E-04	9.94E-04
Total impeller vol, V_{IMP} (m^3)	5.23E-05	4.31E-05
N_p per impeller	0.84	4.6
P/ρ V_{TANK} (W/kg)	0.31	1.72
ε ~ P/ρ V_{IMP} (W/kg)	5.96	39.6
Reynolds number, Re	2638	2638
Mixing time, t_m (min)	9	

4.1.3 Experimental Design

4.1.3.1 Addition Order (F+N)+D

(I) Factorial design at BC 50 ppm

In the previous experiments, it was shown that demulsifier bulk concentration (BC) of 50 ppm is sufficiently high to have a good separation of water droplets. A constant bulk concentration, 50 ppm was used in the first part of the experiment to study the effects of mixing variables. Two variables, mixing energy (J) and injection concentration (IC) were varied, as shown in Table 4-7.

Table 4-7: Variables of 2-level factorial design

Variable	−	+
Mixing Energy, J (J/kg)	Low*	High**
Injection Concentration, IC (wt %)	12	21

  * Low   : $\varepsilon = 1$ W/kg, $t_m = 2$ min
  ** High   : $\varepsilon = 40$ W/kg, $t_m = 10$ min

Table 4-8: 2-level factorial design

Run	J	IC
1	-	-
2	-	+
3	+	-
4	+	+

(II) Effect of solids content

Solids content in the batch of froth samples supplied was 24.1 wt%, compared to the normal solids content of 10 wt%. High solids content may affect the settling of water droplets as solids stabilize the water emulsion (Binks et al. 2002). An experiment was conducted with a sample with lower solids content 10.23 wt% to observe the effect of high solids content on the performance of the demulsifier.

(III) Effect of Increasing Bulk Concentration

Due to higher water content in the froth sample compared to diluted bitumen, a demulsifier bulk concentration of 50 ppm was not sufficient to achieve a low final water content. Several experiments were conducted at favorable mixing conditions with increasing bulk concentration, 0, 50, 100 and 150 ppm to observe the effect of bulk concentration on the performance of the demulsifier at addition order (F+N)+D, Table 4-9.

Table 4-9: Experiments at increasing bulk concentration (F+N)+D

Run	BC (ppm)	J (J)	IC (wt%)
1	0	High*	12
2	50	High*	12
3	100	High*	12
4	150	High*	12

* High : ε = 40 W/kg, t_m = 10 min

(IV) Effect of mixing at a high bulk concentration

It was found that a bulk concentration of 150 ppm was needed in order to have good demulsifier performance in froth samples which had a high water content. However, all the experiments to study the effect of bulk concentration were conducted with favorable mixing conditions. Therefore an experiment with unfavorable mixing conditions, low mixing energy (ε = 1 W/kg, t_m = 2 min) and high injection concentration (21 wt%), was carried out at a bulk concentration of 150 ppm to observe the effect of mixing.

4.1.3.2   Addition Order (F+D)+N

(I) Effect of Increasing Bulk Concentration

Several experiments were conducted at favorable mixing conditions with increasing bulk concentration, 0, 50, 100 and 150 ppm to study the effect of bulk concentration on the performance of the demulsifier at addition order (F+D)+N. The conditions of the experiments are shown in Table 4-10.

Table 4-10: Experiments at increasing bulk concentration (F+D)+N

Run	BC (ppm)	J (J)	IC (wt%)
1	0	High*	12
2	50	High*	12
3	100	High*	12
4	150	High*	12

* Rushton impellers were used

(II) Effect of mixing at a high bulk concentration

An experiment with unfavorable mixing conditions, low mixing energy and high injection concentration, was carried out to observe the effect of mixing. The A310 impellers at a rotational speed of 600 rpm, with 0.15 times the mixing energy of the Rushton and an injection concentration of 21 wt% were used in the experiment. A bulk concentration of 300 ppm was used in the experiment.

4.1.4 Sampling and Test

For addition order (F+N)+D, samples were obtained at the end of naphtha blending, 60 seconds after demulsifier injection and 30 seconds before the end of demulsifier dispersion. For addition order (F+D)+N, samples were obtained at the end of demulsifier dispersion, 3 minutes after naphtha was added and at the end of naphtha blending. All samples were obtained for water content determination and microscope analysis. For naphtha diluted froth, samples were taken by sampling the bulk mixtures 3.2 cm below the liquid surface using 0.25" ID polyethylene tubing attached to an auto-pipette. For viscous froth, sampling was done 1 cm below the liquid surface using an auto-pipette.

After naphtha blending and demulsifier dispersion, the impellers were stopped and the sample in the CIST was allowed to settle by gravity for 60 minutes. Samples were taken at 3.2 cm and 11.5 cm below the liquid surface at 1, 3, 5, 7, 10, 30 and 60 minutes. The samplings in both addition orders were same during the settling. Microscope images of samples were obtained after 1, 3, 5, 7, 10 and 30 minutes of settling. At the end of the 60 minute settling, 100 mL samples were obtained for O/W/S analysis at height $z/H = 0.1$, 0.5 and 0.9. Tables 4-11 and 4-12 summarize the sampling time, location and methods in the experiments for different addition orders.

Table 4-11: Summary of sampling during the experiment for addition order (F+N)+D

Label	Time	Location	Method	Volume (ml)
P	End of premixing	1 cm below the liquid surface	Auto-pipette	1
A	End of blending	3.2 cm below the liquid surface	Tubing attached to an auto-pipette	1
B,C	During demulsifier dispersion (60 s after demulsifier added and 30 s before mixing ends)	3.2 cm below the liquid surface	Tubing attached to an auto-pipette	1
1, 3, 5, 7, 10, 30, 60	During settling	3.2 cm below the liquid surface	Tubing attached to an auto-pipette	1
1a, 3a, 5a, 7a, 10a, 30a	During settling	11.5 cm below the liquid surface ($z/H = 0.5$)	Tubing attached to an auto-pipette	1
DS_0.1, DS_0.5, DS_0.9	End of settling	At $z/H = 0.1, 0.5, 0.9$	Tubing connected to a 100 ml syringe	100

Table 4-12: Summary of sampling during the experiment for addition order (F+D)+N

Label	Time	Location	Method	Volume (ml)
P	End of premixing	1 cm below the liquid surface	Auto-pipette	1
A	End of demulsifier dispersion	1 cm below the liquid surface	Auto-pipette	1
B,C	During naphtha blending (3 min and at the end of mixing)	3.2 cm below the liquid surface	Tubing attached to an auto-pipette	1
1, 3, 5, 7, 10, 30, 60	During settling	3.2 cm below the liquid surface	Tubing attached to an auto-pipette	1
1a, 3a, 5a, 7a, 10a, 30a	During settling	11.5 cm below the liquid surface ($z/H = 0.5$)	Tubing attached to an auto-pipette	1
DS_0.1, DS_0.5, DS_0.9	End of settling	At $z/H = 0.1, 0.5, 0.9$	Tubing connected to a 100 ml syringe	100

4.2 Results and Discussion

4.2.1 Addition Order (F+N)+D

Figure 4-6 shows the results from the factorial design at bulk concentration 50 ppm. The initial water concentration of naphtha diluted froth ranged from 17.56 to 19.19 wt%. At demulsifier bulk concentration 50 ppm, the water content varied from 4.45 to 7.67 wt% at the end of settling.
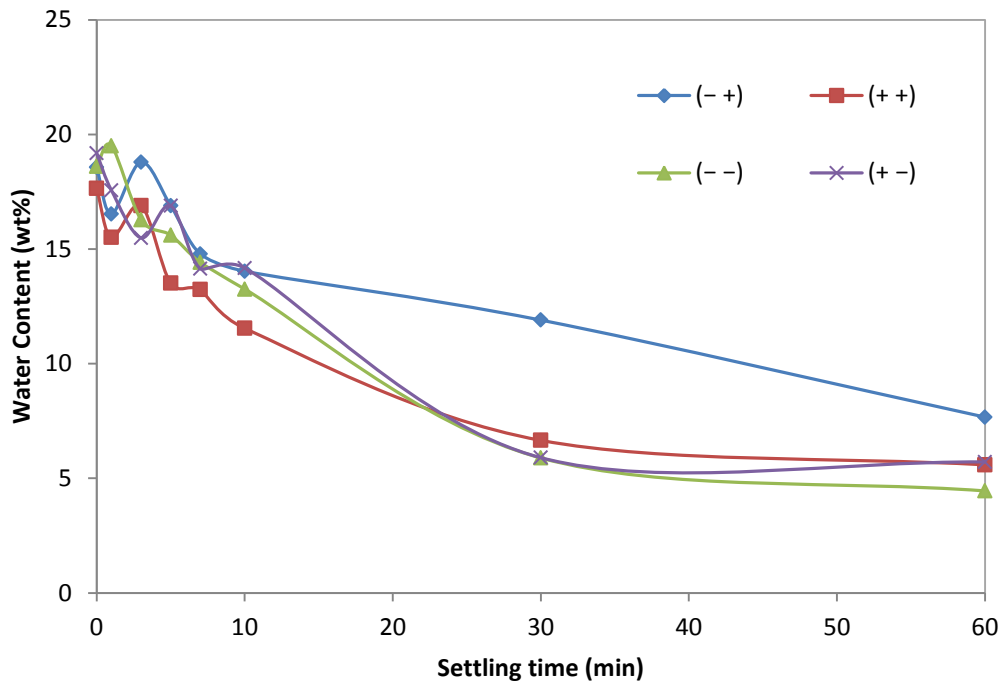
Figure 4-6: Naphtha diluted froth water content during batch gravity settling. Variable order: (X_J and X_{IC})

When the mixing conditions were unfavorable, low mixing energy and high injection concentration, (− +), the water content only reduced to 7.67 wt% at the end of settling. However, when either one of the mixing variables was favorable, in experiment (− −) and (+ +), the final water content dropped to 4.45 and 5.59 wt%, respectively. The final water content was 5.71 wt% in experiment (+ −) when both of the mixing variables were favorable. Three of the experiments (− −), (+ +) and (+ −) had a similar final water content and settling curve. By

improving either one or both of the mixing variables, the removal of water droplets can be improved by 30 minutes settling time.

By comparing the settling curve with experiments in Chapter 2 and 3, where demulsifier was added to diluted bitumen, the initial settling of the water droplet was slower in the naphtha diluted froth. The initial settling rate also ended longer than 10 minutes for naphtha diluted froth and there was a large reduction of water content from 10 to 30 minutes of settling. The slow initial settling can be due to low demulsifier bulk concentration used as the final water content was higher than in the diluted bitumen. The high solids content may also hinder the settling of water droplets and cause slow settling. The effect of solids is discussed in the next section.
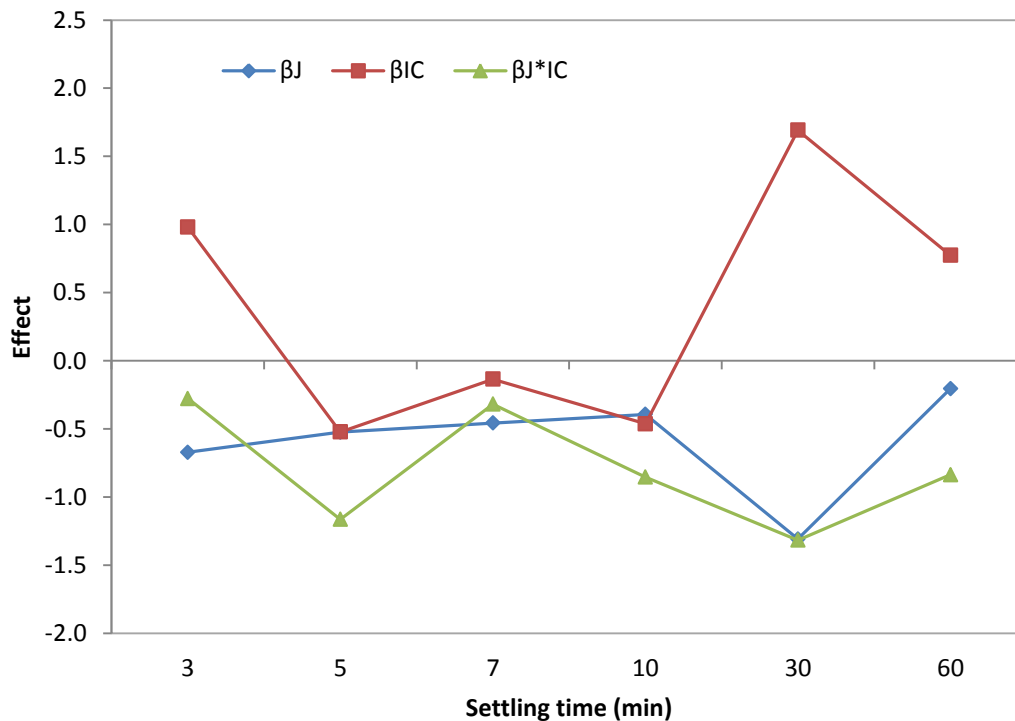
Figure 4-7: Effects of the variables at different time of settling

The effects of the variables on water content during the settling are shown in Figure 4-7. The effect of injection concentration was high at the beginning of settling, at 3 minutes and at the end of the settling from 30 to 60 minutes. The effect of mixing energy was relatively small and showed a large impact at 30 minutes of settling. The interaction effect only appeared to be significant at 5 and 30 minutes of settling. The effects of the variables were the highest during 30 minutes settling. As observed from the settling curve, the water content was very much reduced at 30 minutes if either or both of the mixing variables were favorable.

Effect of Solids
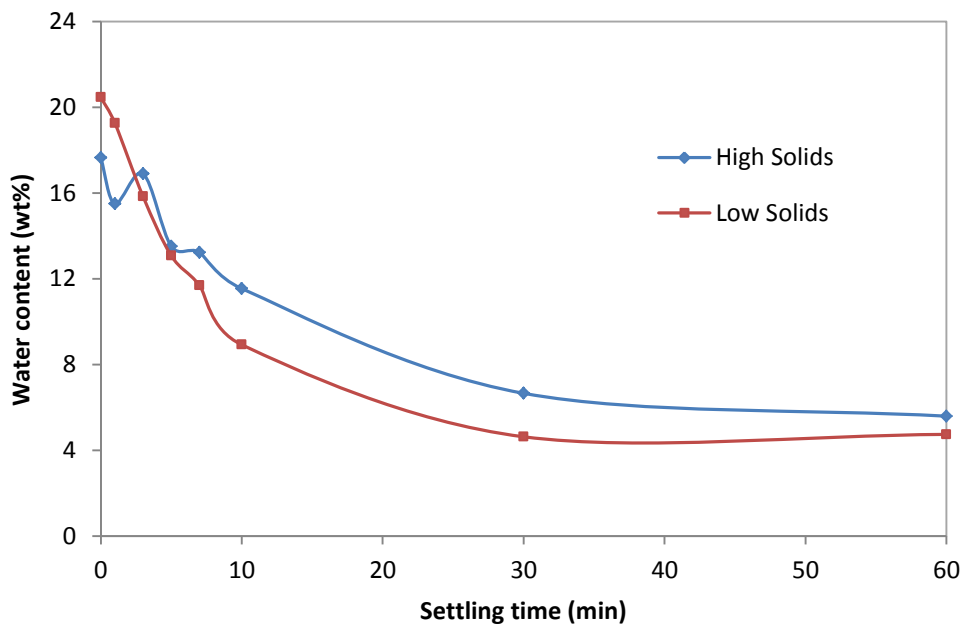
Figure 4-8: Water content of naphtha diluted froth with different solids content during batch gravity settling

An experiment was carried out with a sample with a lower solids content. Figure 4-8 shows the water contents during settling at bulk concentration 50 ppm, high mixing energy and injection concentration 21 wt%. The initial settling was slightly

faster when the solids content was lower, which resulted a lower final water content. High solids content may stabilize water droplets and slow down the settling (Feng et al. 2009). Layers of solids may also get trapped between water droplets and prevent coalescence when the solids content is very high (Sztukowski 2005). Therefore the quality of froth will also affect the performance of demulsifier.

Effect of Bulk Concentration
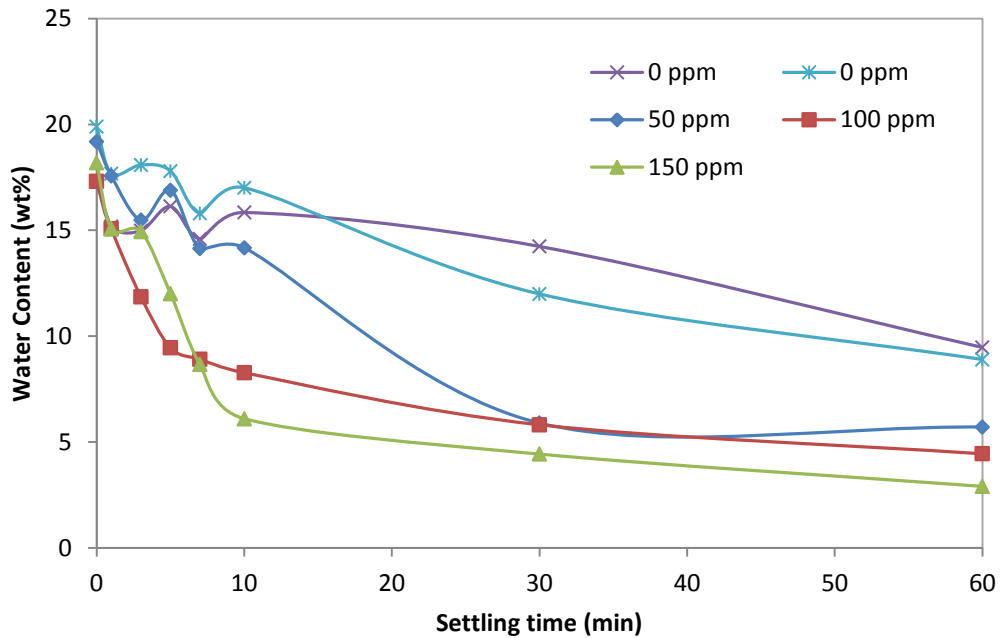
Figure 4-9: Naphtha diluted froth water content during batch gravity settling at increasing BC

Figure 4-9 shows the water content at different bulk concentrations for favorable mixing conditions. At demulsifier bulk concentration 0 ppm, the final water contents were 8.90 and 9.47 wt% in two experiments. Water droplets in naphtha diluted froth settled without the effect of demulsification, where coalescence and flocculation of water droplets were limited. As only large water droplets will settle readily, the water removed in these runs was mainly free

water, estimated as about 50 % of the total water content in the samples. The remaining water can only be removed with the use of demulsifier.

At bulk concentration 50 and 100 ppm, the water contents were similar at 30 and 60 minutes of settling. The final water content was slightly lower at bulk concentration 100 ppm, 4.45 wt%, compared to 50 ppm, 5.71 wt%. However, the initial settling rate was higher at BC 100 ppm. The high initial settling rate may be due to the formation of flocs and large water droplets at the beginning of the settling as larger size flocs or water droplets are required for fast settling. Flocculation and coalescence may be slower at bulk concentration 50 ppm.

At bulk concentration 150 ppm, fast initial settling was also observed during the first 10 minutes of settling. The high initial settling rate was similar to the experiments with diluted bitumen in Chapter 2 and 3. The final water content was also lower, 2.91 wt%. The increase of bulk concentration further improved the performance of demulsifier. A higher bulk concentration is required in naphtha diluted froth as the water content is higher.

Effect of Mixing and Bulk Concentration

At bulk concentration 150 ppm, the final water content only dropped to 7.65 wt% when the mixing energy was low and injection concentration was high, Figure 4-10 (High BC, Bad MX). Bulk concentration 150 ppm was sufficient to remove significant amount of water content but the demulsifier will only perform well at good mixing conditions.

By combining experiments with different bulk concentration and mixing condition, a 2-variable factorial design can be formed to illustrate the effects of bulk concentration and mixing conditions, Table 4-13. Since injection concentration was varied together with mixing energy, mixing conditions include both mixing energy and injection concentration.

At a low bulk concentration of 50 ppm, the performance of the demulsifier can be improved by good mixing conditions but only after 10 minutes of settling. The initial settling was slow, as discussed in the previous section. However, at high bulk concentration 150 ppm, the performance of the demulsifier was improved significantly by good mixing conditions especially at the beginning of the settling. This again demonstrates the importance of good mixing. High bulk concentration alone will not improve the performance of the demulsifier.

Table 4-13: Variables of 2-level factorial design

Variable	−	+
Bulk Concentration, BC (ppm)	50	150
Mixing Condition, MX	Low*	High**

* Low   : ε = 1 W/kg, t_m = 2 min, IC = 21 wt%

** High   : ε = 40 W/kg, t_m = 10 min, IC = 12 wt%
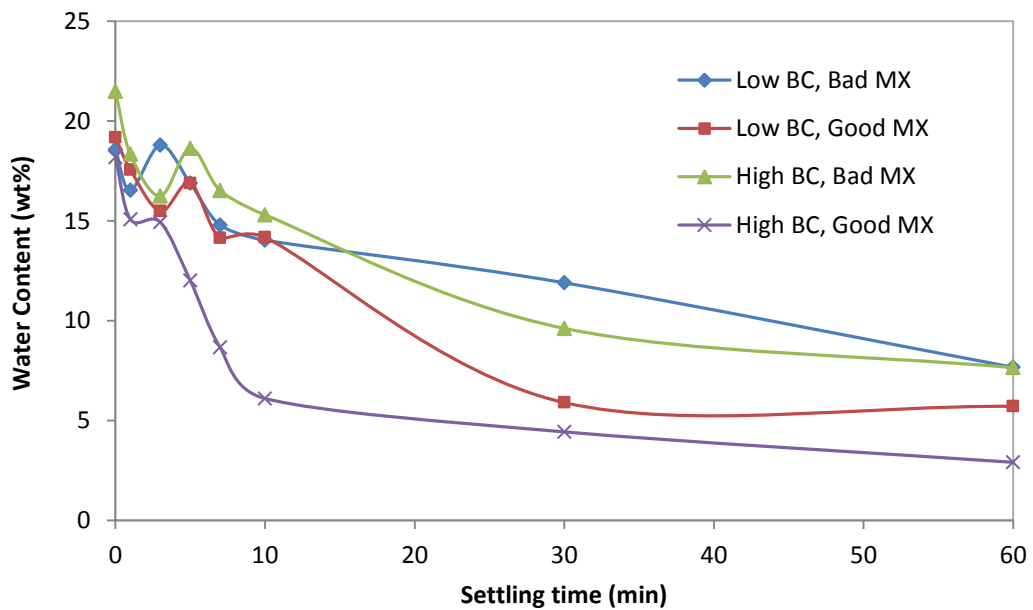
Figure 4-10: Naphtha diluted froth water content during batch gravity settling
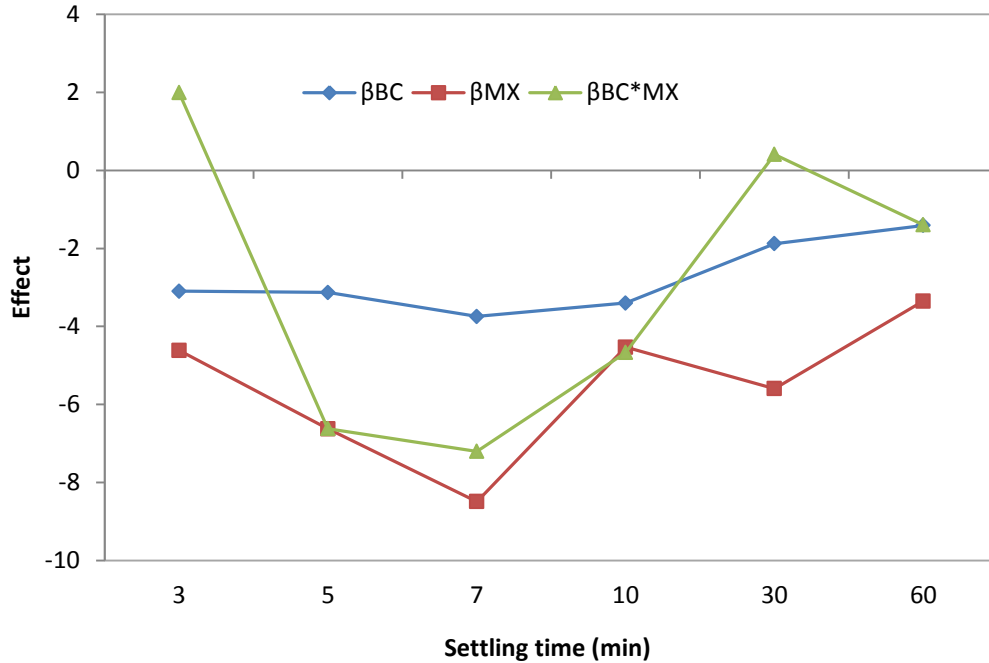
Figure 4-11: Effects of the variables at different time of settling

From the effect analysis shown in Figure 4-11, the combined mixing conditions have a large impact on the demulsifier performance throughout the whole settling. The large effect shows the important of good mixing but also due to the combination of all mixing variables. The effect of mixing was relatively high at 5 and 7 minutes of settling. Therefore better mixing leads to good demulsifier performance and fast initial settling.

4.2.2 Addition Order (F+D)+N

The study of different addition order was started with good mixing conditions, high mixing energy and low injection concentration, at increasing demulsifier bulk concentration from 0 to 150 ppm. The results are shown in Figure 4-12.

In the experiment without demulsifier added, water content was reduced from 22.23 wt% to 8.02 wt% by the end of settling. The reduction of water was higher

compared to addition order (F+N)+D, but the final water contents of these 0 ppm runs were similar, ranging from 8 to 9.5 wt%. Therefore, there is about 8 to 9.5 wt% water content contributed by stabilized water droplets in the froth which needs to be removed through demulsification.
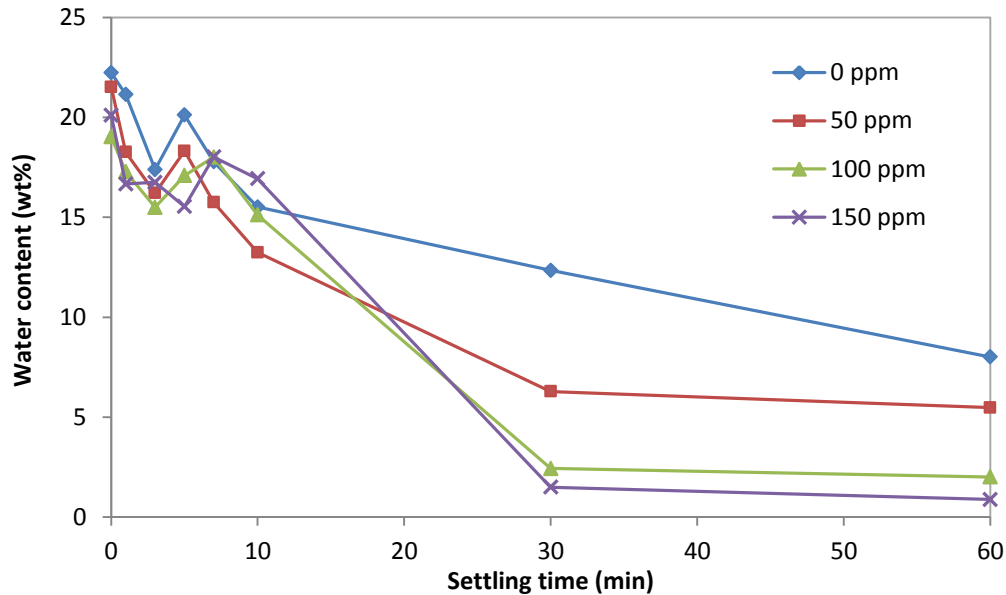
Figure 4-12: Naphtha diluted froth water content during batch gravity settling at increasing BC with addition order (F+D)+N

When the demulsifier bulk concentration was increased to 50 ppm, the final water content dropped to 5.48 wt%. The final water content was similar to the value obtained in experiment with addition order (F+N)+D at the same bulk concentration, 5.71 wt%. In addition, the settling behaved similarly, with high settling rate from 10 to 30 minutes.

When the bulk concentration was further increased to 100 and 150 ppm, the final water content was reduced to 2.01 and 0.88 wt%, respectively. Both of these final water contents were lower than the value determined in addition order (F+N)+D where the final water content only reached 2.91 wt% at bulk

concentration 150 ppm. Furthermore, the final water content of 0.88 wt% is close to the results obtained in experiments with diluted bitumen when demulsifier was performing well. Dispersion of demulsifier in froth was shown to be more effective compared to dispersion to naphtha diluted froth.

However, the fast settling started late in addition order (F+D)+N and the water concentration did not change during the first 10 minutes of settling. The settling behaviour was different compared to cases with addition order (F+N)+D and diluted bitumen, where the initial settling was fast in the first 10 minutes. The stable water content at the beginning of settling may indicate that flocculation and coalescence start slower for (F+D)+N.

An experiment was conducted with a lower mixing energy and high injection concentration and the result is shown in Figure 4-13. Though the mixing energy was only 0.15 time the energy used in the high mixing energy run, the final water content was low, 1.87 wt%. The final water content was also lower than the case when mixing was favorable at addition order (F+N)+D.

There are several reasons for the good performance of demulsifier at the run with unfavorable mixing conditions. First, the bulk concentration used may be too high and overshadow the effect of mixing. Besides, the mixing energy difference might be too small to observe a significant difference in final water content, or the laminar mixing during the demulsifier dispersion may have a very high energy in both cases and contribute to the good performance of the demulsifier.
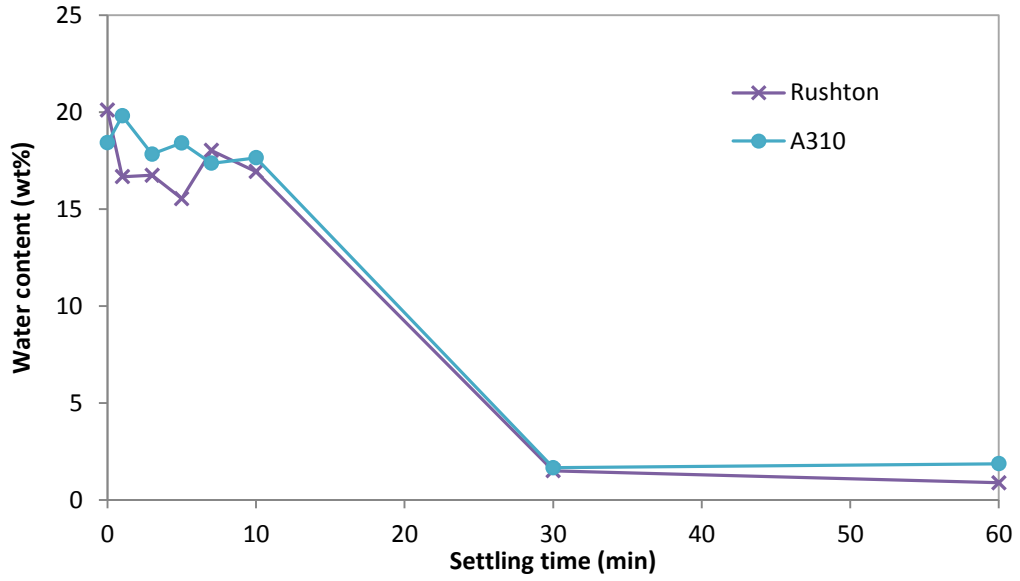
Figure 4-13: Naphtha diluted froth water content during batch gravity settling at different mixing conditions with addition order (F+D)+N

4.2.3 Effect of Mixing Order

By comparing the final water content at the end of settling, Figure 4-9 and 4-12, the performance of the demulsifier is improved with the addition order (F+D)+N. The good settling of water droplets could be due to several reasons such as better dispersion of demulsifier and higher flocculation and coalescence rate.

Though the dispersion of demulsifier at addition order (F+D)+N was in the laminar regime, the bulk concentration of demulsifier was higher as the froth sample was not diluted by naphtha. Effective demulsifier adsorption could be driven by the high bulk concentration. However, due to high viscosity of the froth sample, flocculation and coalescence may be limited. When naphtha was added, viscosity was reduced and flocculation could happen more easily. The dispersion step could be an additional dilution of demulsifier.

Late settling for the addition order (F+D)+N may be due to the coalescence of water droplets at the top layers. The water content was relatively unstable in the first 10 minutes and increased at 5 and 7 minutes in most of the runs. The instability can be due to difference in settling, coalescence and flocculation rate in the CIST. Water droplets at the top layer may coalesce and settle to the sampling height. Population Balance Modeling is required to give a more comprehensive understanding of the different rates.

As sampling was done at 10 and 30 minutes of settling, there is no information about the water concentration in between these two sampling times. There may be a fast settling rate at a particular point at this period of time. It is also difficult to compare the mixing energy in laminar and turbulent flow. The better result could be due to a higher total mixing energy at mixing order (F+D)+N.

4.2.4 Vertical Profile and the Formation of Rag Layer

The water and solids content along the CIST may not be uniform due to high solids and water content in the naphtha diluted froth. High solids may lead to slow settling and rag layer may form at the middle of the tank (Czarnecki et al. 2007). 5 samples along the CIST were taken at the end of the experiment and the water content profiles are shown in Figure 4-14. The water contents were same at the top 30 % of the tank. However, there was a drastic change in water content below z/H = 0.3. The settling of water droplets and solids were good at the top of the tank. Water and solids accumulates at the bottom half of the tank. Settling at the bottom half of the tank may be limited by the formation of rag layers. The mechanisms of rag layer build up are not yet well understood but it could be due to the accumulation of fine oil-wet solids which stabilize the dispersed water droplet, or the low water droplets coalescence rate compared to accumulation rate (Saadatmand et al. 2008; Frising et al. 2006).
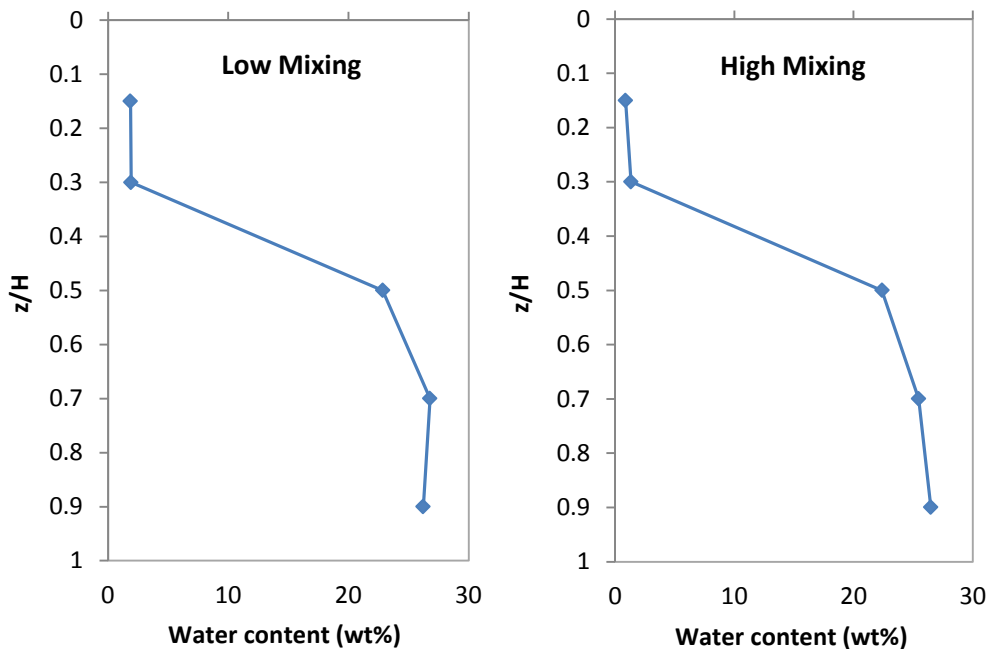
Figure 4-14: Vertical profile of water content along CIST at the end of settling. BC = 150 ppm, Addition Order (F+D)+N

4.3 Conclusions:

In addition order (F+N)+D, high mixing energy and low injection concentration improve the performance of the demulsifier in the naphtha diluted froth. This observation is consistent with the experiments where diluted bitumen is used as the feed samples. However, due to higher water content in naphtha diluted froth, about 20% compared to approximately 2.5% in diluted bitumen, a higher demulsifier bulk concentration is required. Solids content also affects the settling of the water droplets.

The demulsifier works better when it is added to the bitumen froth at addition order (F+D)+N. The good results may be due to the higher bulk concentration during the dispersion before naphtha is added, as the dispersion step acts like an additional demulsifier dilution step. However, settling occurs later in this addition order and further study is needed to determine the critical time for the settling to occur.

In conclusion, mixing improves the performance of the demulsifier in both diluted bitumen and bitumen froth. Mixing strategies developed from the diluted bitumen system are equally applicable to bitumen froth. The total mixing energy and the injection concentration are two key mixing variables. The CIST is an excellent way to perform lab scale mixer/settler experiments.

References

Angle, C. W. (2001). "Chemical demulsification of stable crude oil and bitumen emulsions in petroleum recovery—A review." in Encyclopedic Handbook of Emulsion Technology, ed. Sjöblom, J. New York, Marcel Dekker, Inc.

Anthieren, G. L. (2003). "Eulerian-Lagrangian model of turbulent mixing for silver halide." MSc. Thesis, University of Alberta, Canada.

Bhardwaj, A. and S. Hartland (1994). "Dynamics of emulsification and demulsification of water in crude oil emulsions." Industrial & Engineering Chemistry Research **33**(5): 1271-1279.

Bhardwaj, A. and S. Hartland (1994). "Kinetics of coalescence of water droplets in water-in-crude oil emulsions." Journal of Dispersion Science and Technology **15**(2): 133-146.

Binks, B. P. (2002). "Particles as surfactants: similarities and differences." Current Opinion in Colloid & Interface Science **7**(1-2): 21-41.

Box, G. E. P. and D. W. Behnken (1960). "Some new three level designs for the study of quantitative variables." Technometrics **2**(4): 455-457.

Chen, H. T. and S. Middleman (1967). "Drop size distribution in agitated liquid-liquid systems." AIChE J. **13(5)**: 989-995.

Christensen, J. R., P. B. Sørensen, G. L. Christensen and J. A. Hansen (1993). "Mechanisms for overdosing in sludge conditioning." Journal of Environmental Engineering **119**(1): 159-171.

Czarnecki, J., K. Moran and X. Yang (2007). "On the "rag Layer" and diluted froth dewatering." Canadian Journal of Chemical Engineering **85**(5): 748-755.

Davies, J. T. (1987). "A physical interpretation of drop sizes in homogenizers and agitated tanks, including the dispersion of viscous oils." Chem. Eng. Sci. **42**: 1671-1676.

Deng, S., G. Yu, Z. Jiang, R. Zhang and Y. P. Ting (2005) "Destabilization of oil droplets in produced water from ASP flooding." Colloids and Surfaces A: Physicochem. Eng. Aspects **252**(2-3): 113–119.

Dimitrov, A.N., D.I. Yordanov and P.S. Petkov (2012). "Study on the effect of demulsifiers on crude oil and petroleum products." International Journal of Environmental Research **6**(2): 435-442.

ERCB (2013). "ST98-2013: Alberta's Energy Reserves 2012 and Supply/Demand Outlook 2013-2022." Calgary.

Ese, M. H. and P. K. Kilpatrick (2004). "Stabilization of water-in-oil emulsions by naphthenic acids and their salts: Model compounds, role of pH, and soap: Acid ratio." Journal of Dispersion Science and Technology **25**(3): 253-261.

Feng, X., P. Mussone, S. Gao, S. Wang, S. Y. Wu, J. H. Masliyah and Z. Xu (2010). "Mechanistic study on demulsification of water-in-diluted bitumen emulsions by ethylcellulose." Langmuir **26**(5): 3050-3057.

Feng, X., Z. Xu and J. Masliyah (2009). "Biodegradable polymer for demulsification of water-in-bitumen emulsions." Energy Fuels **23**(1): 451–456.

Frising, T., C. Noïka and C. Dalmazzonea (2006). "The liquid/liquid sedimentation process: from droplet coalescence to technologically enhanced water/oil emulsion gravity separators: A review." Journal of Dispersion Science and Technology **27**(7): 1035-1057.

Gao, S. (2010). "Stability of water-in-diluted bitumen emulsion droplets." PhD Thesis, University of Alberta, Canada.

Gregory, J. and S. Barany (2011). "Adsorption and flocculation by polymers and polymer mixtures." Advances in Colloid and Interface Science **169**(1): 1-12.

Hinze, J. O. (1955). "Fundamentals of the hydrodynamic mechanism of splitting in dispersion process." AIChE Journal **1**(3): 289-295.

Ibemere, S. and S. Kresta (2007). "Modelling the mixing and dissolution kinetics of partially miscible liquids." Chemical Engineering Research and Design **85**(5 A): 710-720.

Liu, J., Z. Xu and J. Masliyah (2005). "Processability of oil sand ores in Alberta." Energy and Fuels **19**(5): 2056-2063.

Kim, Y. H. and D. T. Wasan (1996). "Effect of demulsifier partitioning on the destabilization of water-in-oil emulsions." Industrial and Engineering Chemistry Research **35**(4): 1141-1149.

Kresta, S. M. (2013). Mixing in the Process Industry, CH E 620. University of Alberta, Edmonton, Canada.

Kukukova, A., J. Aubin and S. M. Kresta (2009). "A new definition of mixing and segregation: Three dimensions of a key process variable." Chemical Engineering Research and Design **87**(4): 633-647.

Laplante, P. G (2011). "On Mixing and Demulsifier Performance in Oil Sands Froth Treatment." MSc. Thesis, University of Alberta, Canada.

Long, Y., T. Dabros and H. Hamza (2007). "Selective solvent deasphalting for heavy oil emulsion treatment" in Asphaltenes, Heavy Oils and Petroleomics, ed. O. C. Mullins, E. Y. Sheu, A. Hammami and A. G. Marshall. New York, Springer.

Machado, M. B. and S. M. Kresta (2013). "The confined impeller stirred tank (CIST): A bench scale testing device for specification of local mixing conditions required in large scale vessels." Chemical Engineering Research and Design In Press.

Masliyah, J., Z. Xu and J. Czarnecki (2011). Handbook on Theory and Practice of Bitumen Recovery from Athabasca Oil Sands. Canada.

Masliyah, J., Z. Zhou, Z. Xu, J. Czarnecki and H. Hamza (2004). "Understanding water-based bitumen extraction from Athabasca oil sands." Canadian Journal of Chemical Engineering **82**(4): 628-654.

Mason, S. L., K. May and S. Hartland (1995). "Drop size and concentration profile determination in petroleum emulsion separation." Colloids and Surfaces A: Physicochemical and Engineering Aspects **96**(1-2): 85-92.

McLean, J. D. and P. K. Kilpatrick (1997). "Effects of asphaltene solvency on stability of water-in-crude-oil emulsions." Journal of Colloid and Interface Science **189**(2): 242-253.

Menon, V. B. and D. T. Wasan (1988). "Characterization of oil-water interfaces containing finely divided solids with applications to the coalescence of water-in-oil Emulsions: A review." Colloids and Surfaces **29**(1): 7-27.

Mullins, O. C., E. Y. Sheu, A. Hammami and A. G. Marshall (2007). Asphaltenes, Heavy Oils and Petroleomics. New York, Springer.

OGJ 2012, "Worldwide Look at Reserves and Production." Oil & Gas Journal.

Paul, E. L., V. A. Atiemo-Obeng and S. M. Kresta (2004). Handbook of Industrial Mixing : Science and Practice. Hoboken, New Jersey, John Wiley & Sons, Inc.

Peña, A. A., G. J. Hirasaki and C. A. Miller (2005). "Chemically induced destabilization of water-in-crude oil emulsions." Industrial and Engineering Chemistry Research **44**(5): 1139-1149.

Rahmani, N. H. G., T. Dabros and J. H. Masliyah (2004). "Evolution of asphaltene floc size distribution in organic solvents under shear." Chemical Engineering Science **59**(3): 685-697.

Ramakrishna, D. (2001). Population Balances. New York, Wiley.

Rushton, J. H., E. W. Costich and H. J. Everett (1950). "Power characteristics of mixing impellers." Chem. Eng. Progr. **46**(8): 395-476.

Rastegari, K., W. Y. Svrcek and H. W. Yarranton (2004). "Kinetics of asphaltene flocculation." Industrial and Engineering Chemistry Research **43**(21): 6861-6870.

Saadatmand, M. and H. W. Yarranton (2008). "Rag layers in oil sand froths." Industrial and Engineering Chemistry Research **47**(22): 8828-8839.

Shelfantook, W. E. (2004). "A perspective on the selection of froth treatment processes." Canadian Journal of Chemical Engineering **82**(4): 704-709.

Sjöblom, J., E.E. Johnsen, A.Westvik, et al. (2001). Encyclopedic Handbook of Emulsion Technology. Page 595. New York, Marcel Dekker.

Stewart, M., and K. Arnold (2009). Emulsions and Oil Treating Equipment: Selection, Sizing and Troubleshooting. Elsevier.

Sullivan, A. P. and P. K. Kilpatrick (2002). "The effects of inorganic solid particles on water and crude oil emulsion stability." Industrial and Engineering Chemistry Research **41**(14): 3389-3404.

Sztukowski, D. M. and H. W. Yarranton (2005). "Oilfield solids and water-in-oil emulsion stability." Journal of Colloid and Interface Science **285**: 821-833.

Xu, Y., J. Wu, T. Dabros and H. Hamza (2005) "Optimizing the polyethylene oxide and polypropylene oxide contents in diethylenetriamine-based surfactants for destabilization of a water-in-oil emulsion." Energy & Fuels **19**(3): 916-921.

Yan, N., M. R. Gray and J. H. Masliyah (2001). "On water-in-oil emulsions stabilized by fine solids." Colloids and Surfaces A: Physicochemical and Engineering Aspects **193**(1-3): 97-107.

Zhang, Z., G. Xu , F. Wang, S. Dong and Y. Chen (2005). "Demulsification by amphiphilic dendrimer copolymers." Journal of Colloid and Interface Science **282**(1): 1–4.

Zhou, G. and S. M. Kresta (1998). "Evolution of drop size distribution in liquid-liquid dispersions for various impellers." Chem. Eng. Sci. **53**: 2099-2113.

Appendix A: Feed Rate Calculation

Mesomixing time can be expressed as (Paul et al. 2004):

$$t_{meso} = \frac{Q_I}{U D_t} \qquad \text{A-1}$$

where Q_I is the injection flowrate (m³/s), U is the mean velocity of surrounding fluid at the feed point (m/s) and D_t is the local turbulent diffusivity (m²/s) which can be expressed as a function of the turbulent kinetic energy, k and its dissipation, ε:

$$D_t = 0.1 \frac{k^2}{\varepsilon} \qquad \text{A-2}$$

$$t_{meso} = \frac{Q_I \varepsilon}{U \cdot 0.1 k^2} \qquad \text{A-3}$$

Micromixing time can be expressed as:

$$t_{micro} = t_m = 12 \left(\frac{\nu}{\varepsilon}\right)^{0.5} =? \, 17.24 \left(\frac{\nu}{\varepsilon}\right)^{0.5} \qquad \text{A-4}$$

where ν is the kinematic viscosity (m²/s) and ε is the energy dissipation (W/kg). There are two different coefficients, 12 which is theoretical and 17.24 which is experimental (engulfment). For a more conservative experimental design where the mesomixing time is smaller and will be achieved faster, 12 is used in the calculation below.

To avoid mesomixing during the injection, $t_{meso} < 0.2 \, t_{micro}$ (Anthieren 2003).
Let, $t_{meso} = 0.2 \, t_{micro}$

$$5 = \frac{t_{micro}}{t_{meso}} = 12 \left(\frac{\nu}{\varepsilon}\right)^{0.5} \cdot \frac{U \cdot 0.1 k^2}{Q_I \varepsilon} \qquad \text{A-5}$$

$$k = \frac{1}{2}\left(v_z'^2 + v_r'^2 + v_\theta'^2\right) = \frac{3}{2} v_z'^2 \qquad \text{A-6}$$

$$\varepsilon = \frac{A v_z'^3}{L} \qquad \text{A-7}$$

where v_z' is the local fluctuating velocity (m/s), constant A is unity and L is the characteristic local integral length scale.

3 different length scales (1) $L = d_p$, (2) $L = D_{imp}/10$, (3) $L = T/5$ can be used, where d_p is the feed pipe diameter, D_{imp} is the impeller diameter and T is the tank diameter. Feed pipe diameter is chosen as the length scale as it will affect the size of droplet during the injection. The injection flowrate can be express as:

$$Q_I = 0.54 \frac{v^{0.5} \cdot U_z \cdot d_p^{1.5}}{v_z'^{0.5}} \qquad \textbf{A-8}$$

Appendix B: Chapter 2 Experimental Data

Table B-1: Batch gravity settling data from Karl Fischer titration (in wt% water) for Campaign 1

Run	Label	Settling time (min)							
		0	1	3	5	7	10	30	60
E001	(0,0,0,0)	2.43	2.44	2.28	2.40	2.30	2.23	1.47	1.37
E002	(0,0,0,0)	2.71	2.67	2.66	2.37	2.20	2.19	1.57	1.30
E003	(-1,-1,0,0)	2.37	2.05	2.04	2.09	2.04	1.86	1.85	1.69
E004	(-1,1,0,0)	2.38	2.21	2.13	2.18	1.89	1.92	1.70	1.69
E005	(1,-1,0,0)	2.61	2.52	2.56	2.22	1.96	2.04	1.75	1.39
E006	(1,1,0,0)	2.43	2.56	2.46	2.11	2.11	1.80	1.30	1.07
E007	(0,0,1,1)	2.57	2.43	2.39	1.88	1.93	1.70	1.67	1.53
E008	(0,0,1,-1)	2.65	2.59	1.20	0.66	0.55	0.50	0.37	0.24
E009	(0,0,-1,1)	2.82	2.82	2.40	2.16	2.19	2.07	1.61	1.19
E010	(0,0,-1,-1)	2.54	2.70	1.50	0.93	0.90	0.81	0.62	0.36
E011	(0,0,0,0)	2.63	2.44	2.35	2.39	2.34	2.04	1.34	1.29
E012	(0,0,0,0)	2.49	2.46	2.40	2.45	2.41	2.13	1.46	1.29
E013	(-1,0,0,-1)	2.20	2.36	2.27	2.25	1.97	1.88	1.63	1.33
E014	(1,0,0,-1)	2.27	2.23	2.07	0.47	0.42	0.35	0.21	0.13
E015	(1,0,0,1)	2.45	2.35	2.27	2.10	2.03	1.97	1.45	1.20
E016	(-1,0,0,1)	2.42	2.24	2.23	2.30	2.17	2.00	1.93	1.58
E017	(0,-1,-1,0)	2.47	2.45	2.43	2.29	2.30	2.18	1.90	1.63
E018	(0,1,-1,0)	2.49	2.37	2.41	2.33	2.29	2.15	1.78	1.78
E019	(0,-1,1,0)	2.54	2.50	2.44	2.40	2.28	2.22	1.83	1.61

E020	(0,1,1,0)	2.54	2.40	2.48	2.42	2.36	1.90	1.38	0.98
E021	(-1,0,-1,0)	2.47	2.37	2.38	2.31	2.32	2.16	1.76	1.42
E022	(1,0,-1,0)	2.36	2.36	2.32	2.26	2.31	2.08	1.52	1.10
E023	(-1,0,1,0)	2.58	2.24	2.31	2.32	2.26	2.20	1.86	1.54
E024	(1,0,1,0)	2.56	2.37	2.37	1.95	1.56	1.28	1.00	0.66
E025	(0,-1,0,1)	2.43	2.37	2.24	2.23	2.16	2.12	2.03	1.76
E026	(0,1,0,-1)	2.40	2.32	2.28	1.82	1.31	0.93	0.62	0.43
E027	(0,1,0,1)	2.50	2.32	2.42	2.21	2.20	2.13	1.74	1.57
E028	(0,-1,0,-1)	2.49	2.41	1.31	0.93	0.84	0.66	0.63	0.39
E029	(0,0,0,0)	2.41	2.39	2.38	2.31	2.17	2.15	1.63	1.32
E030	(0,0,0,0)	2.41	2.39	2.36	2.24	2.30	2.30	1.76	1.42

Table B-2: Data from Dean Stark O/W/S analysis (only solids and water, in wt%) for Campaign 1

Run	Label	Solids				Water			
		Pre-Mix	0.1	0.5	0.9	Pre-Mix	0.1	0.5	0.9
E001	(0,0,0,0)	0.38	0.27	0.29	0.30	3.9	3.05	2.21	2.69
E002	(0,0,0,0)	0.41	0.34	0.32	0.33	5.91	3.62	1.92	3.28
E003	(-1,-1,0,0)	0.39	0.36	0.31	0.35	5.24	4.78	4.69	2.56
E004	(-1,1,0,0)	0.38	0.33	0.33	0.36	4.13	3.99	2.54	3.42
E005	(1,-1,0,0)	0.34	0.23	0.26	0.27	5.52	3.05	5.35	2.77
E006	(1,1,0,0)	0.41	-	0.36	0.38	2.64	-	1.69	1.54
E007	(0,0,1,1)	0.45	0.36	0.42	0.37	3.4	2.45	2.05	2.44

E008	(0,0,1,-1)	0.46	0.08	0.04	0.68	2.54	1.01	0.94	3.8
E009	(0,0,-1,1)	0.33	0.27	0.28	0.31	3.6	3.09	4.87	3.97
E010	(0,0,-1,-1)	0.38	0.10	0.11	0.47	3.64	1.32	2.67	3.11
E011	(0,0,0,0)	0.37	0.34	0.30	0.33	3.55	2.13	3.04	3.22
E012	(0,0,0,0)	0.41	0.29	0.33	0.38	4.71	2.29	2.49	4.13
E013	(-1,0,0,-1)	0.42	0.37	0.40	0.38	5.19	3.37	3.87	2.59
E014	(1,0,0,-1)	0.42	0.10	0.07	0.85	3.09	0.64	0.48	4.16
E015	(1,0,0,1)	0.52	0.51	0.43	0.42	3.48	1.56	2.15	1.6
E016	(-1,0,0,1)	0.50	0.47	0.49	0.52	3.02	2.08	2.38	2.08
E017	(0,-1,-1,0)	0.53	0.47	0.45	0.46	2.86	2.23	2.36	2.83
E018	(0,1,-1,0)	0.54	0.43	0.51	0.47	2.8	1.31	1.61	2.14
E019	(0,-1,1,0)	0.46	0.49	0.49	0.51	3.15	1.86	2.14	1.87
E020	(0,1,1,0)	0.56	0.41	0.41	0.41	4.93	0.96	0.98	1.06
E021	(-1,0,-1,0)	0.44	0.39	0.34	0.33	2.71	3.74	1.87	1.69
E022	(1,0,-1,0)	0.41	0.37	0.39	0.37	2.85	4.51	1.39	3.33
E023	(-1,0,1,0)	0.51	0.49	0.46	0.49	3.21	2.77	2.05	2.11
E024	(1,0,1,0)	0.55	0.39	0.33	0.47	4.53	2.36	1.69	2.44
E025	(0,-1,0,1)	0.46	0.39	0.36	0.40	2.53	3.04	2.22	3.54
E026	(0,1,0,-1)	0.45	0.10	0.11	0.31	4.18	1.31	2.42	2.94
E027	(0,1,0,1)	0.40	0.35	0.37	0.39	3.7	3.68	3.65	3.04
E028	(0,-1,0,-1)	0.44	0.13	0.10	0.50	3.83	1.79	0.62	1.91
E029	(0,0,0,0)	0.50	0.37	0.30	0.31	2.42	2.51	1.02	1.35
E030	(0,0,0,0)	0.36	0.28	0.28	0.25	2.37	1.67	1.83	1.21

Table B-3: Batch gravity settling data from Karl Fischer titration (in wt% water) for Campaign 2

Run	Label	Settling time (min)							
		0	**1**	**3**	**5**	**7**	**10**	**30**	**60**
D001	(– – –)	1.21	1.13	1.11	1.08	1.10	1.10	0.95	0.84
D002	(– + –)	1.21	1.03	1.06	1.01	0.92	0.81	0.63	0.52
D003	(+ – +)	1.44	1.33	1.29	1.24	1.19	1.12	0.86	0.77
D004	(+ + +)	1.44	1.17	1.13	0.85	0.74	0.67	0.55	0.46
D005	(– – +)	1.04	0.94	0.96	0.93	0.95	0.92	0.88	0.82
D006	(+ + –)	1.04	0.86	0.86	0.64	0.54	0.46	0.37	0.31
D007	(– + +)	1.36	1.22	1.21	1.20	1.17	1.14	0.89	0.80
D008	(+ – –)	1.36	1.27	1.25	1.22	1.14	0.96	0.69	0.62

Table B-4: Data from Dean Stark O/W/S analysis (only solids and water, in wt%) for Campaign 2

Run	Label	Solids				Water			
		Pre-Mix	0.1	0.5	0.9	Pre-Mix	0.1	0.5	0.9
D001	(− − −)	0.37	0.36	0.37	0.34	1.14	0.68	0.77	0.77
D002	(− + −)	0.37	0.25	0.27	0.3	1.14	0.63	0.79	1.09
D003	(+ − +)	0.42	0.27	0.28	0.25	2.34	0.83	1.41	1.85
D004	(+ + +)	0.42	0.15	0.18	0.21	2.34	1.26	1.17	1.68
D005	(− − +)	0.44	0.3	0.25	0.33	1.31	0.71	1.28	1.44
D006	(+ + −)	0.44	0.1	0.09	0.4	1.31	1.44	3.88	1.25
D007	(− + +)	0.34	0.27	0.32	0.24	2.42	1.11	0.8	1.11
D008	(+ − −)	0.34	0.27	0.25	0.34	2.42	0.43	0.54	0.59

Appendix C: Chapter 3 Experimental Data

Table C-1: Batch gravity settling data from Karl Fischer titration (in wt% water) for Campaign 3

Run	Label	Settling time (min)							
		0	1	3	5	7	10	30	60
D009	(− +)	1.21	1.15	1.11	1.14	1.13	1.10	1.11	0.99
D010	(+ −)	1.21	1.00	1.01	0.89	0.63	0.49	0.32	0.21
D011	(+ +)	1.45	1.35	1.11	0.78	0.70	0.63	0.49	0.52
D012	(− −)	1.45	1.36	1.34	1.35	1.24	1.27	0.91	0.77

Table C-2: Data from Dean Stark O/W/S analysis (only solids and water, in wt%) for Campaign 3

Run	Label	Solids				Water			
		Pre-Mix	0.1	0.5	0.9	Pre-Mix	0.1	0.5	0.9
D009	(− +)	1.21	0.99	0.94	0.94	0.39	0.37	0.43	0.47
D010	(+ −)	1.21	0.21	0.24	2.02	0.39	0.11	0.13	1.34
D011	(+ +)	1.45	0.52	0.51	0.78	0.44	0.27	0.21	0.28
D012	(− −)	1.45	0.77	0.76	0.78	0.44	0.22	0.24	0.26

Appendix D: Chapter 4 Experimental Data

Table D-1: Batch gravity settling data from Karl Fischer titration (in wt% water) at addition order (F+N)+D

Run	Label	Settling time (min)							
		0	**1**	**3**	**5**	**7**	**10**	**30**	**60**
F001	(− +)	18.56	16.53	18.79	16.89	14.78	14.04	11.90	7.67
F002	(+ +)	17.64	15.50	16.90	13.52	13.23	11.54	6.66	5.59
F003	(− −)	18.60	19.50	16.28	15.61	14.42	13.25	5.89	4.45
F004	(+ −)	19.19	17.56	15.49	16.89	14.14	14.17	5.90	5.71
F005	**Low Solids**	20.46	19.26	15.84	13.08	11.69	8.92	4.63	4.74
F006	**0 ppm**	17.31	15.18	14.98	16.13	14.59	15.84	14.24	9.47
F007	**0 ppm**	19.90	17.68	18.08	17.80	15.80	17.01	12.00	8.90
F008	**100 ppm**	17.31	15.07	11.86	9.46	8.91	8.27	5.82	4.45
F009	**150 ppm**	18.19	15.08	14.94	12.01	8.67	6.11	4.44	2.91
F010	**150 ppm Intermig**	21.49	18.34	16.24	18.63	16.51	15.30	9.62	7.65

Table D-2: Batch gravity settling data from Karl Fischer titration (in wt% water) at addition order (F+D)+N

Run	Label	Settling time (min)							
		0	1	3	5	7	10	30	60
F011	0 ppm	22.23	21.15	17.39	20.12	17.78	15.51	12.34	8.02
F012	50 ppm	21.52	18.26	16.21	18.32	15.75	13.24	6.29	5.48
F013	100 ppm	19.03	17.28	15.50	17.10	18.01	15.12	2.43	2.01
F014	150 ppm	20.10	16.67	16.75	15.54	18.02	16.93	1.50	0.88
F015	150 ppm A310	18.42	19.81	17.83	18.41	17.37	17.64	1.66	1.87